



**Systematic Revision of *Thomasomys cinereus*
(Rodentia: Cricetidae: Sigmodontinae) from Northern
Peru and Southern Ecuador, With Descriptions of Three
New Species**

Authors: Pacheco, Víctor, and Ruelas, Dennisse

Source: Bulletin of the American Museum of Natural History, 461(1) : 1-72

Published By: American Museum of Natural History

URL: <https://doi.org/10.1206/0003-0090.461.1.1>

BioOne Complete (complete.BioOne.org) is a full-text database of 200 subscribed and open-access titles in the biological, ecological, and environmental sciences published by nonprofit societies, associations, museums, institutions, and presses.

Your use of this PDF, the BioOne Complete website, and all posted and associated content indicates your acceptance of BioOne's Terms of Use, available at www.bioone.org/terms-of-use.

Usage of BioOne Complete content is strictly limited to personal, educational, and non - commercial use. Commercial inquiries or rights and permissions requests should be directed to the individual publisher as copyright holder.

BioOne sees sustainable scholarly publishing as an inherently collaborative enterprise connecting authors, nonprofit publishers, academic institutions, research libraries, and research funders in the common goal of maximizing access to critical research.

SYSTEMATIC REVISION OF
THOMASOMYS CINEREUS
(RODENTIA: CRICETIDAE: SIGMODONTINAE) FROM
NORTHERN PERU AND SOUTHERN ECUADOR,
WITH DESCRIPTIONS OF THREE NEW SPECIES

VÍCTOR PACHECO

*Departamento de Mastozoología, Museo de Historia Natural,
Universidad Nacional Mayor de San Marcos, Lima, Perú;
Instituto de Ciencias Biológicas “Antonio Raimondi,” Facultad de Ciencias Biológicas,
Universidad Nacional Mayor de San Marcos, Lima, Perú*

DENNISSE RUELAS

*Departamento de Mastozoología, Museo de Historia Natural,
Universidad Nacional Mayor de San Marcos, Lima, Perú;
Instituto de Ciencias Biológicas “Antonio Raimondi,” Facultad de Ciencias Biológicas,
Universidad Nacional Mayor de San Marcos, Lima, Perú;
Institut des Sciences de l’Evolution, Université Montpellier II, Montpellier, France*

BULLETIN OF THE AMERICAN MUSEUM OF NATURAL HISTORY

Number 461, 71 pp., 26 figures, 4 tables

Issued June 21, 2023

Copyright © American Museum of Natural History 2023

ISSN 0003-0090

CONTENTS

Abstract.....	3
Introduction.....	3
Material and Methods	4
Molecular Analyses	8
Morphological and Morphometric Analyses.....	11
Results.....	15
Intraspecific Analyses	15
Phylogenetic Analyses.....	15
Morphometric Analyses	17
Taxonomic Accounts	17
<i>Thomasomys cinereus</i> (Thomas, 1882)	21
<i>Thomasomys lojapiuranus</i> , new species	35
<i>Thomasomys shallqukucha</i> , new species.....	44
<i>Thomasomys pagaibambensis</i> , new species.....	48
Discussion	53
Biogeographic Implications	55
Acknowledgments.....	56
References.....	57
Appendix 1. Selected Collecting Localities.....	63
Appendix 2. Phylogenetic Relationships of <i>Thomasomys</i> Based on Maximum-Likelihood Analysis	66
Appendix 3. ANOVA Test Results	67
Appendix 4. Factor Loadings for Principal Components and Discriminant Function Analyses	69
Appendix 5. Results of Principal Components Analyses	70

ABSTRACT

Thomasomys cinereus is the type species of *Thomasomys*, type genus of the sigmodontine tribe Thomasomyini. As currently recognized, *Thomasomys* includes 48 species, all of which are endemic to humid montane or premontane forests in the tropical Andes. Although it has been suggested that *T. cinereus* is a species complex, this hypothesis has yet to be critically evaluated. Herein we provide a revision of the species based on a qualitative assessment of external, craniodental, and soft morphological traits; morphometric analyses; a phylogenetic analysis based on cytochrome *b* gene sequences; species delimitation methods; and first-hand examination of type material. Our analyses of genetic data recovered four distinct clades within *T. cinereus*, one corresponding to *T. cinereus* sensu stricto (restricted to the montane forests delimited by the Río Marañón, Río Huancabamba, and Río Tablachaca in Cajamarca department, Peru) and three new species: *Thomasomys lojapiuranus*, sp. nov., from the montane forests of Piura department, Peru, and Loja province, Ecuador; *T. shallqukucha*, sp. nov., restricted to the Kañaris montane forests in the Peruvian department of Lambayeque; and *T. pagaibambensis*, sp. nov., restricted to the montane forests of Pagaibamba in Cajamarca department, Peru. These species can be distinguished by several discrete morphological traits of the skull, dentition, mandible, stomach, palatal rugae, and glans penis. Genetic distances among these taxa range from 5.06%–7.65% at the cytochrome *b* locus, and delimitation analyses based on cytochrome *b* sequence data support their recognition as distinct species. Our results suggest the existence of previously unsuspected dispersal barriers in the Andes of northern Peru, and they confirm that the Río Marañón is a formidable barrier that limits the distribution of species of *Thomasomys* as well as other sigmodontine rodents.

INTRODUCTION

Thomasomys Coues, 1884, is the type genus of the tribe Thomasomyini in the cricetid rodent subfamily Sigmodontinae. The genus currently includes 48 species (Pacheco et al., 2015; Brito et al., 2019, 2021; Ruelas and Pacheco, 2021a; Lee et al., 2022), all of which are endemic to the tropical Andes from about 1150 m to 4600 m above sea level, where most of them appear to be restricted to montane forests (Patton, 1987; Pacheco et al., 2015). Although several new species have been described in recent years (e.g., *T. onkiro* Luna and Pacheco, 2002; *T. ucucha* Voss, 2003; *T. andersoni* Salazar-Bravo and Yates, 2007; *T. salazari* Brito et al., 2019; *T. pardignasi* Brito et al., 2021; *T. antoniobracki* Ruelas and Pacheco, 2021; and *T. burneoi* Lee et al., 2022) the genus as a whole remains unrevised.

The type species of *Thomasomys* is *Hesperomys cinereus* Thomas, 1882, which was based on a holotype collected at Cutervo in Cajamarca department, Peru. Thomas (1882) described *T. cinereus* using external morphology and basic

morphometric values, and Voss (1993) subsequently described additional key external, cranial, dental, and soft-anatomical characters. Pacheco (2003) confirmed these diagnostic morphological attributes and added several others. More recently, Pacheco (2015) provided an updated account of *Thomasomys cinereus*, describing the species afresh, comparing it with other congeners known at that time, and reporting marginal localities from the Peruvian departments of Cajamarca (west of the Río Marañón), La Libertad, Lambayeque, and Piura. Subsequently, *T. cinereus* has also been reported from the province of Loja in southern Ecuador (Lee et al., 2018; Moreno-Cárdenas and Novillo-Gonzalez, 2020). Although Pacheco (2015) considered *T. cinereus* monotypic, he suggested that it might be a species complex. To date, however, no taxonomic revision of the material currently referred to *T. cinereus* has been undertaken.

Based on a phylogeny using external, cranial, dental, postcranial, and soft-anatomical characters, Pacheco (2003, 2015) proposed seven informal species groups for *Thomasomys*, of

which the Cinereus Group was the most diverse with 23 species. This group includes mainly small to medium-size rodents (head and body length: 89–161 mm) distributed in montane forests from Venezuela and Colombia to Bolivia. The species that Pacheco (2003, 2015) included in the Cinereus Group included *T. australis* Anthony, 1925; *T. bombycinus* Anthony, 1925; *T. caudivarius* Anthony, 1923; *T. cinereiventer* J.A. Allen, 1912; *T. cinereus* (Thomas, 1882); *T. cinnamomeus* Anthony, 1924; *T. contradictus* Anthony, 1925; *T. daphne* Thomas, 1917; *T. dispar* Anthony, 1925; *T. emeritus* Thomas, 1916; *T. erro* Anthony, 1926; *T. fumeus* Anthony, 1924; *T. hudsoni* Anthony, 1923; *T. hylophilus* Osgood, 1912; *T. laniger* (Thomas, 1895); *T. monochromos* Bangs, 1900; *T. niveipes* (Thomas, 1896); *T. onkiro* Luna and Pacheco, 2002; *T. paramorum* Thomas, 1898; *T. silvestris* Anthony, 1924; *T. ucucha* Voss, 2003; *T. vestitus* (Thomas, 1898); and *T. vulcani* (Thomas, 1898). Recently, Brito et al. (2019) described *T. salazari* and included it along with two undescribed taxa in the Cinereus Group, bringing the potential total membership to 26 species.

Phylogenetic analyses of cytochrome *b* sequence data have provided molecular support for some of Pacheco's (2003, 2015) species groups (Salazar-Bravo and Yates, 2007; Lee et al., 2015, 2018; Brito et al., 2019, 2021). In particular, Lee et al. (2018) and Brito et al. (2019) both recovered a monophyletic Cinereus Group, but *T. cinereus* was represented in their analyses only by Ecuadorian specimens, the identification of which has yet to be convincingly established. Genetic data obtained from topotypical specimens of *T. cinereus* and specimens from other Peruvian populations currently referred to *T. cinereus* have yet to be analyzed. As a result, the phylogenetic position of *T. cinereus* is still unclear, nor has the distributional range of the species been critically evaluated with either phenotypic or genetic analyses.

Herein, we review the taxonomy of *Thomasomys cinereus* sensu lato (i.e., as this name was applied by Pacheco, 2015) and provide a

hypothesis about its phylogenetic relationships. Based on phylogenetic analyses of cytochrome *b* sequence data, qualitative morphological comparisons, and morphometric analyses, we recognize four species among specimens previously identified as *T. cinereus*, three of which are described as new. Our results contribute to a better taxonomic understanding of the genus, and they provide a framework for future biogeographic studies of small mammals in northern Peru.

MATERIAL AND METHODS

SOURCE OF MATERIAL: For morphological assessment we examined 350 specimens (skulls, skins, and fluid-preserved material) previously referred to *Thomasomys cinereus* (including the holotype) from throughout the distributional range of the species as it has been identified in the past (appendix 1). This morphological material is deposited in the following institutions (acronyms in parentheses): American Museum of Natural History, New York (AMNH); Natural History Museum, London (formerly the British Museum of Natural History, BMNH); Field Museum of Natural History, Chicago (FMNH); Museum of Zoology, Louisiana State University, Baton Rouge (LSUMZ); Museo de la Escuela Politécnica Nacional, Quito (MEPN); Museo de Historia Natural, Universidad Nacional Mayor de San Marcos, Lima (MUSM); Museum of Vertebrate Zoology, University of California, Berkeley (MVZ); Sección de Mastozoología, Museo de Zoología de la Pontificia Universidad Católica del Ecuador, Quito (QCAZ-M); University of Michigan Museum of Zoology, Ann Arbor (UMMZ); and the National Museum of Natural History, Smithsonian Institution, Washington D.C. (USNM).

Collection localities for examined specimens of *Thomasomys cinereus* (sensu Pacheco, 2015; including the new specimens described herein) are mapped in figure 1 and gazetteered in appendix 1. The specimens we sequenced for cytochrome *b* are listed in table 1.

TABLE 1

Ingroup and outgroup taxa sequenced for cytochrome *b* used in phylogenetic tree reconstruction.

Species include new taxa (marked with an asterisk) described in this report. Voucher provides museum catalog number or collector's field number. Locality numbers in parentheses (for members of the *Thomasomys cinereus* complex) are mapped in figure 1.

Abbreviations: CBF, Colección Boliviana de Fauna; LCM, Laboratorio de Citogenética de Mamíferos, Universidad de Chile; MECN, Museo Ecuatoriano de Ciencias Naturales; MSB, Museum of Southwestern Biology, University of New Mexico; TTU, Museum of Texas Tech University; UFMG, Collection at Universidade Federal de Minas Gerais; ASA, Anderson Solis Alvaro (field number); EV, Elena Vivar (field number); JLP, James L. Patton (field number); MNFS, M.N.F da Silva (field number); TEL, Tom Lee (field number); UP, Ulyses Pardiñas (field number); other abbreviations are listed in Material and Methods.

Species	Voucher	Locality	GenBank #	Source
<i>Abrothrix olivaceus</i>	FMNH 129876	Chile, Aysén	AF297892	Smith et al. (2001)
<i>Akodon boliviensis</i>	MVZ 171607	Peru, Puno	M35691	Smith and Patton (1999)
<i>Andinomys edax</i>	—	Bolivia, Tarija	AF159284	Anderson and Yates (2000)
<i>Auliscomys micropus</i>	MVZ 182661	Argentina, Rio Negro	AF108690	Smith and Patton (1999)
<i>Chilomys instans</i>	JLP 16693	Colombia, Risaralda	AF108679	Smith and Patton (1999)
<i>Chilomys instans</i>	TEL 2775	Ecuador, Carchi	KR818906	Lee et al. (2015)
<i>Microrzomys minutus</i>	MVZ 173975	Peru, Cusco	AF108698	Smith and Patton (1999)
<i>Oecomys bicolor</i>	MNFS 1499	Brazil, Acre	U58382	Patton and da Silva (1995)
<i>Oxymycterus rufus</i>	UP AC04	Argentina	AY275126	D'Elía (2003)
<i>Phyllotis magister</i>	LCM 1817	Chile, Antofagasta	AF484213	Kuch et al. (2002)
<i>Rhagomys longilingua</i>	CBF 7620	Bolivia, Bajo Hornuni	KX423691	Salazar-Bravo et al. (2016)
<i>Rhagomys rufescens</i>	—	Brazil, Minas Gerais	AY206770	Percequillo et al. (2004)
<i>Rhipidomys albujaí</i>	MEPN 12196	Ecuador, Morona Santiago	KY366344	Brito et al. (2017)
<i>Rhipidomys latimanus</i>	QCAZ Z4784	Ecuador, Cotopaxi	KY366338	Brito et al. (2017)
<i>Sigmodon hispidus</i>	TTU-M 80670	United States, Texas	KX866980	Milazzo et al. (2017)
<i>Thomasomys andersoni</i>	MSB 146437	Bolivia, Cochabamba	DQ914643	Salazar-Bravo and Yates (2007)
<i>Thomasomys andersoni</i>	AMNH 268734	Bolivia, Cochabamba	DQ914644	Salazar-Bravo and Yates (2007)
<i>Thomasomys aureus</i>	MECN 5666	Ecuador, Chimborazo	MN557077	Brito et al. (2019)
<i>Thomasomys auricularis</i>	MECN 4695	Ecuador, Loja	MN557061	Brito et al. (2019)
<i>Thomasomys australis</i>	AMNH 268736	Bolivia, Cochabamba	DQ914645	Salazar-Bravo and Yates (2007)
<i>Thomasomys australis</i>	MSB 70447	Bolivia, Cochabamba	DQ914650	Salazar-Bravo and Yates (2007)
<i>Thomasomys baeops</i>	MSB 70704	Ecuador, Bolivar	DQ914654	Salazar-Bravo and Yates (2007)
<i>Thomasomys bombycinus</i>	MECN 4957	Ecuador, Carchi	MN557062	Brito et al. (2019)
<i>Thomasomys caudivarius</i>	MECN 4687	Ecuador, Loja	MN557059	Brito et al. (2019)
<i>Thomasomys caudivarius</i>	MECN 4692	Ecuador, Loja	MN557060	Brito et al. (2019)

TABLE 1 *continued*

Species	Voucher	Locality	GenBank #	Source
<i>Thomasomys caudivarius</i>	MECN 4699	Ecuador, Loja	MN557126	Brito et al. (2019)
<i>Thomasomys caudivarius</i>	MEPN 12491	Ecuador, Loja	MZ490799	This study
<i>Thomasomys cinereus</i>	MUSM 24169	Peru, La Libertad (51)	MZ490800	This study
<i>Thomasomys cinereus</i>	MUSM 24172	Peru, La Libertad (51)	MZ490801	This study
<i>Thomasomys cinereus</i>	MUSM 38007	Peru, Cajamarca (45)	MZ490802	This study
<i>Thomasomys cinereus</i>	MUSM 41103	Peru, La Libertad (54)	MZ490803	This study
<i>Thomasomys cinereus</i>	MUSM 42010	Peru, La Libertad (54)	MZ490804	This study
<i>Thomasomys cinereus</i>	MUSM 42011	Peru, La Libertad (54)	MZ490805	This study
<i>Thomasomys cinereus</i>	MUSM 46716	Peru, Cajamarca (25)	MZ490806	This study
<i>Thomasomys cinereus</i>	MUSM 46756	Peru, Cajamarca (29)	MZ490807	This study
<i>Thomasomys cinereus</i>	MUSM 46757	Peru, Cajamarca (29)	MZ490808	This study
<i>Thomasomys cinereus</i>	MUSM 46909	Peru, Cajamarca (33)	MZ490809	This study
<i>Thomasomys cinereus</i>	MUSM 51110	Peru, Cajamarca (48)	MZ490810	This study
<i>Thomasomys cinereus</i>	MUSM 51115	Peru, Cajamarca (48)	MZ490811	This study
<i>Thomasomys cinereus</i>	MUSM 51117	Peru, Cajamarca (48)	MZ490812	This study
<i>Thomasomys cinereus</i>	MUSM:EV1626	Peru, La Libertad	MZ490813	This study
<i>Thomasomys cinnameus</i>	TEL 2806	Ecuador, Carchi	KR818895	Lee et al. (2015)
<i>Thomasomys cinnameus</i>	TEL 2811	Ecuador, Carchi	KR818896	Lee et al. (2015)
<i>Thomasomys cinnameus</i>	TEL 2690	Ecuador, Carchi	KR818897	Lee et al. (2015)
<i>Thomasomys cinnameus</i>	QCAZ 14919	Ecuador, Carchi	MN557099	Brito et al. (2019)
<i>Thomasomys cinnameus</i>	QCAZ 14920	Ecuador, Carchi	MN557100	Brito et al. (2019)
<i>Thomasomys daphne</i>	MVZ 171502	Peru, Puno	AF108673	Smith and Patton (1999)
<i>Thomasomys daphne</i>	AMNH 268737	Bolivia, La Paz	DQ914649	Salazar-Bravo and Yates (2007)
<i>Thomasomys daphne</i>	MUSM 9369	Peru, Cusco	MZ736561	This study
<i>Thomasomys daphne</i>	MVZ 171501	Peru, Puno	KY754167	Steppan and Schenk (2017)
<i>Thomasomys daphne</i>	MVZ 171502	Peru, Puno	MZ490814	This study
<i>Thomasomys erro</i>	TEL 1663	Ecuador, Napo	EU579476	Hanson (2008)
<i>Thomasomys fumeus</i>	TEL 1894	Ecuador, Napo	KR818901	Lee et al. (2015)
<i>Thomasomys gracilis</i>	MVZ 166668	Peru, Cusco	AF108674	Smith and Patton (1999)
<i>Thomasomys gracilis</i>	MVZ 166669	Peru, Cusco	MZ736560	This study
<i>Thomasomys hudsoni</i>	MSB 140583	Ecuador, Azuay	DQ914646	Salazar-Bravo and Yates (2007)
<i>Thomasomys hudsoni</i>	TEL 2243	Ecuador, Chimborazo	KR818894	Lee et al. (2015)
<i>Thomasomys hudsoni</i>	MECN 5664	Ecuador, Chimborazo	MN557076	Brito et al. (2019)
<i>Thomasomys hudsoni</i>	MECN 5667	Ecuador, Chimborazo	MN557078	Brito et al. (2019)
<i>Thomasomys hudsoni</i>	MECN 5668	Ecuador, Chimborazo	MN557079	Brito et al. (2019)
<i>Thomasomys</i> cf. <i>incanus</i>	MUSM 40809	Peru, Junín	MZ736562	This study
<i>Thomasomys kalinowskii</i>	MVZ 172598	Peru, Junín	AF108678	Smith and Patton (1999)

TABLE 1 *continued*

Species	Voucher	Locality	GenBank #	Source
<i>Thomasomys ladewi</i>	MSB 68484	Bolivia, La Paz	DQ914647	Salazar-Bravo and Yates (2007)
<i>Thomasomys lojapiuranus</i> *	QCAZ 16230	Ecuador, Loja (4)	MN557119	Brito et al. (2019)
<i>Thomasomys lojapiuranus</i> *	QCAZ 16231	Ecuador, Loja (4)	MN557120	Brito et al. (2019)
<i>Thomasomys lojapiuranus</i> *	QCAZ 16328	Ecuador, Loja (4)	MN557121	Brito et al. (2019)
<i>Thomasomys lojapiuranus</i> *	QCAZ 16329	Ecuador, Loja (4)	MN557122	Brito et al. (2019)
<i>Thomasomys lojapiuranus</i> *	QCAZ 16330	Ecuador, Loja (4)	MN557123	Brito et al. (2019)
<i>Thomasomys lojapiuranus</i> *	MEPN 12549	Ecuador, Loja (2)	MZ490815	This study
<i>Thomasomys lojapiuranus</i> *	MUSM 23758	Peru, Piura (6)	MZ490816	This study
<i>Thomasomys lojapiuranus</i> *	MUSM 511	Peru, Piura (3)	MZ490817	This study
<i>Thomasomys lojapiuranus</i> *	MUSM:ASA11	Peru, Piura (1)	OK318983	This study
<i>Thomasomys lojapiuranus</i> *	MUSM:ASA12	Peru, Piura (1)	OK318984	This study
<i>Thomasomys lojapiuranus</i> *	MUSM:ASA16	Peru, Piura (1)	OK318985	This study
<i>Thomasomys macrotis</i>	LSUMZ 27287	Peru, San Martín	KY754168	Steppan and Schenk (2017)
<i>Thomasomys notatus</i>	UMMZ 160588	Peru, Cusco	MN557128	Brito et al. (2019)
<i>Thomasomys onkiro</i>	USNM 582124	Peru, Junín	KY754169	Smith and Patton (1999)
<i>Thomasomys oreas</i>	MSB 87126	Bolivia, Cochabamba	DQ914651	Smith and Patton (1999)
<i>Thomasomys oreas</i>	MVZ 166704	Peru, Cusco	MN557091	Brito et al. (2019)
<i>Thomasomys pagaibambensis</i> *	MUSM 40973	Peru, Cajamarca (22)	MZ419564	This study
<i>Thomasomys pagaibambensis</i> *	MUSM 41009	Peru, Cajamarca (19)	MZ419565	This study
<i>Thomasomys pagaibambensis</i> *	MUSM 39526	Peru, Cajamarca (23)	MZ490823	This study
<i>Thomasomys pagaibambensis</i> *	MUSM 39529	Peru, Cajamarca (20)	MZ490824	This study
<i>Thomasomys paramorum</i>	TEL 2244	Ecuador, Chimborazo	KR818891	Lee et al. (2015)
<i>Thomasomys paramorum</i>	TEL 2247	Ecuador, Chimborazo	KR818892	Lee et al. (2015)
<i>Thomasomys paramorum</i>	TEL 2380	Ecuador, Chimborazo	KR818893	Lee et al. (2015)
<i>Thomasomys paramorum</i>	MEPN 12631	Ecuador, Chimborazo	MN557087	Lee et al. (2015)
<i>Thomasomys paramorum</i>	MEPN 12634	Ecuador, Chimborazo	MN557088	Brito et al. (2019)
<i>Thomasomys paramorum</i>	QCAZ 11986	Ecuador, Chimborazo	MN557094	Brito et al. (2019)
<i>Thomasomys paramorum</i>	QCAZ 12602	Ecuador, Pichincha	MN557096	Brito et al. (2019)
<i>Thomasomys pardignasi</i>	QCAZ 17489	Ecuador, Morona Santiago	MN557083	Brito et al. (2019)
<i>Thomasomys salazari</i>	TEL 2271	Ecuador, Chimborazo	KR818888	Lee et al. (2015)
<i>Thomasomys salazari</i>	TEL 2293	Ecuador, Chimborazo	KR818889	Lee et al. (2015)
<i>Thomasomys salazari</i>	MECN 5634	Ecuador, Morona Santiago	MN557065	Brito et al. (2019)
<i>Thomasomys salazari</i>	MECN 5653	Ecuador, Morona Santiago	MN557073	Brito et al. (2019)
<i>Thomasomys shallqukucha</i> *	MUSM 46883	Peru, Lambayeque (15)	MZ490818	This study
<i>Thomasomys shallqukucha</i> *	MUSM 46886	Peru, Lambayeque (15)	MZ490819	This study
<i>Thomasomys shallqukucha</i> *	MUSM 47227	Peru, Lambayeque (14)	MZ490820	This study
<i>Thomasomys shallqukucha</i> *	MUSM 47228	Peru, Lambayeque (14)	MZ490821	This study

TABLE 1 *continued*

Species	Voucher	Locality	GenBank #	Source
<i>Thomasomys shallqukucha</i> *	MUSM 47229	Peru, Lambayeque (14)	MZ490822	This study
<i>Thomasomys silvestris</i>	QCAZ 13067	Ecuador, Cotopaxi	KR818900	Lee et al. (2015)
<i>Thomasomys silvestris</i>	MECN 5238	Ecuador, Pichincha	MN557063	Brito et al. (2019)
<i>Thomasomys silvestris</i>	MECN 5394	Ecuador, Pichincha	MN557064	Brito et al. (2019)
<i>Thomasomys cf. aureus</i> ¹	MVZ 170076	Peru, Cusco	U035402	Smith and Patton (1999)
<i>Thomasomys taczanowskii</i>	MVZ 181999	Peru, Cajamarca	AF108675	Smith and Patton (1999)
<i>Thomasomys ucucha</i>	TEL 2692	Ecuador, Carchi	KR818898	Lee et al. (2015)
<i>Thomasomys ucucha</i>	TEL 2800	Ecuador, Carchi	KR818899	Lee et al. (2015)
<i>Thomasomys ucucha</i>	QCAZ 11707	Ecuador, Imbabura	MN557093	Brito et al. (2019)
<i>Thomasomys vulcani</i>	TEL 2703	Ecuador, Carchi	KR818902	Lee et al. (2015)
<i>Thomasomys vulcani</i>	TEL 2728	Ecuador, Carchi	KR818903	Lee et al. (2015)
<i>Thomasomys</i> sp. 1	MSB 70714	Ecuador, Bolivar	DQ914648	Salazar-Bravo and Yates (2007)
<i>Thomasomys</i> sp. 2 ²	QCAZ 15621	Ecuador, Loja	MN557110	Brito et al. (2019)
<i>Thomasomys</i> sp. 2 ²	QCAZ 15612	Ecuador, Loja	MN557101	Brito et al. (2019)
<i>Thomasomys</i> sp. 2 ²	QCAZ 15614	Ecuador, Loja	MN557103	Brito et al. (2019)
<i>Thomasomys</i> sp. 2 ²	QCAZ 15617	Ecuador, Loja	MN557106	Brito et al. (2019)
<i>Thomasomys</i> sp. 2 ²	QCAZ 15619	Ecuador, Loja	MN557108	Brito et al. (2019)
<i>Wiedomys pyrrhorhinos</i>	UFMG -LC43	Brazil, Bahia	AF108685	Smith and Patton (1999)

¹ *Thomasomys* sp. 1 of Pacheco (2003).² *Thomasomys cinereus* sensu Lee et al. (2018), not *T. cinereus* as recognized in this report.

MOLECULAR ANALYSES

DNA ISOLATION: We isolated genomic DNA from 28 specimens of *Thomasomys cinereus* (sensu Pacheco, 2015) from Piura, Cajamarca, Lambayeque, and La Libertad departments in Peru and from one specimen of *T. cinereus* (sensu Moreno-Cárdenas and Novillo-Gonzalez, 2020) from Loja province, Ecuador (table 1). DNA was isolated from portions of liver and muscle preserved in alcohol or from fragments of dried skin using Wizard® SV Genomic DNA Purification System Kit (Promega Corp.). We amplified and sequenced the mitochondrial gene cytochrome *b* (*cytb*) by polymerase chain reaction using primers MVZ05, MVZ45, MVZ04, MVZ16, and MVZ14 of Smith and Patton (1993). The thermal profile of PCR reactions consisted of an initial denaturation step at 94° C for 4 min,

followed by 33 cycles of PCR (denaturation at 93° C for 1 min, annealing at 45° C for 1 min, polymerization at 72° C for 2 min), and a final extension at 72° C for 10 min. Gene isolation and amplification were performed in the Evolutionary Biology Lab of the Mammalogy Department of MUSM. Amplified products were sequenced by an external sequencing service (Macrogen. Inc. Seoul, South Korea). The sequences were manually checked using CodonCode 6.0.2 (CodonCode Corporation, Centerville, Massachusetts). New sequences were deposited in GenBank (table 1).

INTRASPECIFIC ANALYSES: Genetic relationships among geographic samples of *Thomasomys cinereus* sensu lato were determined by the median-joining approach (Bandelt et al., 1999) using R 4.1.3 (R Core Team 2022) with the packages: “ape,” “pegas,” and “scales.” Then, we per-

formed an Analysis of Molecular Variance (AMOVA; Excoffier et al., 1992) and computed fixation indices (F_{ST}) using Arlequin 3.5 (Excoffier and Lischer, 2010) to assess genetic isolation among the geographic populations currently referred to this species.

PHYLOGENETIC ANALYSES: For phylogenetic analysis, we used the following taxa as outgroups: 10 representatives of other sigmodontine tribes (*Sigmodon hispidus*, *Wiedomys pyrhorhinos*, *Microrhynchomys minutus*, *Oecomys bicolor*, *Abrothrix olivaceus*, *Akodon boliviensis*, *Oxymyzomys rufus*, *Andinomys edax*, *Auliscomys micropus*, and *Phyllotis magister*), 5 representatives of other thomatomyine genera (*Chilomys instans*, *Rhagomys longilingua*, *Rhagomys rufescens*, *Rhipidomys albujaui*, *Rhipidomys latimanus*), and 14 species of *Thomasomys* representing other species groups of *Thomasomys* (*Thomasomys* sp. 1 [sensu Pacheco, 2003], *T. andersoni*, *T. aureus*, *T. auricularis*, *T. baeops*, *T. gracilis*, *T. cf. incanus*, *T. kalinowskii*, *T. ladewi*, *T. macrotis*, *T. notatus*, *T. oreas*, *T. pardignasi*, and *T. taczanowskii*). Members of the Cinereus Group (as defined in the Introduction) were considered the ingroup (table 1), among which we included 34 partial sequences of *Thomasomys cinereus* sensu lato.

Phylogenetic relationships were inferred by maximum likelihood (ML) and Bayesian inference (BI). The model and parameters used in both analysis were previously selected under the Akaike Information criterion using JModelTest 2.1.10 (Darriba et al., 2012). The best model was GTR+I+G with the following parameters: rate matrix (1.0886, 6.9496, 1.0512, 0.3431, 11.6214, 1.0000), base frequencies (0.3101, 0.3319, 0.0820, 0.2760), $p\text{-inv} = 0.4530$, gamma distribution shape parameter (0.8350). ML analyses were performed using IQ-TREE multicore 1.6.3 (Nguyen et al., 2015) with 10,000 nonparametric bootstrap replicates to search for the best tree and to compute bootstrap support (BS) values. Bayesian analysis was performed in MrBayes 3.2.6 (Ronquist et al., 2012) with 10 million generations, four simultaneous Markov chains, and trees sam-

pled every 1000 generations per chain. The first 25% of the trees were discarded as burn-in, and the remaining trees were used to compute a 50% majority rule consensus tree and to obtain the Bayesian posterior probability (BPP) for each node. Chain convergence was evaluated using the ESS (effective sample size) indicator, which was greater than 200 in all priors using Tracer 1.7 (Rambaut et al., 2018). Consensus trees were edited using iTOL v 4 (Letunic and Bork, 2016).

SPECIES DELIMITATION: We performed four single-locus species-delimitation analyses using the *cytb* dataset: Automatic Barcode Gap Discovery (ABGD; Puillandre et al., 2011), Assemblage of Species by Automatic Partitioning (ASAP; Puillandre et al., 2021); Poisson Tree Processes (PTP; Zhang et al., 2013), and General Mixed Yule Coalescent (GMYC; Fujisawa and Barraclough, 2013; Pons et al., 2006). For the ABGD method, we uploaded the FASTA alignment in the ABGD online version (<https://bioinfo.mnhn.fr/abi/public/abgd/>) with settings: $pmin = 0.001$, $pmax = 0.10$, $X = 1.00$, and using simple distance. For ASAP method, we uploaded the FASTA alignment in the ASAP web (<https://bioinfo.mnhn.fr/abi/public/asap/>) using the default settings and simple distance. For PTP method, we uploaded trees of BI in bPTP web server (<https://species.h-its.org/>; Zhang et al., 2013) with 5×10^5 MCMC generations. For these three methods, we used only ingroup species (members of the Cinereus Group as defined above). The GMYC method was performed in the GMYC web server (<https://species.h-its.org/gmyc/>), using a calibrated tree by the uncorrelated relaxed-clock log-normal model with multiple secondary calibration points performed in Beast (Bouckaert et al., 2019). We followed Parada et al. (2021) for the crown ages of sigmodontine tribes.

GENETIC DISTANCES: We calculated the corrected *cytb* genetic distances using the Kimura 2-parameter model and pairwise deletion option within and among candidate species using MEGA v. 7.0 (Kumar et al., 2016).

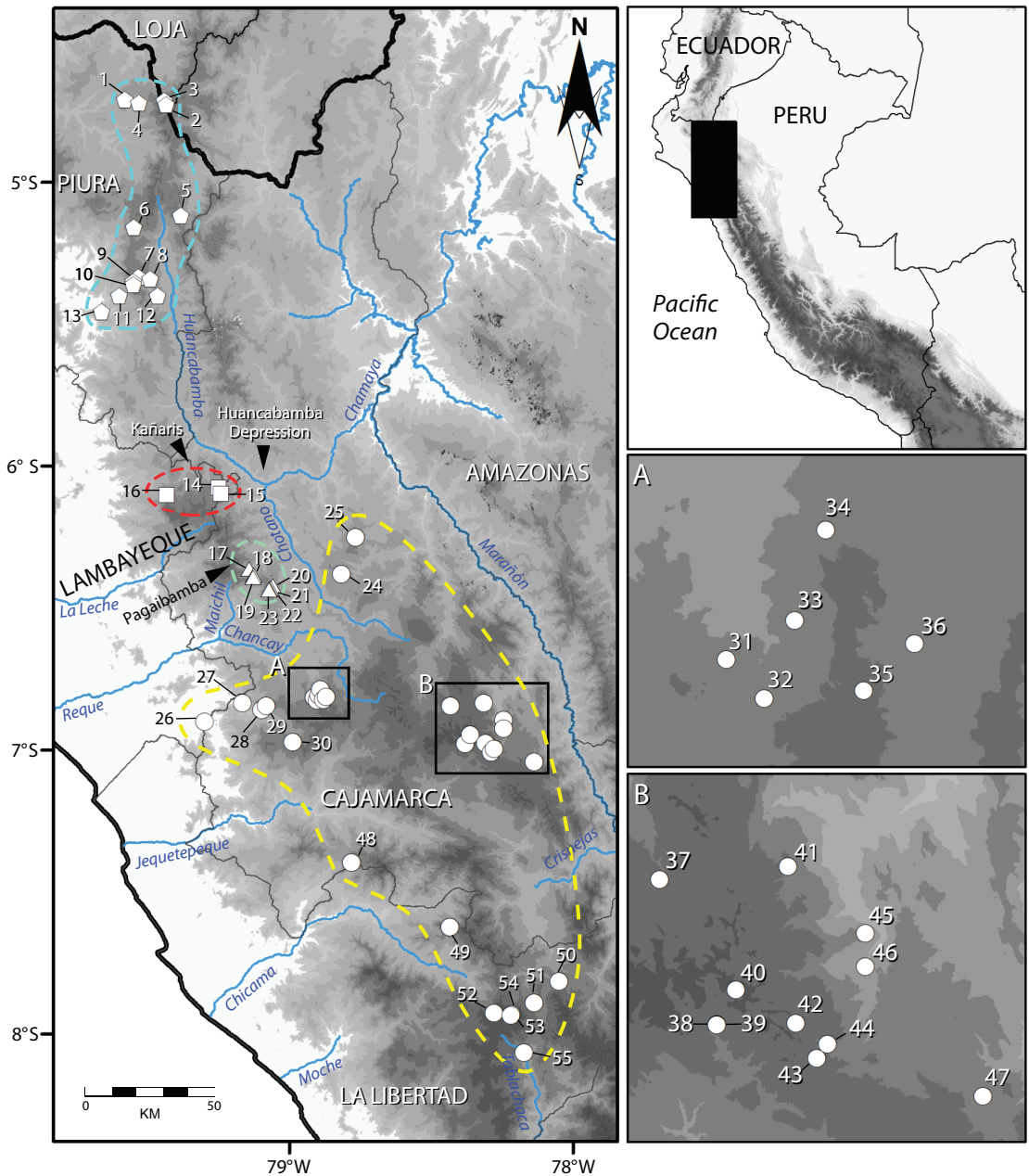


FIGURE 1. Collecting localities for examined specimens of the *Thomasomys cinereus* complex from northern Peru and southern Ecuador: *T. cinereus* sensu stricto (circles), *T. lojapiuranus* (pentagons), *T. pagaibambensis* (triangles), and *T. shallukucha* (squares). Numbers are keyed to gazetteer entries (appendix 1).

SPECIES CONCEPT: We recognize species in accordance with the general lineage species concept (de Queiroz, 2007) considering the morphological (qualitative and quantitative evidence), reciprocal monophyly, large genetic distances (Baker and Bradley, 2006), ecological evidence, and molecular species delimitation.

MORPHOLOGICAL AND MORPHOMETRIC ANALYSES

EXTERNAL AND CRANIODENTAL MEASUREMENTS: Skin measurements (total length, TL; length of tail, LT; hind foot length, HFL) and weight were transcribed from specimen tags. However, we sometimes remeasured the length of hind foot (HFL) on fluid or dry specimens to check the accuracy of values recorded by the collector, and we used our value rather than the collector's value whenever large discrepancies were found. Head-and-body length (HBL) was estimated by subtracting tail length from total length. We use the ratios "Tail%" (= $LT/HBL \times 100$) and "HFL%" (= $HFL/HBL \times 100$) to quantify proportions of the tail and hind foot with respect to head-and-body length for descriptive purposes. All external measurements are reported to the nearest millimeter (mm) and all weights to the nearest gram (g). All cranial and mandibular variables were measured to the nearest 0.01 mm using dial calipers following Tribe (1996), Luna and Pacheco (2002), and Voss (2003). The following variables were measured (fig. 2):

Greatest length of skull (GSL): measured from the tip of the nasals to the posterior margin of occiput
 Condylolincisive length (CIL): distance from the greater curvature of an upper incisor to the articular surface of the occipital condyle on the same side
 Condylomolar length (CML): distance from the anterior edge of the first upper molar to the articular surface of the occipital condyle on the same side

Length of orbital fossa (LOF): greatest distance of the orbital fossa inside the maxillary and squamosal roots of the zygomatic arch.
 Length of nasals (LN): the greatest length of either nasal bone
 Rostral length (RL): the greatest diagonal distance from the zygomatic notch to the tip of the nasal bone on the same side.
 Diastema length (LD): measured from the crown of the first upper molar to the exposed lesser curvature of the upper incisor on the same side
 Length of incisive foramina (LIF): distance from the anterior to the posterior edge of one incisive foramen
 Length of maxillary toothrow (LM): occlusal length of the upper molar row
 Breadth of incisive foramina (BIF): the greatest distance across the incisive foramina
 Breadth of rostrum (BR): the least breadth between the anteroventral edges of the zygomatic plates
 Breadth of palatal bridge (BPB): measured between the protocones of first maxillary molars
 Breadth of first upper molar (BM1): measured across the protocone-paracone cusp pair of the first upper molar
 Breadth of nasals (BN): the greatest distance across both nasal bones
 Least interorbital breadth (LIB): the least interorbital breadth
 Zygomatic breadth (ZB): the greatest distance across the zygomatic arches
 Braincase breadth (BB): measured immediately posterodorsal to the squamosal roots of the zygomatic arches
 Breadth of zygomatic plate (BZP): the distance between the anterior and posterior edges of the zygomatic plate
 Depth of incisor (DI): distance between greater and lesser curvature of the upper incisor
 Height of braincase (HBC): distance from the top of the braincase to the ventral surface of the basisphenoid and basioccipital bones

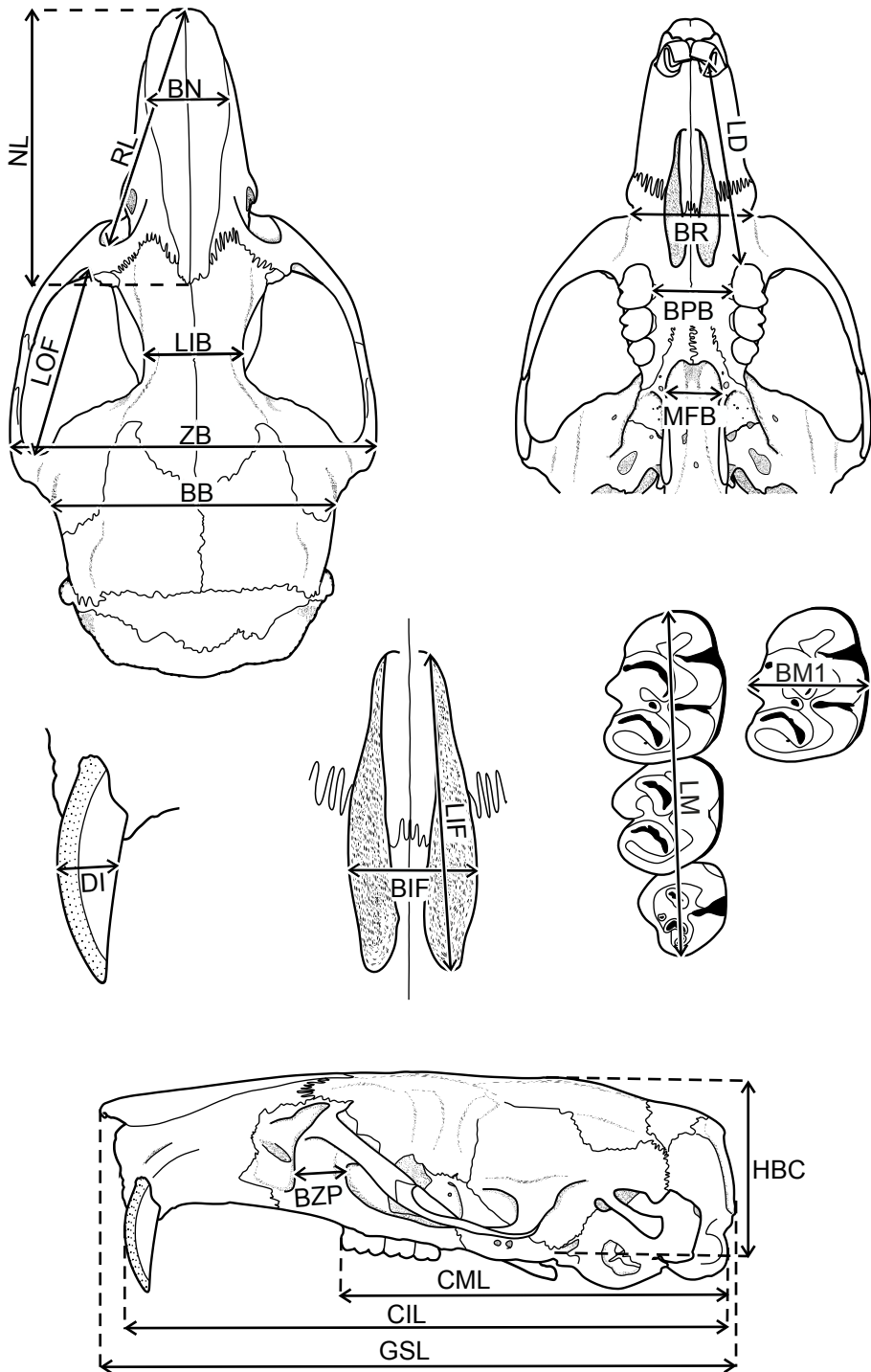


FIGURE 2. Dorsal, ventral, and lateral cranial views of *Thomasomys cinereus*, showing the anatomical limits of craniodental measurements defined in the text.

Mesopterygoid fossa breadth (MFB): greatest internal width across the mesopterygoid fossa

AGE CRITERIA: An estimate of relative age was based on molar toothwear. Five categories are here defined using a modification of the scheme presented by Voss (1991) for *Zygodontomys* and by Carleton and Musser (1989) for *Microroryzomys*:

Age class 0: M3 incompletely erupted

Age class 1: M3 erupted but essentially unworn

Age class 2: M3 little worn (some dentine exposed), paracone tuberculate and prominent, paraflexus distinct. M1–2 primary cusps prominent

Age class 3: M3 worn, occlusal surface flat or concave but hypoflexus still distinct; M1–2 moderately worn, primary cusps well-defined, distinct, but not prominent; flexus distinct

Age class 4: M1–3 worn, occlusal surface essentially flat or concave, hypoflexus obliterated

Hereafter, we consider specimens in age classes 0–1 as “juveniles,” age class 2 as “sub-adult,” and age classes 3 and 4 as “adults.”

MORPHOLOGY: We followed Smithe (1975) for the characterization of fur coloration. Anatomical terminology follows Brown (1971) and Brown and Yalden (1973) for external characters; Reig (1977, 1980) and Carleton and Musser (1989) for dental nomenclature; Voss (1988) for cephalic arteries; Wahlert (1985) for cranial foramina; Howell (1926) for postcranial characters; Sprague (1941) and Carleton (1980) for the hyoid apparatus; Carleton and Musser (1984) and Voss (1988) for general features of murid anatomy; Carleton (1973) for gross stomach morphology; Quay (1954), Carleton (1980), and Pacheco (2003) for transverse palatal rugae; Pacheco (2003, 2015) and Zavodszky and Russo (2020) for chevron bones of the caudal vertebrae; Hooper and Hart (1962), Hooper and Musser (1964), and Myers et al. (1990) for the glans

penis; and Pacheco (2003, 2015) for other anatomical features of thomasmomyines. Descriptions of right upper and right lower molar rows were used. Glandes penes were dissected carefully from the prepuce of fluid-preserved specimens, and some were lightly stained (for 1–3 hours) with 0.3% alizarin. Dissected glands were maintained in 70% ethanol. The presence or absence of preputial glands was also observed macroscopically. Stomachs were dissected following Carleton (1973) and preserved, with the gastric contents, in 70% ethanol; some contents were identified.

MORPHOMETRIC ANALYSES: Standard univariate statistics (mean, range, standard error, coefficient of variation, skewness, and kurtosis) were calculated for each external and craniodental variable for each taxon in the *Thomasomys cinereus* complex (i.e., *T. cinereus* and the three species recognized as new in this report). Multivariate normality was assessed utilizing the results of the Royston’s H test. ANOVAs were calculated to test the null hypothesis of no significant differences in each variable between the sexes. In addition, MANOVA with Wilk’s Lambda and Pillai trace criteria based on the largest available population sample ($N_{\text{females}} = 29$, $N_{\text{males}} = 24$) from Huancabamba, department of Piura, was performed for an overall sex effect, but no significant differences were found ($\lambda = 1.021$, $p > 0.05$). Therefore, the sexes were combined for subsequent morphometric analyses. Then, ANOVA followed by the statistical post hoc analysis Tukey-Kramer test for unbalanced groups was performed for each variable among taxa. Only normally distributed variables were used in ANOVAs.

Multivariate analyses were performed on measurements of adult specimens (age classes 3 and 4) to reduce intraspecific variation due to age (Rengifo and Pacheco, 2015; Pacheco, 2021). The variables RL and MFB (which were measured only on MUSM specimens) and GSL and CML (which were highly correlated with CBL) were not used in the multivariate analyses. We extracted principal components (PCs) from the variance-covariance

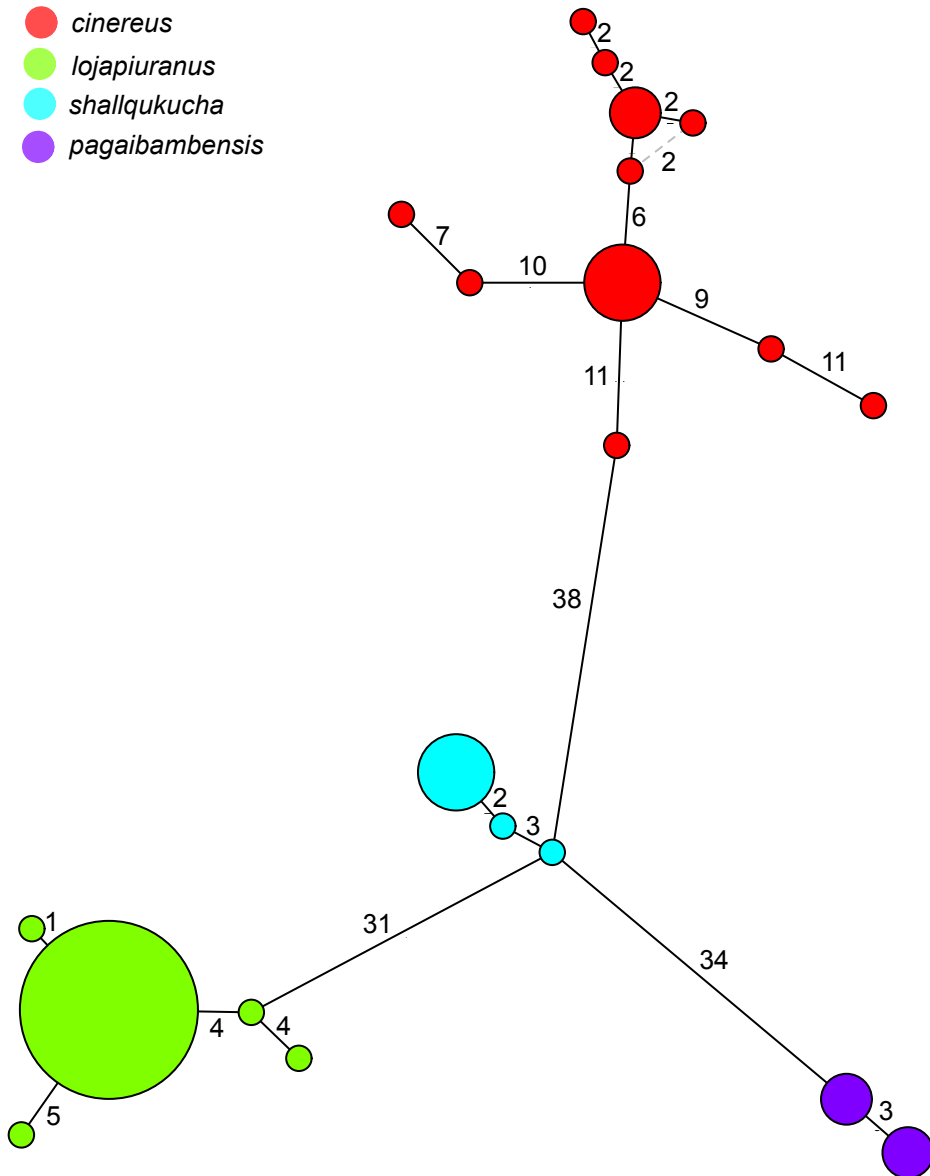


FIGURE 3. Median-joining network of the relationships among haplotypes of the *Thomasomys cinereus* complex from northern Peru and southern Ecuador. Numbers of mutations are shown along the branches.

matrix using \log_{10} -transformed data for the four species in the *Thomasomys cinereus* complex and in pairwise analyses. Specimens scores of the first three components were used to project two-dimensional patterns of variation. Additionally, we performed a discriminant function analysis (DFA) with Jackknife (Lance et al., 2000) to estimate the

percentage of accurate classification. Statistical significance for all analyses was assessed as $p < 0.05$. All analyses were executed in SPSS v 23 and R v 4.1.3 (R Core Team, 2022) with the complementary packages “MVN” (Korkmaz et al., 2014) for the multivariate normality test and “MASS” (Venables and Ripley, 2002) for DFA.

RESULTS

In order to simplify the presentation of our results in the following text, tables, and figures, we anticipate our taxonomic conclusions and use Latin binomina for the allopatric lineages we recognize as full species within *Thomasomys cinereus* sensu lato. The geographic sense in which these names (*T. cinereus* sensu stricto, *T. lojapiuranus*, *T. pagaibambensis*, and *T. shallqukucha*) are applied is illustrated in figure 1. The phrase “intraspecific” as applied below, however, refers to *T. cinereus* sensu lato (i.e., as previously employed by Pacheco, 2015).

INTRASPECIFIC ANALYSES

More than 30 mutational steps separate *Thomasomys cinereus* sensu stricto from the candidate taxa recognized in this study (fig. 3). Additionally, AMOVA recovered a high fixation index ($F_{ST} = 0.89$) among them and between species pairs (*T. cinereus* versus *T. lojapiuranus*, $F_{ST} = 0.88$; *T. cinereus* versus *T. pagaibambensis*, $F_{ST} = 0.87$; *T. cinereus* versus *T. shallqukucha*, $F_{ST} = 0.88$; *T. lojapiuranus* versus *T. pagaibambensis*, $F_{ST} = 0.87$; *T. lojapiuranus* versus *T. shallqukucha*, $F_{ST} = 0.94$; and *T. pagaibambensis* versus *T. shallqukucha*, $F_{ST} = 0.96$). Both lines of evidence suggest the absence of gene flow among these taxa.

PHYLOGENETIC ANALYSES

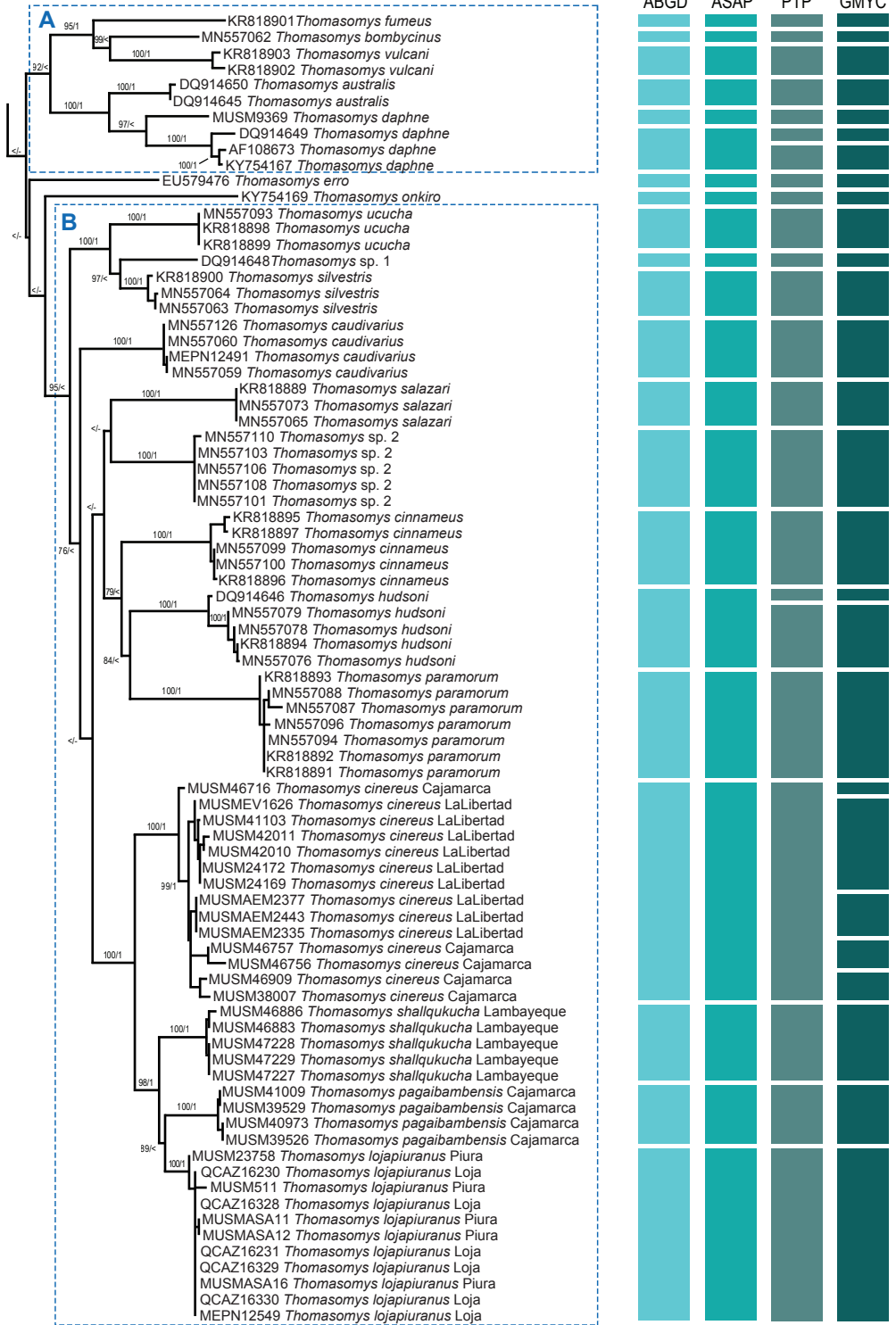
We analyzed fragments (403–801 bp) of the *cytb* gene from 116 specimens, among which 399 sites were invariant, 74 were singletons, and 328 were parsimony informative. Both ML and BI analyses of *cytb* recovered similar topologies (fig. 4). The monophyly of *Thomasomys* was recovered with strong support in both analysis (BS = 99%, BPP = 1.00) (appendix 2). The monophyly of the Cinereus Group was also recovered, but with low or moderate support (BS = 49%, BPP = 0.74). Within the Cinereus Group, two strongly supported clades (labelled A and B in fig. 4) were

recovered, but two members of the Cinereus Group, *T. erro* and *T. onkiro*, were not members of either clade; their relationships remain effectively unresolved by our analyses.

Clade A includes *Thomasomys australis*, *T. daphne*, *T. fumeus*, *T. bombycinus*, and *T. vulcani*. Within this clade, a lineage consisting of *T. australis* and *T. daphne*, and another consisting of *T. fumeus*, *T. bombycinus*, and *T. vulcani* were each recovered with strong support. None of the members of this clade have ever been identified as or associated with *T. cinereus*.

Clade B includes *Thomasomys ucucha*, *T. silvestris*, *T. cinnameus*, *T. caudivarius*, *T. paramorum*, *T. hudsoni*, *T. salazari*, two unnamed forms (*Thomasomys* sp. 1 and *Thomasomys* sp. 2), and four species belonging to a complex that correspond to *T. cinereus* sensu lato (i.e., sensu Pacheco [2015] and Moreno-Cárdenas and Novillo-Gonzalez [2020]): *T. cinereus* sensu stricto, *T. lojapiuranus*, *T. pagaibambensis*, and *T. shallqukucha*. Within clade B, *T. ucucha* is sister to a lineage that includes *T. silvestris* and *T. sp. 1*, whereas *T. cinereus* sensu stricto is sister to a lineage that includes *T. shallqukucha*, *T. lojapiuranus*, and *T. pagaibambensis* (of which the last two are sister species). All other relationships within this clade have only weak to moderate support, but it is noteworthy that the Ecuadorean taxon identified as *T. cinereus* by Lee et al. (2018)—denoted as *T. “sp. 2”* in these results—is not closely associated with the species complex that includes *T. cinereus* sensu stricto.

Observed genetic distances among species of the Cinereus Group of *Thomasomys* (table 2) range from $6.67 \pm 0.92\%$ (between *T. cinereus* and *T. lojapiuranus*) to $16.39 \pm 1.65\%$ (between *T. onkiro* and *T. fumeus*). Within the *T. cinereus* complex, the genetic distances among *T. cinereus* sensu stricto, *T. lojapiuranus*, *T. pagaibambensis*, and *T. shallqukucha* are all in the range of 5.06%–7.65%. By comparison, intragroup divergences in this complex range from $0.22 \pm 0.07\%$ in *T. lojapiuranus* (11 sequences from five localities) to $1.39 \pm 0.2\%$ in *T. cinereus* sensu stricto (14 sequences from eight localities).



The results of the ABGD, ASAP, and PTP species-delimitation analyses all suggest that *Thomasomys cinereus* sensu lato is comprised of four putative species as recognized above, whereas the GMYC analysis inferred eight putative species, of which five correspond to *T. cinereus* sensu stricto (fig. 4). The divergence threshold estimated by the GMYC analysis was 0.210 Mya.

MORPHOMETRIC ANALYSES

Descriptive statistics for adult specimens of *Thomasomys cinereus*, *T. lojapiuranus*, *T. shallqukucha*, and *T. pagaibambensis* are provided in table 3. The variables CML, LN, LD, LIF, LM, BPB, BN, LIB, BZP, DI, and HBC had distributions that did not depart significantly from normality. The results of ANOVAs applied to these variables (appendix 3) showed that *T. cinereus* sensu stricto and *T. lojapiuranus* differ significantly in LD, LIF, LM, and DI; that *T. cinereus* and *T. shallqukucha* differ significantly in CML, LD, LIF, and LIB; that *T. cinereus* and *T. pagaibambensis* differ significantly in all variables except LN, LM, BN, and BZP; that *T. lojapiuranus* and *T. pagaibambensis* differ significantly in all variables except LD and BZP; that *T. lojapiuranus* and *T. shallqukucha* differ significantly only in CML and LIB; and that *T. pagaibambensis* and *T. shallqukucha* differ significantly only in BPB, BN, and HBC.

Factor loadings and percentages of variation of the first three principal components (PC1–PC3) for the analysis with the *Thomasomys cinereus* complex are presented in appendix 4, where the first principal component has uniformly positive coefficient values, indicating that this axis is predominantly related to variation in skull size (and size-correlated proportions). Plots

of PC1 versus PC2 (fig. 5A) exhibit broad overlap among *Thomasomys cinereus* sensu stricto, *T. lojapiuranus*, *T. shallqukucha*, and *T. pagaibambensis*; but plots of PC2 versus PC3 (fig. 5B) are less overlapped. These three axes account for 56.31% of the total variance (PC1: 31.75%, PC2: 12.79%, PC3: 11.77%). By contrast, discriminant function analysis provided an almost complete separation by group (fig. 5C), with each group identified by a candidate taxon. DF1 explained 52.48% of the variance, and the most important variables were CML and LOF; DF2 explained 41.53% with LM and BB as the most important variables, and DF3 explained 5.98% with ZB and BM1 as the most important variables (appendix 4). Overall, 86.4% of the specimens were accurately classified by Jackknife. By species, 90.91% of *T. cinereus* sensu stricto, 87.18% of *T. lojapiuranus*, 95% of *T. pagaibambensis*, and 60% of *T. shallqukucha* were accurately classified. Additionally, plots of PC1 versus PC2 of *Thomasomys cinereus* sensu stricto versus *T. lojapiuranus* (appendix 5A), *T. cinereus* versus *T. pagaibambensis* (appendix 5B), and *T. cinereus* versus *T. shallqukucha* (appendix 5C) showed these taxa partially overlapped. Plots of PC1 and PC2 for *T. lojapiuranus* versus *T. pagaibambensis* (appendix 5D) and *T. lojapiuranus* versus *T. shallqukucha* (appendix 5E) showed these taxa also partially overlapped. Finally, the plot of PC1 and PC2 for *T. pagaibambensis* versus *T. shallqukucha* showed these taxa overlapped (appendix 5F).

TAXONOMIC ACCOUNTS

Our molecular analyses revealed that *Thomasomys cinereus* sensu lato comprises four genetically differentiated populations that represent reciprocally monophyletic lineages, and our morphometric analyses suggest mod-

FIGURE 4. Phylogenetic tree (minus outgroup taxa) based on *cytb* sequences of the Cinereus Group reconstructed by Bayesian analysis. Branch labels indicate maximum likelihood bootstrap values (BS) and Bayesian posterior probabilities (PP); a less-than sign (<) indicates that support is <75% of BS or <0.95 of PP; and a dash (–) indicates that the clade was not recovered. Colored columns indicate the results of species delimitation analyses: ABGD (21 spp.), ASAP (21 spp.), PTP (23 spp.), and GMYC (27 spp.).

TABLE 2
 Corrected average pairwise genetic distances using the Kimura 2-parameter model (below diagonal) and standard errors (above diagonal) among species of the Cineret Group of *Thomasonys*
 Diagonal values (in parentheses) are average intraspecific distances.

Species	1	2	3	4	5	6	7	8	9	10	11	12	13	14	15	16	17	18	19	20
1. <i>australis</i>	(0.39)	1.31	1.25	1.43	1.46	0.94	1.33	1.37	1.44	1.45	1.53	1.52	1.5	1.42	1.47	1.35	1.49	1.41	1.63	1.5
2. <i>bombycinus</i>	11.32	—	1.31	1.32	1.29	1.3	1.38	1.29	1.36	1.28	1.57	1.46	1.43	1.47	1.33	1.36	1.22	1.21	1.57	1.39
3. <i>caudivarius</i>	10.82	11.36	(0.15)	1.25	1.15	1.2	1.25	1.39	1.22	1.13	1.35	1.33	1.23	1.16	1.26	1.17	1.16	1.3	1.43	1.17
4. <i>cineret</i>	13.02	12.25	10.81	(1.39)	1.22	1.29	1.23	1.4	1.15	0.92	1.39	0.95	1.2	1.31	0.98	1.13	1.14	1.35	1.32	1.2
5. <i>cinnamens</i>	13.4	11.67	9.29	10.43	(0.82)	1.33	1.47	1.51	1.18	1.18	1.42	1.36	1.33	1.35	1.34	1.16	1.13	1.42	1.4	1.23
6. <i>daphne</i>	8.12	12.95	12.16	13.76	13.43	(4.11)	1.24	1.36	1.29	1.32	1.38	1.36	1.43	1.38	1.39	1.25	1.33	1.29	1.5	1.37
7. <i>erro</i>	11.37	12.44	10.96	10.9	13.66	12.41	—	1.47	1.28	1.36	1.37	1.41	1.52	1.41	1.41	1.28	1.32	1.52	1.46	1.33
8. <i>fumeus</i>	11.57	10.85	12.15	12.66	13.77	13.01	13.28	—	1.42	1.46	1.65	1.55	1.48	1.41	1.49	1.45	1.42	1.29	1.7	1.49
9. <i>hudsoni</i>	13.81	13.7	10.53	10.04	10.25	13.71	12.03	13.08	(0.81)	1.07	1.4	1.23	1.31	1.23	1.2	1.21	1.29	1.32	1.46	1.23
10. <i>lojapiuranus</i>	13.86	11.57	8.65	6.67	9.7	13.88	12.59	13.57	8.32	(0.22)	1.43	0.78	1.17	1.18	0.82	1.23	1.17	1.25	1.47	1.13
11. <i>onkiro</i>	14.52	14.84	12.16	13.43	12.95	13.92	12.75	16.39	13.28	13.06	—	1.38	1.63	1.48	1.45	1.27	1.36	1.57	1.64	1.41
12. <i>pagaibambensis</i>	13.99	13.2	11.54	6.85	11.89	14.13	12.53	14.21	10.56	5.06	12.81	(0.25)	1.34	1.28	0.9	1.24	1.26	1.35	1.51	1.29
13. <i>paramorum</i>	14	12.89	10.08	10.67	11.56	15.19	13.8	13.66	11.63	9.77	15.64	12.34	(0.67)	1.34	1.28	1.38	1.29	1.37	1.73	1.3
14. <i>salazari</i>	13.41	12.64	8.98	11.44	11.5	15	13.15	12.06	10.33	9.1	13.97	10.65	11.76	(0.17)	1.16	1.32	1.23	1.49	1.51	1.31
15. <i>shallukucha</i>	13.61	11.7	10.02	7.65	11.51	14.6	12.07	13.61	10.17	5.09	13.44	6.27	10.95	9.14	(0.39)	1.31	1.22	1.37	1.53	1.3
16. <i>silvestris</i>	11.23	11.84	9.01	9.12	9.01	11.84	10.68	12.78	10.51	9.67	10.69	10.01	11.4	11.23	10.17	(0.52)	0.95	1.43	1.09	1.22
17. <i>ucucha</i>	12.57	10.44	9.23	9.48	9.05	12.32	11.39	12.77	11.66	9.16	11.21	10.02	11.13	9.9	9.51	6.69	—	1.41	1.21	1.26
18. <i>vulcani</i>	13.2	9.76	11.15	11.89	12.88	12.3	13.94	10.88	11.95	10.3	14.69	12.13	12.32	13.36	11.85	13.05	12.24	(1.18)	1.64	1.39
19. sp. 1	14.05	13.38	11.23	10.74	11.27	14.12	12.53	13.98	12.59	12.08	14.22	12.31	14.39	12.36	12.89	6.49	8.47	13.79	—	1.63
20. sp. 2 ¹	13.49	11.73	8.96	9.32	9.25	13.7	11.77	13.84	9.88	8.48	12.46	9.83	10.67	10.28	10.12	9.4	10.52	11.86	13.16	(0.16)

¹ *Thomasonys cinereus* sensu Lee et al. (2018), not *T. cinereus* as recognized in this report.

TABLE 3

**External and craniodental measurements (mm) and weights (g) for members of the
Thomasomys cinereus complex**

Table entries include the sample mean, standard deviation, observed range (in parentheses), and sample size. GSL and CML (marked with an asterisk) were not used in multivariate analyses to reduce the number of highly correlated variables.

	<i>T. cinereus</i>	<i>T. lojapiuranus</i>	<i>T. shallqukucha</i>	<i>T. pagaibambensis</i>
LT	135 ± 9 (121–161) 45	151 ± 7 (136–165) 41	157 ± 8 (145–171) 12	164 ± 8 (142–181) 46
HBL	132 ± 8 (114–148) 46	130 ± 8 (107–146) 41	132 ± 7 (116–142) 12	135 ± 8 (121–158) 46
Tail%	103 ± 8 (90–120) 45	117 ± 11 (96–145) 41	119 ± 6 (110–128) 12	122 ± 8 (110–139) 46
HFL	30 ± 1 (27–33) 45	30 ± 1 (28–32) 48	31 ± 1 (30–33) 12	31 ± 1 (28–34) 46
HFL%	22.72 ± 1.69 (19.42–27.12) 44	23.43 ± 1.77 (19.20–28.97) 42	23.48 ± 1.15 (22.06–25.86) 12	23.35 ± 1.44 (20.57–26.98) 46
EL	20 ± 1 (17–22) 37	22 ± 2 (18–26) 49	21 ± 2 (19–26) 12	21 ± 1 (20–24) 46
Wt	60.17 ± 10.42 (38–86) 44	58.84 ± 7.39 (44–75) 28	59.95 ± 7.33 (40.40–70) 12	62.98 ± 6.96 (48–78) 45
GSL*	32.66 ± 0.87 (31.30–36.52) 39	33.28 ± 0.75 (31.85–35.05) 49	33.83 ± 0.69 (32.87–34.76) 12	33.85 ± 0.84 (32.14–35.86) 39
CIL	30.26 ± 0.96 (28.55–34.45) 42	30.61 ± 0.69 (29.25–32.25) 53	31.29 ± 0.56 (30.41–32.47) 12	31.44 ± 0.69 (29.83–33.34) 41
CML*	19.75 ± 0.58 (18.57–21.94) 42	19.75 ± 0.46 (18.70–20.60) 53	20.16 ± 0.36 (19.49–20.75) 12	20.32 ± 0.44 (19.24–21.70) 41
LOF	11.01 ± 0.35 (10.36–11.79) 48	10.85 ± 0.22 (10.35–11.30) 53	10.86 ± 0.30 (10.22–11.31) 12	10.95 ± 0.34 (10.24–11.71) 45
LN	12.74 ± 0.67 (11.39–14.69) 46	12.56 ± 0.54 (11.22–13.70) 52	12.96 ± 0.42 (12.33–13.58) 12	13.18 ± 0.54 (11.95–14.62) 45
RL	11.33 ± 0.52 (10.36–13.24) 31	11.29 ± 0.37 (10.71–11.74) 7	12.09 ± 0.39 (11.32–12.65) 12	12.04 ± 0.49 (10.95–13.07) 43
LD	8.91 ± 0.38 (8.32–10.76) 51	9.22 ± 0.30 (8.55–10.00) 53	9.51 ± 0.25 (9.20–10.14) 12	9.40 ± 0.40 (8.52–10.14) 45
LIF	6.86 ± 0.34 (6.27–7.83) 51	6.43 ± 0.26 (5.70–7.05) 49	6.56 ± 0.18 (6.35–6.85) 12	6.64 ± 0.24 (6.19–7.19) 45
LM	5.34 ± 0.17 (5.00–5.74) 51	5.15 ± 0.16 (4.80–5.50) 53	5.23 ± 0.11 (5.05–5.41) 12	5.37 ± 0.16 (5.00–5.75) 45
BIF	2.47 ± 2.20 (2.10–3.00) 50	2.35 ± 0.12 (2.10–2.67) 51	2.37 ± 0.10 (2.22–2.54) 12	2.36 ± 0.11 (2.12–2.61) 45
BR	5.55 ± 0.28 (4.90–6.28) 50	5.35 ± 0.18 (4.85–5.70) 53	5.38 ± 0.20 (5.05–5.59) 12	5.41 ± 0.20 (4.90–5.86) 45
BPB	3.58 ± 0.21 (3.10–4.30) 51	3.52 ± 0.16 (3.15–3.85) 52	3.54 ± 0.20 (3.21–3.75) 12	3.74 ± 0.18 (3.37–4.08) 45
BM1	1.68 ± 0.08 (1.49–1.88) 51	1.69 ± 0.06 (1.58–1.85) 53	1.75 ± 0.10 (1.59–1.95) 12	1.69 ± 0.06 (1.57–1.85) 45
BN	4.13 ± 0.29 (3.39–4.87) 47	4.28 ± 0.22 (3.85–4.75) 52	4.34 ± 2.20 (3.98–4.69) 12	4.14 ± 0.26 (3.63–4.80) 45
LIB	4.97 ± 0.18 (4.65–5.38) 50	5.07 ± 0.13 (4.75–5.30) 53	5.27 ± 0.17 (5.05–5.53) 12	5.37 ± 0.18 (5.00–5.84) 45
ZB	17.48 ± 0.59 (16.32–19.82) 46	17.39 ± 0.39 (16.60–18.50) 48	17.45 ± 0.48 (16.63–18.42) 12	18.08 ± 0.41 (17.09–18.84) 44
BB	14.13 ± 0.45 (13.15–15.10) 42	14.26 ± 0.39 (13.45–15.00) 53	14.11 ± 0.25 (13.59–14.40) 11	14.00 ± 0.35 (12.95–14.50) 41
BZP	2.67 ± 0.18 (2.26–3.19) 51	2.63 ± 0.17 (2.30–3.05) 53	2.74 ± 0.17 (2.47–3.06) 12	2.66 ± 0.13 (2.37–2.93) 45
DI	1.68 ± 0.10 (1.46–1.95) 51	1.71 ± 0.07 (1.55–1.90) 53	1.72 ± 0.05 (1.65–1.81) 12	1.76 ± 0.07 (1.61–1.90) 45
HBC	9.30 ± 0.24 (8.65–9.74) 41	9.23 ± 0.27 (8.35–9.80) 50	9.33 ± 0.25 (8.96–9.68) 12	9.57 ± 0.26 (9.06–10.32) 41
MFB	2.21 ± 0.29 (1.72–3.03) 32	2.58 ± 0.20 (1.72–3.03) 32	2.50 ± 0.14 (2.27–2.76) 12	2.58 ± 0.19 (2.18–3.05) 43

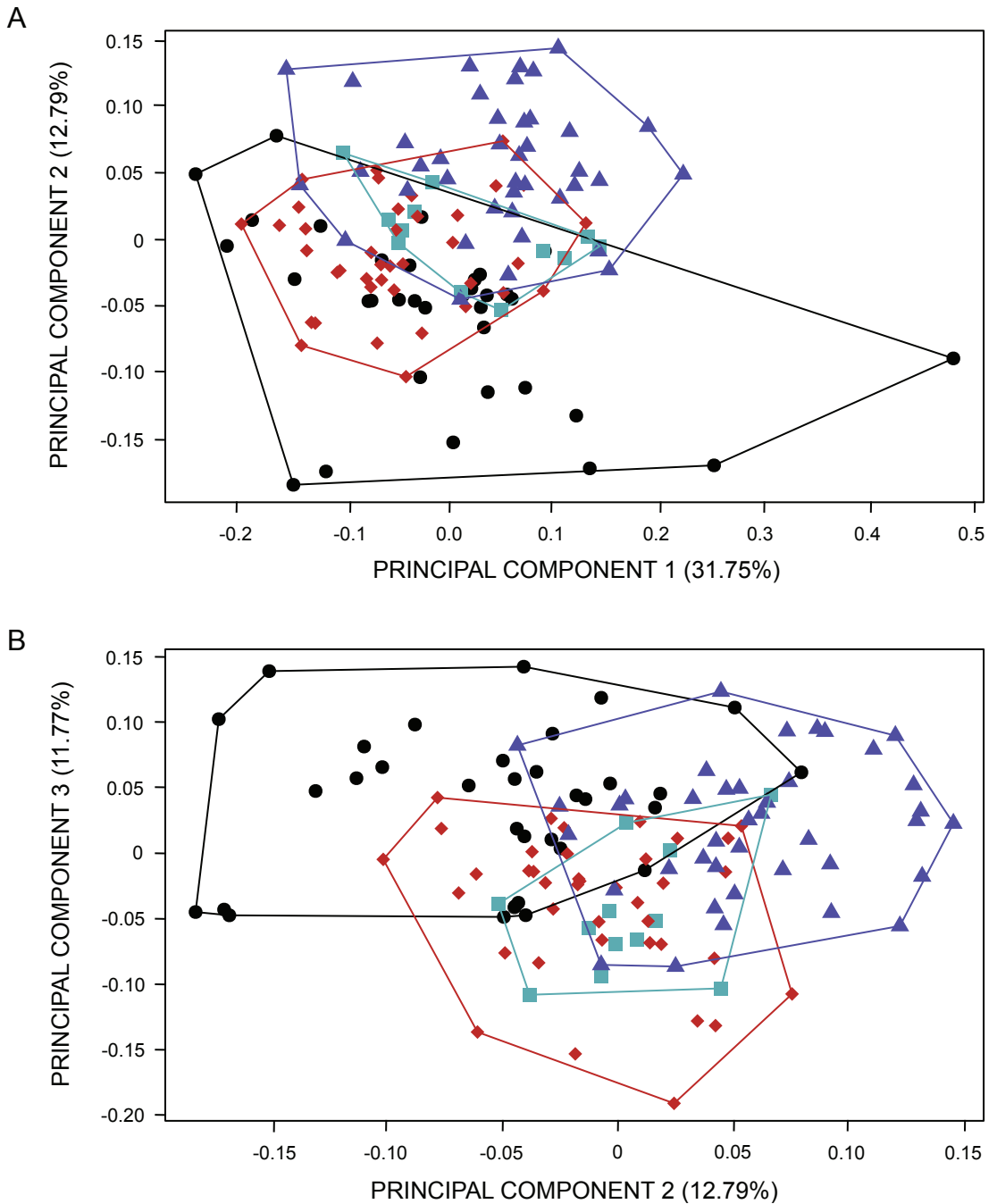
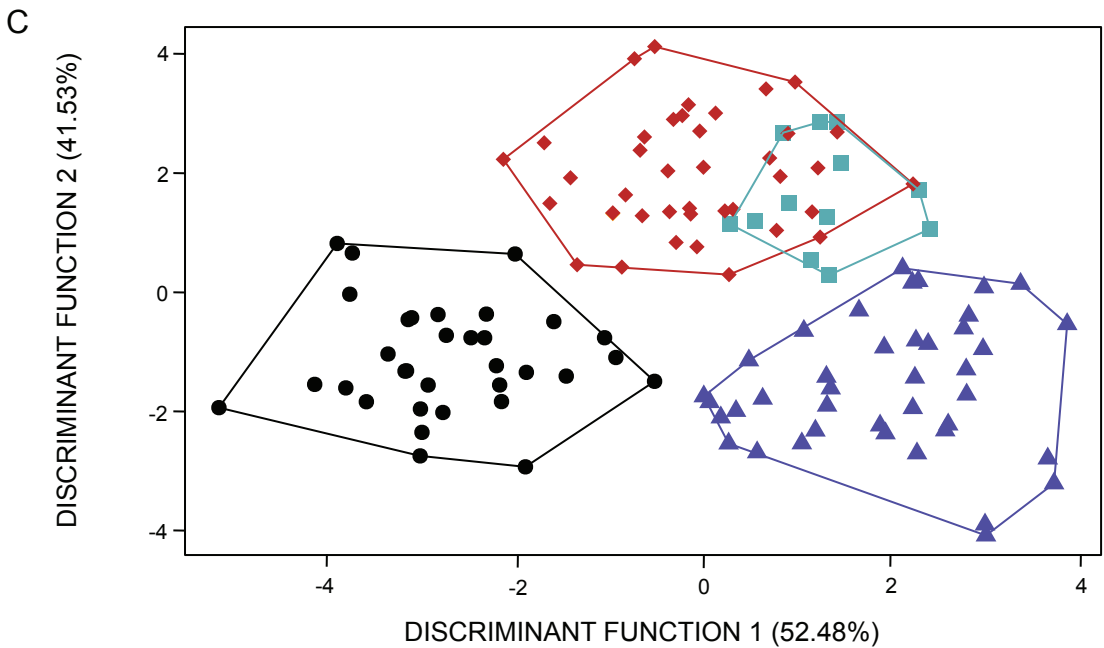


FIGURE 5. Results of principal components analyses and discriminant function analysis using craniodental measurement data of *Thomasomys cinereus* sensu stricto (circles), *T. lojapiuranus* (diamonds), *T. pagaibambensis* (triangles), and *T. shallqukucha* (squares). Plots of the first two principal components (A), second and third principal components (B), and the first two discriminant functions (C, opposite page). Percentage of variance is shown into parenthesis.



est phenotypic divergence in craniodental size and proportions. Additionally, side-by-side visual comparisons of specimens indicate that these lineages can be diagnosed by differences in multiple external, skeletal, and soft-anatomical characters (table 4). We hypothesize that they are distinct species that should be recognized as follows.

Thomasomys cinereus (Thomas, 1882)

Olive-gray *Thomasomys*

Figures 6A, 7, 8, 9, 10A, 11A, 11E, 12A, 13A, 14, 15A, 16A, 17A, 18A, 19A, 19E, 20A, 21, 22A

H[esperomys]. (*Rhipidomys*) *cinereus* Thomas, 1882: 108; type locality “Cutervo, 9,200 feet [2,804 m]” Cajamarca, Peru.

Hesperomys (*Vesperimus*) *cinereus*: Thomas, 1884: 449; name combination.

Hesperomys (*Thomasomys*) *cinereus*: Coues, 1884: 1275; name combination.

Peromyscus (*Thomasomys*) *cinereus*: Trouessart, 1898: 512; name combination.

Thomasomys cinereus: Thomas, 1906: 443; first use of current name combination.

TYPE: A subadult (age 2) female specimen (BMNH 81.9.7.29) collected at Cutervo, Chota [Cutervo] Province, department of Cajamarca, Peru; 9200 ft (2804 m), in February or March 1879 by the well-known Polish collector Jan Stanislaw Stolzmann. The specimen is preserved in alcohol with skull removed. Thomas’s description was based on a single uncataloged specimen that Gyldenstolpe (1932) later identified as BMNH 81.9.7.29 (the holotype by monotypy).

EMENDED DIAGNOSIS: A medium-sized species (table 3) of *Thomasomys* distinguished from congeneric taxa by the following combination of characters: pelage long and soft, above ashy gray with hair tips brownish; mystacial vibrissae short, extending barely beyond posterior margin of pinnae; metatarsals whitish; tail equal to or less than head-and-body length, moderately bicolored (paler ventrally than dorsally), without a white tip and without a terminal pencil; thenar and hypothenar pads closely approximated; nasals long, expanded anteriorly, tapering poste-

TABLE 4

Selected morphological comparisons among *Thomasomys cinereus* sensu stricto, *T. lojapiuranus*, *T. shallqukucha*, and *T. pagaibambensis*

Mystacial vibrissae are "short" when they barely extend behind the posterior margins of pinnae or "long" if they extend conspicuously behind the pinnae. Incisive foramina are "long" when they extend to or between the first molar crowns or "short" if they do not extend to or between the first molars. Capsular process is of the lower incisor alveolus.

	<i>T. cinereus</i>	<i>T. lojapiuranus</i>	<i>T. shallqukucha</i>	<i>T. pagaibambensis</i>
Mystacial vibrissae	short	long	short	long
Metatarsal pelage	whitish	pale brownish	pale brownish	pale brownish
Tail length (LT)	≤HBL	>HBL	>HBL	>HBL
Tail color	indistinctly bicolored, tip not white	unicolored, tip not white	unicolored, tip not white	unicolored, tip usually white
Plantar skin of hind foot	pale	pale	dark	slightly dark
Thenar and hypothenar pads of hind foot	closely approximated	widely separated	widely separated	widely separated
Zygomatic notch	deep (55%) or shallow	shallow	very shallow	shallow
Interparietal	moderately long anteroposteriorly	moderately long anteroposteriorly	long anteroposteriorly	long anteroposteriorly
Zygomatic plate	vertical	slope backward	sloped backward	vertical
Zygomatic processes of maxilla and squamosal	closely approximated	usually closely approximated	closely approximated	distinct space between both processes
Incisive foramina	long	long	short	short
Median palatal process	usually present	usually present	absent	absent or indistinct
Bullae	small, not inflated	moderately inflated	moderately inflated	moderately inflated
Stapedial process of bulla	distinct	reduced	reduced	reduced
Eustachian tube	short and narrow	short and broad	short and narrow	short and narrow
Orbicular apophysis	knob-shaped	elongated without basal constriction	elongated with basal constriction on anterior margin	elongated with basal constriction and recurved
Capsular process	absent	absent	absent	distinctly swollen
M1 anteromedian flexus	distinct	weak	distinct	distinct
M3 hypoflexus	conspicuous	reduced	conspicuous	reduced
m1 anteromedian flexid	distinct	weak	distinct	distinct

riorly to lacrimals, and extending slightly behind premaxillae; zygomatic notch relatively deep; interorbital region narrow; zygomatic plate moderately broad, anterior edge vertical; incisive foramina long, extending posteriorly to or between first molars; posterior margin of palatal bridge usually with a median process; mesop-

terygoid fossa usually narrow with subparallel sides; Eustachian tube short and narrow; stapedial process of bulla conspicuous; capsular process of lower incisor alveolus absent; upper incisors orthodont; M1 anteromedian flexus distinct; M3 hypoflexus conspicuous; and m1 anteromedian flexid distinct.

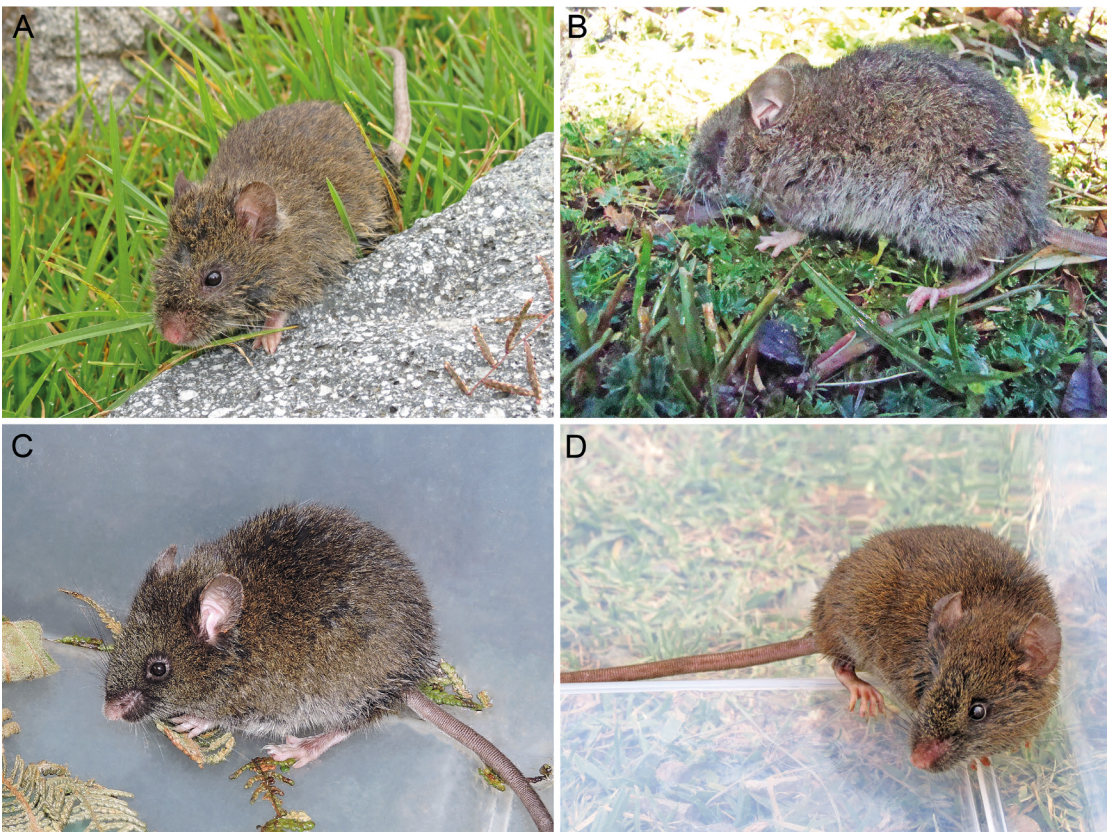


FIGURE 6. Living specimens of *Thomasomys*. **A**, *T. cinereus* (subsequently released) from La Libertad, El Fundo, Río Chuyuhual. **B**, *T. lojapiuranus* (MEPN 12549) from southern Loja, Ecuador. **C**, *T. shallqukucha* (MUSM 46882) from Lambayeque, Kañaris, Geomarca. **D**, *T. pagaibambensis* (MUSM 40358) from Cajamarca, La Granja, Quebrada Agua de la Montaña. Photos taken by Víctor Pacheco, except *T. lojapiuranus* that was taken by Pablo Moreno.

MORPHOLOGICAL DESCRIPTION: Medium sized *Thomasomys* (HBL = 114–148 mm) with long, soft, and dense dorsal fur (individual hairs about 13–14 mm). Dorsal coloration is grizzled ashy gray to dark gray with hairs being slate colored at the base (Blackish Neutral Gray, color 82) and white at tips, sprinkled with longer and brownish hairs (Vandyke Brown, color 221) or Raw Umber (color 123). Ventral pelage is pale yellowish (Pale Horn Color, color 92) or pale gray (Pale Neutral Gray, color 86), hairs are also slate colored at the base, and moderately countershaded with dorsal pelage (figs. 8, 9). The ears are short (EL = 17–22 mm) and pale. Postauricular patches of cream-colored fur are con-

spicuous. The mystacial and supraorbital vibrissae are short, extending barely behind the posterior margin of the pinnae when laid back alongside the head. The genal vibrissae are absent. Females have three pairs of mammae in thoracic, abdominal, and inguinal position (sensu Pacheco, 2003). The tail is comparatively thick, moderately bicolored, and without a conspicuous white tip. The tail is, on average, about as long as the combined length of the head and body (Tail% = 103). The manus is whitish with digit II larger than digit V. The hind feet are moderately long (27–33 mm) and narrow, with metatarsals covered by pure white shining hairs that extend to the digits. The pedal digits (dII–



FIGURE 7. Dorsal, ventral, and lateral views of the cranium and mandible of *Thomasomys cinereus* (MUSM 46716), an adult female from Parque Nacional Cutervo, 100 m over Tragadero, San Andres district, Cutervo province, Cajamarca department, Peru. Scale bar = 10 mm.

dV) exhibit long and dense unguis tufts that cover the claws. The plantar surface of the hind foot is pale (unpigmented), and the thenar and hypothenar pads are not widely separated (fig. 10A). Digit I of the hind foot (hallux) is moderately long, its claw extending close to or to the first interphalangeal joint of dII. Digit V of hind

foot is long, with the claw extending about half the length of phalanx 2 of dIV.

Cranium: The skull is moderately large (CIL = 28.55–34.45 mm) with a flat or barely convex profile, without a bump on the frontal region. The rostrum is relatively long and moderately broad (fig. 11A). A rostral tube is absent, and the



FIGURE 8. Dorsal pelage of species of *Thomasomys* from northern Peru and southern Ecuador. From left to right: *T. cinereus* (MUSM 46716), *T. lojapiuranus* (MUSM 23758), *T. shallqukucha* (MUSM 47230), and *T. pagaibambensis* (MUSM 40973).

gnathic process is small (figs. 12A, 15A). The nasals are long and tapering; the posterior margins are narrow, extending posteriorly to the lacrimals and beyond the premaxillae. The zygomatic notches are usually comparatively deep (55%) or shallow (fig. 13A). The lacrimals are small without a posterior process. The inter-

orbital region is narrow and hourglass shaped with rounded margins, and the frontal sinuses are not inflated. The braincase is broad and squarish. The lateral parietal processes are moderately large and subtriangular. The interparietal is wide and moderately long anteroposteriorly, straplike in some specimens, but rhomboidal in



FIGURE 10. Left feet of adult specimens of *Thomasomys* species treated in this report: **A**, *T. cinereus* (MUSM 38493); **B**, *T. lojapiuranus* (MUSM 23758); **C**, *T. shallqukucha* (MUSM 46882); **D**, *T. pagaibambensis* (MUSM 40965). Abbreviations: **t**, thenar; **h**, hypothenar.

The carotid circulatory pattern is pattern 1 (sensu Voss, 1988): a stapedial foramen, a groove on the inner surface of the squamosal and the alisphenoid, and a sphenofrontal foramen are all present. In the medial wall of the orbit, the ethmoid foramen is placed dorsal to M2; the ethmoturbinals are moderate in size; the sphenopalatine foramen is bordered by the maxillary, ethmoid, and palatine bones; and the optic foramen is moderate in size and slightly posterior to M3. The paraoccipital process is small, slightly curved, and not bifurcated. The incisive foramina are long, and extend posteriorly to, or usually (in 73% of examined specimens) slightly between, the anterior margins of the first molars; the maxillary septum is long but less than half the incisive foramina length (fig. 17A). The palate is short and wide (sensu Hershkovitz, 1962). The mesopterygoid fossa is narrow (in 76% of examined specimens) with subparallel sides; a median posterior process of the palate is present in 75%

of examined specimens. The sphenopalatine vacuities are usually represented by narrow slits along the basisphenoid and presphenoid bones. The parapterygoid fossa is triangular, shallow, and usually (in 80% of examined specimens) without vacuities. The foramen ovale is moderate in size, the alisphenoid strut is present, and the middle lacerate foramen is narrow but conspicuous. The auditory bullae are small, flask shaped, and not inflated; the Eustachian tube is short and narrow, with two spines that usually do not reach the alisphenoid; the stapedial process of the bulla is conspicuous. The internal carotid canal is bounded by the basioccipital and the ectotympanic (auditory bulla), but not by the periotic. The basioccipital is moderately broad, and the mastoid (the occipital exposure of the periotic) is either imperforate or has only a small fenestra. The lamina of the malleus is squarish and not deep, and the orbicular apophysis is short and knob shaped due to a conspicuous basal con-

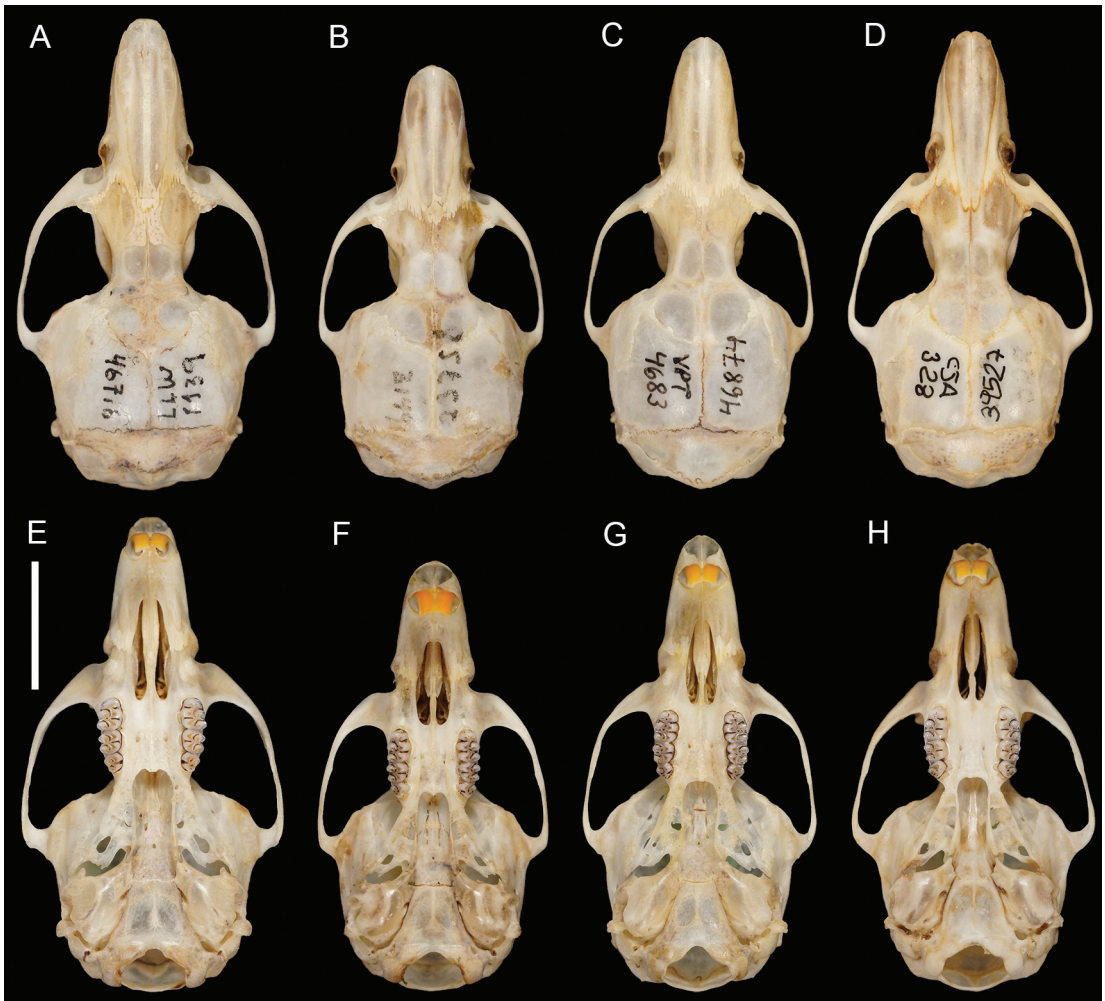


FIGURE 11. Dorsal and ventral views of adult crania of *Thomasomys* species treated in this report: A, E, *T. cinereus* (MUSM 46716); B, F, *T. lojapiuranus* (MUSM 23758); C, G, *T. shallqukucha* (MUSM 46874); D, H, *T. pagaibambensis* (MUSM 39527). Scale bar = 10 mm.

striction (fig. 18A). The processus brevis of the incus is long, narrow, and delicate.

Teeth: The upper incisors are orthodont with orange enamel on their anterior surfaces. The upper molar rows are moderately long (5.00–5.74 mm) and parallel. The upper molars are brachyodont and pentalophodont (sensu Hershkovitz, 1962) without interpenetration of the labial and lingual flexi; labial and lingual cingula are not developed; and accessory labial roots are absent. The procingulum of the first upper molar (M1) is slightly narrower than the protocone-paracone

cuspid pair, and the anteromedian flexus conspicuously divides a slightly smaller anterolingual conule from a larger anterolabial conule. The anteroloph is conspicuous and the paraflexus is recurved to deeply recurved. The paraloph is oriented transversally to the median mure and, in some cases, to the base of the mesoloph. The mesoloph is well developed, reaching the labial margin of the tooth, and it is often fused to the metacone producing a closed metaflexus that is curved or sometimes angular. The posteroloph is usually coalesced with the metacone or persists as

a minute structure in a few specimens. M2 exhibits a strong anteroloph with a recurved paraflexus; the mesoloph is narrow and usually complete, the metaflexus is “comma-shaped,” and the posteroloph is coalesced with the metacone. M3 is much smaller than M2; its paraflexus, mesoflexus, and hypoflexus are conspicuous; and its metacone is obsolete (fig. 19A).

On the lower molars, the main cuspids are conspicuous and slightly alternating. The first lower molar (m1) has a distinct anteromedian flexid; the protolophid is short; the anterolophid is short or obsolete; the anterolabial and anterolingual cingula are poorly developed; the mesoflexid is broad and recurved; the entoflexid is small or coalesced; the posteroflexid is broad and almost straight; the hypoflexid is broad and oriented perpendicularly; and the mesolophid is narrow but complete. On m2, the mesolophid is short or coalesced with the entoconid, and the anterolabial cingulum is small. The m3 has a subtriangular occlusal shape produced by the less-developed entoconid; the mesoflexid and hypoflexid are conspicuous; and the posteroflexid is reduced or coalesced (fig. 19E).

Mandible: The coronoid process of the mandible is narrow, long, falciform, and taller than the condylar process, and produces a deep sigmoid notch. The angular process is short and anterior to the condylar process. The capsular process of the lower incisor alveolus is absent or indistinct. Superior and inferior masseteric ridges are posterior to the anterior margin of m1. The mental foramen is below the diastemal border on the lateral surface of the mandible (fig. 7).

Hyoid apparatus: The basihyal has a slightly convex anterior border, and the posterior border is concave; an entoglossal process is absent. The thyrohyal is shorter than the basihyal, and it is arched laterally. The ceratohyal is much smaller and more slender than the thyrohyal (observation made in five specimens).

Penis: Four fluid-preserved male specimens (MUSM 38005, 38006, 38493, 38497) were examined. The glans is medium sized and subcylindrical, with the dorsum convex and the venter

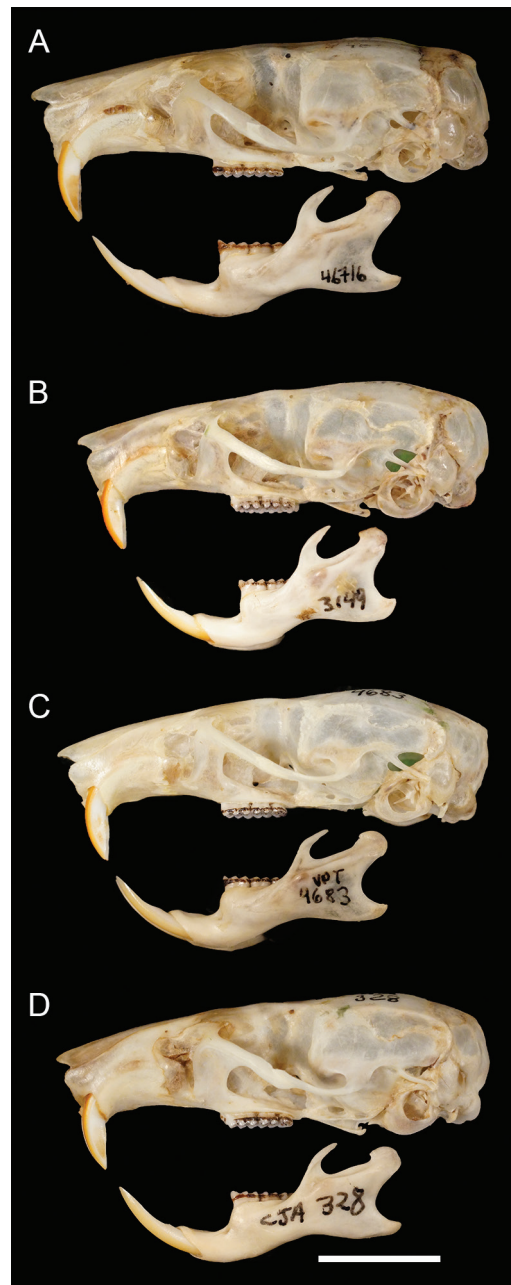


FIGURE 12. Lateral views of adult crania and mandibles of *Thomasomys* species treated in this report: A, *T. cinereus* (MUSM 46 716); B, *T. lojapiuranus* (MUSM 23758); C, *T. shallqukucha* (MUSM 46874); D, *T. pagaibambensis* (MUSM 39527). Scale bar = 10 mm.



FIGURE 13. Dorsal view of the skull of adult male crania showing the zygomatic notch area. From left to right: *Thomasomys cinereus* (MUSM 46716), *T. lojapiuranus* (MUSM 23758), *T. shallqukucha* (MUSM 46874), and *T. pagaibambensis* (MUSM 39527). Abbreviation: **zn**, zygomatic notch.

slightly flat in profile. On average, the midshaft diameter (2.55 mm) is less than the overall length of the glans (4.54 mm) (fig. 20A). A dorsal groove is present and confluent with the crater lip; a ventral groove is also present but is shallow and less developed. Laterally, other shallow depressions divide the glans into 5 or 7 sections on each side. The epidermal spines are rather sparse overall except along the rim, which is spineless. Each spine is in a shallow pit, and the spines are larger at the base of the glans than they are near the apex. The crater lip circumscribes the entire crater opening, and is separated from the spinous epithelium by a narrow fold. The medial bacular mound projects conspicuously from the crater lip and is thus visible externally; the much smaller lateral bacular mounds project only a little and are barely visible externally. The tip of the medial mound is usually oriented ventrally, except in one specimen where it is slightly dorsally oriented. The urethral flaps are well developed, triangular, undivided, and relatively long, but deeply buried within the crater; their tips are well separated, and a few minute spines are present on each. The dorsal papilla is well developed, conical, and bears several small spines on the tip or dorsal surface; it is

surrounded by tissue folds connecting the bacular mound with the inner surface of the crater.

Palatal rugae: Two complete (diastemal) and five incomplete (interdental) transverse palatal ridges (terminology following Quay, 1954, and Carleton, 1980) characterize most known species of *Thomasomys* (Pacheco 2003), including *T. cinereus* and *T. lojapiuranus*. In *T. cinereus*, the first diastemal ridge is slightly triangular and the second ridge is slightly convex. The interdental rugae i1, i2, i3, and i5 are slightly convex and each extends to the palate midline, whereas the interdental ruga i4 is very short and does not reach the palate midline (fig. 21).

Stomach: The stomach corresponds to the unilocular-hemiglandular morphotype (Carleton, 1973; Pacheco, 2003). The incisura angularis is shallow, and the bordering fold is thin and crosses the lesser curvature of the stomach slightly anterior to the incisura angularis; thus, some cornified epithelium extends into the antrum; the bordering fold also recurves moderately to the left but not beyond the esophageal orifice (fig. 22A).

Gall bladder: Present.

Reproductive glands: As described by Pacheco (2003), adult males have one pair each of dorsal

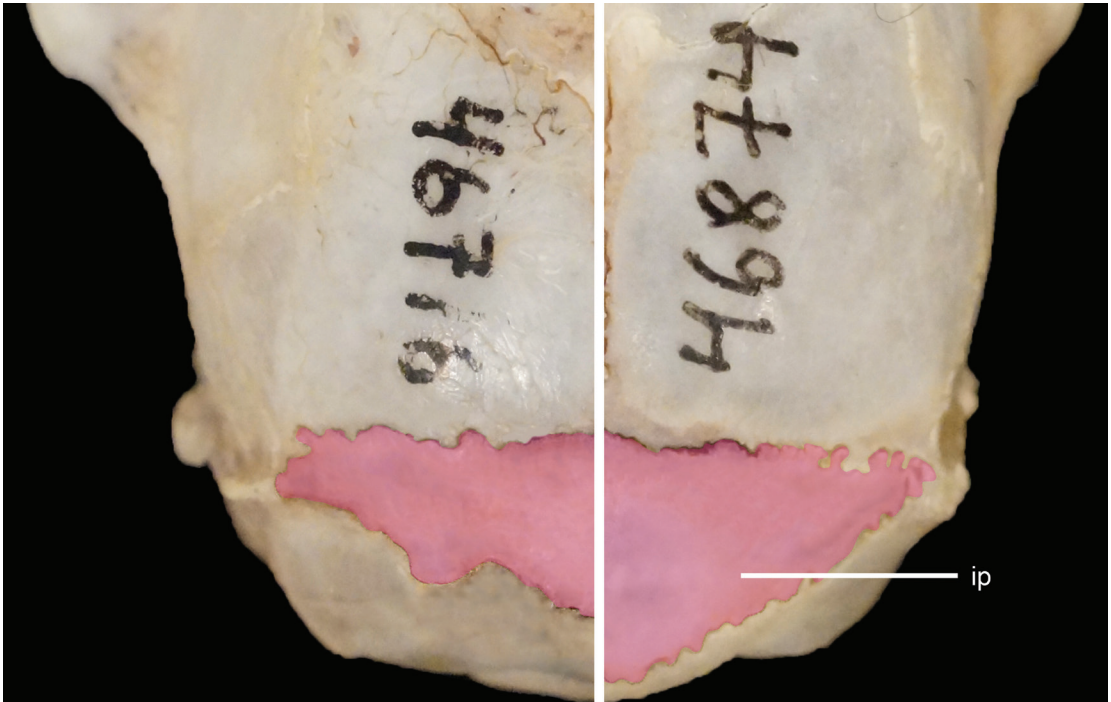


FIGURE 14. Interparietal region of *Thomasomys cinereus* (MUSM 46716) and *T. shallqukucha* (MUSM 46874). Note the interparietal bone (**ip**) is longer anteroposteriorly in *T. shallqukucha* than in *T. cinereus*.

prostate, anterior prostate, ampullary, vesicular, and bulbourethral glands, and two pairs of ventral prostate glands. The medial ventral prostate is much smaller than the lateral ventral prostate. Macroscopic preputial glands are absent.

Skeleton: Two partial skeletons each have 7 cervical, 13 thoracic, 6 lumbar, 4 sacral, and more than 36 caudal vertebrae; and the same skeletons each have 13 pairs of ribs. The first two caudal vertebrae in one specimen, and the first three caudal vertebrae in the second specimen, have chevron bones fused forming a closed arch. In both specimens, the closed arch of the first caudal vertebra has a small spinous process.

Karyotype: Unknown.

MEASUREMENTS OF HOLOTYPE: GSL, 33.05; CIL, 30.95; CML, 20.15; LOF, 11; LN, 12.95; LD, 9.25; LIF, 7.4; LM, 5.7; BIF, 2.4; BR, 6.2; BPB, 3.3; BM1, 1.8; BN, 4.3; LIB, 4.9; ZB, 18; BB, 15.05; BZP, 2.9; DI, 1.7. Measurements of additional specimens are provided in table 3.

DISTRIBUTION: *Thomasomys cinereus* is distributed in northern Peru, west of the Río Marañón and south of the Huancabamba Depression and the Río Chamaya. On the western side of the Andes, the species is distributed south of the Río Chancay from Montesecco in the department of Cajamarca southward to the Río Tablachaca (a main tributary of the Río Santa) in the department of La Libertad. On the eastern side of the species range, all records are on the west (left) side the Río Marañón, from Cutervo (fig. 1: locality 25) in the north to the Río Crisnejas in the south, all within the department of Cajamarca (fig. 1). The altitudinal range is from 1524 m to 3818 m.

NATURAL HISTORY: This species inhabits the humid montane forests or Yungas of northern Peru, which has also been called the Peruvian Yungas ecoregion of the Tropical and Subtropical Moist Broadleaf Forest biome (Dinerstein et al., 2017). Specimens were collected on the ground

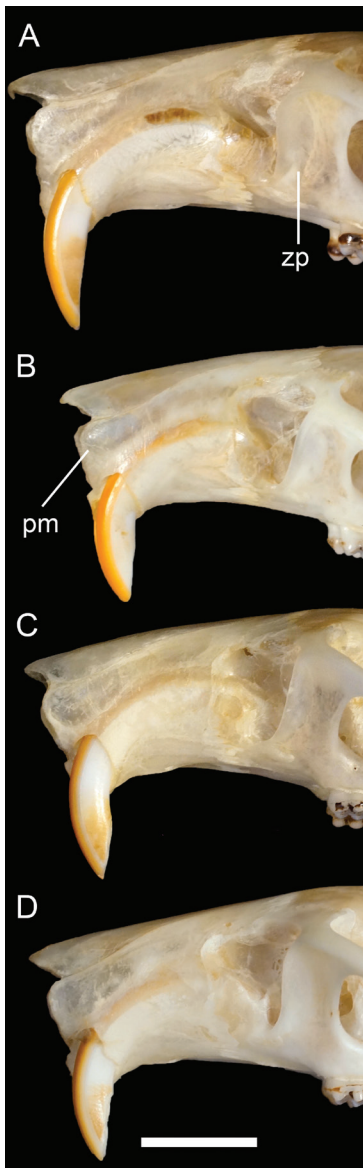


FIGURE 15. Lateral view of the skull showing the rostral and zygomatic plate regions. From top to bottom: *Thomasomys cinereus* (MUSM 46716), *T. loja-piuranus* (MUSM 23758), *T. shallqukucha* (MUSM 46875), and *T. pagaibambensis* (MUSM 40986). Abbreviations: **zp**, zygomatic plate; **pm**, premaxillary bone. Scale bar = 5 mm.

among dense shrubs or inside forests with small trees (fig. 23A). Arboreal or semiarboreal habits are suggested because we observed that some specimens easily climb shrubs and small trees when released.

Among specimens with reproductive data, 21 males were collected from July to October (usually considered the dry season); nine of them had scrotal testes and 12 had abdominal testes. Of eight male specimens collected from November to March (usually considered the wet season), four had scrotal testes and four had abdominal testes. Of 16 females collected from July to October, 14 had closed vaginas, one had an open vagina, and one was lactating. For the wet season, there is only one record of one female with an open vagina in April.

The stomach contents of one specimen was full of insect remains and a second specimen had some insect remains together with plant material.

Johnson (1972) and Durden and Musser (1994) reported *Thomasomys cinereus* as the host for the anopluran louse *Hoplopleura angulata*, but Pacheco (2015) corrected the host identification to *T. ischyryus*. Several species of nematodes of the genus *Trichuris*, *Vianella*, *Malvinema*, *Aspidodera*, and *Pterygodermatites* have been recently reported from specimens of *T. cinereus* collected at Bosque Cachil, Cajamarca (Polo-Gonzales, 2020).

At several localities, *Thomasomys cinereus* is sympatric with *T. taczanowskii* (Thomas, 1882) and *T. pyrrhonotus* Thomas, 1886 (MUSM database). Other natural history information about this species is still unknown.

REMARKS: Pacheco (2015) corrected the identification of some specimens previously identified as *Thomasomys cinereus*, including one collected from Maraynioc (near Chanchamayo), Junín department (Thomas, 1884), another reported near Uchco, Amazonas (Osgood, 1914), and other records from Antioquia (Hooper and Musser, 1964) and Huila (Carleton, 1973) in Colombia. Therefore, the descriptions of penis morphology (Hooper and Musser, 1964) and stomach morphology (Carleton,

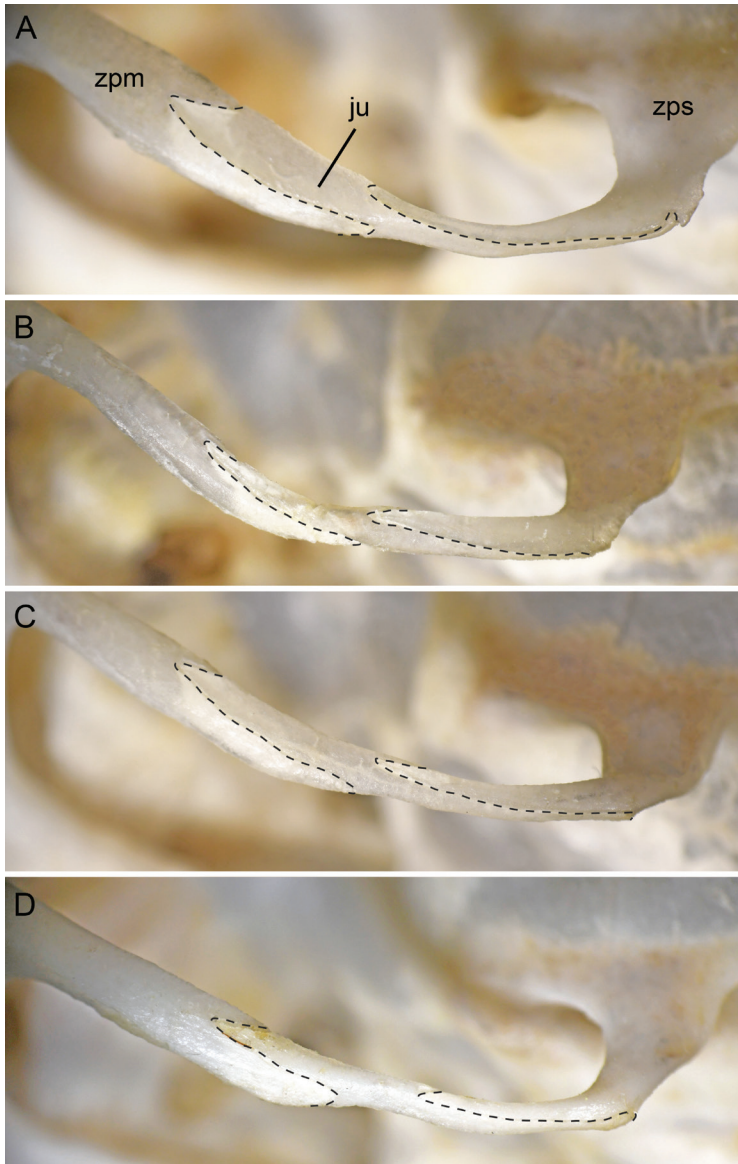


FIGURE 16. Zygomatic arches of **A**, *Thomasomys cinereus* (MUSM 46716); **B**, *T. lojapiuranus* (MUSM 23758); **C**, *T. shallqukucha* (MUSM 46874); **D**, *T. pagaibambensis* (MUSM 39527). Abbreviations: **zpm**, zygomatic process of the maxilla; **zps**, zygomatic process of the squamosal; **ju**, jugal.

1973) previously attributed to *T. cinereus* do not correspond to this species. However, Pacheco (2003) reported on these morphological attributes based on correctly identified specimens, and his observations are expanded here based on examination of additional specimens.

One specimen of *Thomasomys cinereus* LSUMZ 20313 (Esselstyn, 2017) has locality information and geographic coordinates that we believe to be wrong, and this problem merits comment. The specimen was collected from “33 road km SW Chiriaco” in Piura Department by

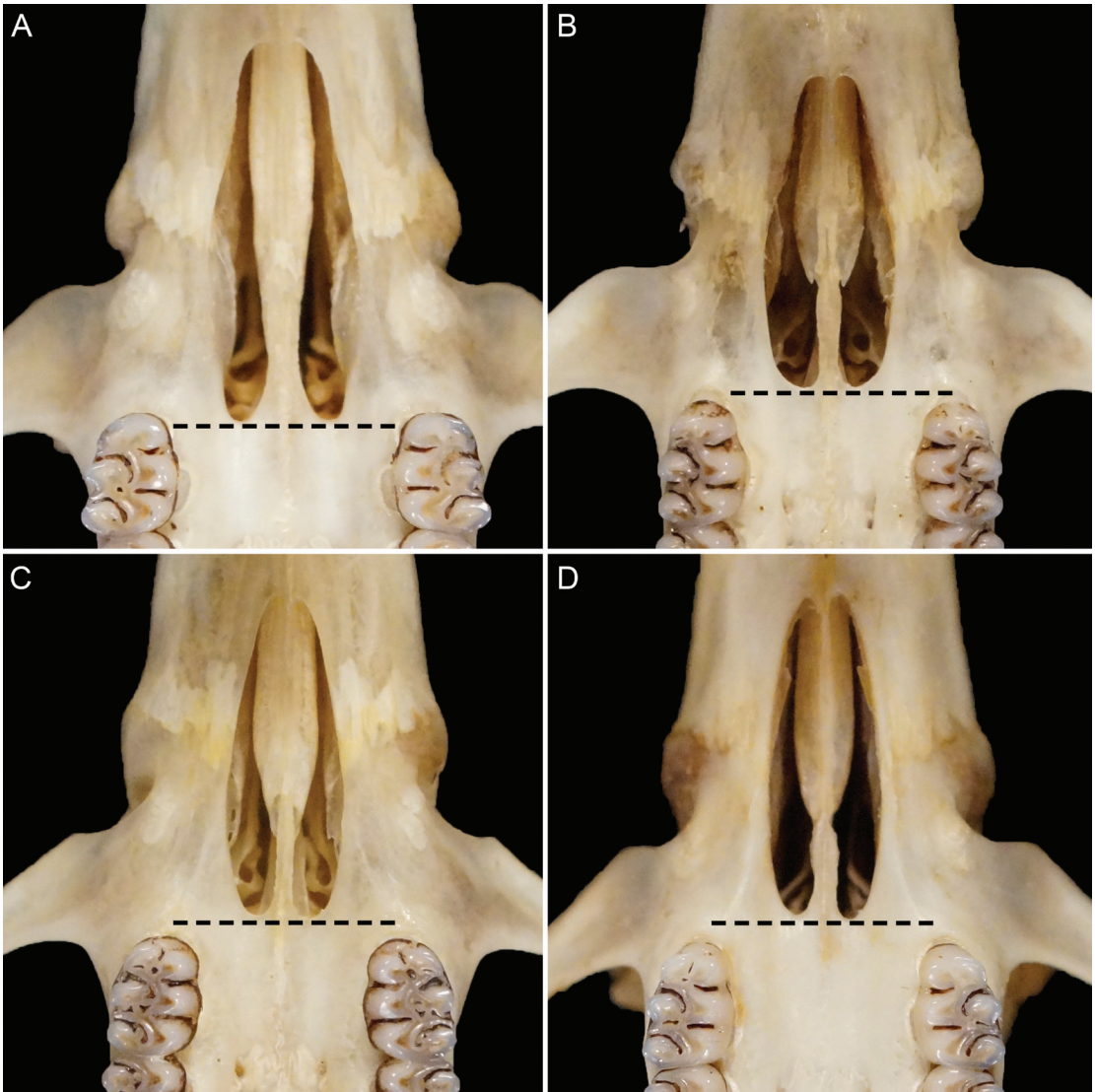


FIGURE 17. Incisive foramina size and position in relation to first molar of **A**, *Thomasomys cinereus* (MUSM 46716); **B**, *T. lojapiuranus* (MUSM 23758); **C**, *T. shallqukucha* (MUSM 46874); **D**, *T. pagaibambensis* (MUSM 39527).

K.R. Thomas. However, the recorded coordinates for this locality (5.372°S, 77.929°W) correspond to a point in the lowlands of Amazonas department far from all other known records of *T. cinereus*. We suggest that either the locality datum is a typographical error for “33 road km SW Huancabamba” in Piura Department (where Thomas also collected), or the specimen (which we have not examined) is misidentified.

Two specimens (AMNH 73127, 73129) were said to have been collected at Seques in Lambayeque department by Watkins on his way to Taulis in Cajamarca, although Lambayeque currently has no locality named Seques, but Cajamarca does. In the province of San Miguel (district of La Florida) there are localities known as “Pampa de Seques” and “Mountain of Seques” (<https://www.deperu.com/centros->

poblados/pampa-de-seques-37687), with approximate coordinates: 6.890384°S, 79.088967°W. These places are on the route that Watkins travelled to Taulis, so it seems likely Watkins collected these specimens in Cajamarca rather than Lambayeque.

Thomasomys lojapiuranus, new species

Loja and Piura *Thomasomys*

Figures 6B, 8, 9, 10B, 11B, 11F, 12B, 13B, 15B, 16B, 17B, 18B, 19B, 19F, 20B, 21, 22B, 24

Thomasomys cinereus Voss, 1993: part,

Thomasomys sp. 2 Brito et al., 2019: 9.

HOLOTYPE: An adult female specimen housed in the Museo de Historia Natural de la Universidad Nacional Mayor de San Marcos (MUSM 23758), collected by V. Pacheco on April 28, 2006 (original field number VPT 3149). The holotype is preserved as skin and skull in good condition.

PARATYPES: Four paratypes from the same locality, two females (MUSM 23759, 23762) and two males (MUSM 23760, 23761).

TYPE LOCALITY: Peru, Department of Piura, Province of Huancabamba, Pariamarca Alto; 5.15867°S, 79.54901°W, 2990 m above sea level.

DIAGNOSIS: A medium-sized *Thomasomys* (table 3) that can be distinguished from its congeners by the following combination of characters: dorsal pelage long and soft, brownish with hair tips yellowish; mystacial vibrissae long, extending beyond posterior margin of pinnae; tail longer than head-and-body length, unicolored and without a white tip; thenar and hypothenar pads separated; plantar surface of hind foot pale; nasal relatively short, expanded anteriorly, and tapering posteriorly to the maxilla-frontal-lacrimal intersection or shorter; zygomatic notch shallow; incisive foramina long, extending posteriorly to the anterior margins of first molars, not between; palatal median process usually present (78%); Eustachian tube short and broad; stapedial process of bulla reduced; capsu-

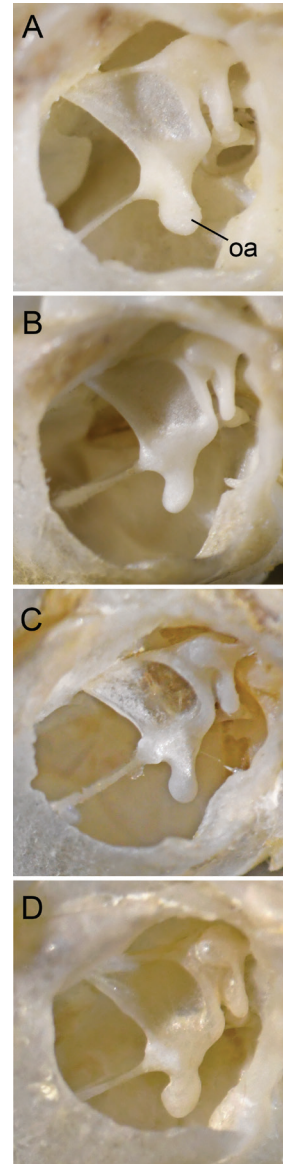


FIGURE 18. Orbicular apophysis of the malleus in **A**, *Thomasomys cinereus* (MUSM 39369); **B**, *T. lojapiuranus* (MUSM 511); **C**, *T. shallqukucha* (MUSM 47229); **D**, *T. pagaibambensis* (MUSM 41006). Abbreviation: **oa**, orbicular apophysis.

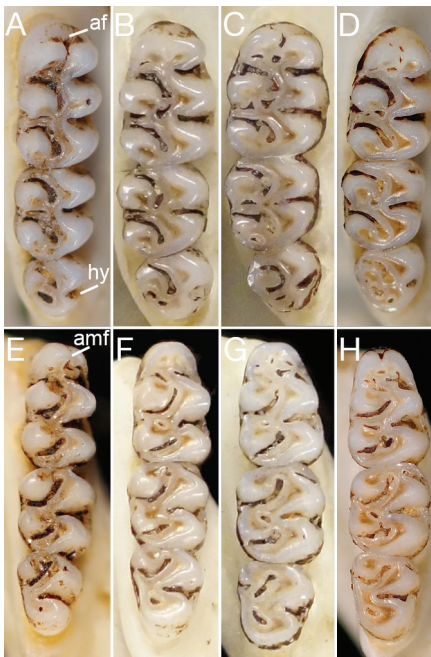


FIGURE 19. Upper and lower molars of *Thomasomys* species treated in this report: **A, E**, *T. cinereus* (MUSM 46716); **B, F**, *T. lojapiuranus* (MUSM 23758); **C, G**, *T. shallqukucha* (MUSM 46874); **D, H**, *T. pagaibambensis* (MUSM 39527). Abbreviations: **af**, anteromedian flexus; **hy**, hypoflexus; **amf**, anteromedian flexid.

lar process of lower incisors alveolus absent; M1 anteromedian flexus weak; M3 hypoflexus weak; and m1 anteromedian flexid weakly produced.

MORPHOLOGICAL DESCRIPTION: *Thomasomys lojapiuranus* is a medium-size *Thomasomys* (HBL = 107–146 mm) with long, soft, and dense dorsal fur (individual hairs about 14–16 mm). Dorsal pelage is brownish (Dark Drab, color 119B) with hairs slate colored at the base. Ventral pelage is gray whitish (Smoke Gray, color 45) or washed with pale brown, individual hairs slate colored basally. Dorsal and ventral pelage are moderately countershaded (figs. 8, 9). The ears are moderately long (EL = 18–26 mm) and paler. Postauricular patches of cream-colored fur are conspicuous. The mystacial vibrissae are long, extending behind the posterior margin of the pinnae by about half the pinnae length when laid

back alongside the head. The supraorbital vibrissae are also relatively long, extending behind the posterior margins of pinnae when laid back alongside the head. The genal 1 vibrissae are absent. The tail is on average longer than the combined length of head and body (Tail% = 117), comparatively thick, mostly unicolored, and without a white tip. The metacarpals are pale brownish. Digit II of manus is larger than digit V. The hindfeet are moderately long (HFL = 28–32 mm) with metatarsal patch pale brownish, and dense ungual tufts. The plantar surface of the hind foot is pale. The thenar and hypothelar pads are separated by a distinct gap (fig. 10B). Digit I of the hind foot (hallux) is moderately long, its claw extending close or to the first interphalangeal joint of dII. Digit V of the hind foot is long, with the claw extending about half the length of phalanx 2 of dIV.

Cranium: The skull is moderately large (CIL = 29–32 mm) with a relatively long and moderately broad rostrum. The skull dorsal profile is slightly convex, never straight, with a small bump at the interorbital region level. A rostral tube is absent, and the gnathic process is small (figs. 12B, 15B). The nasals are short and tapering; the anterior half is expanded; the posterior margins are narrow, extending posteriorly to the maxilla-frontal-lacrimal intersection or shorter and barely beyond the premaxillae. The zygomatic notches are shallow (fig. 13B). The interorbital region is moderately broad and hourglass shaped with rounded margins, and the frontal sinus are relatively inflated. The interparietal is wide and moderately long anteroposteriorly, straplike in some specimens, but rhomboidal in others. The premaxillae are slightly produced anteriorly beyond the incisors (fig. 15B). The zygomatic arches converge anteriorly to a moderate degree. The zygomatic plates are moderately broad, subequal in breadth to the length of M1, and moderately sloped backward (fig. 15B). The zygomatic process of the maxilla and the zygomatic process of the squamosal are closely approximated (80%) or separated by a distinct gap (20%) (fig. 16B). The postglenoid foramen is

small and placed anterior to a relatively larger subsquamosal fenestra. The tegmen tympani is robust and overlaps a distinct suspensory process of the squamosal. The carotid circulatory pattern is pattern 1 (sensu Voss, 1988): a stapedia foramen, a groove on the inner surface of the squamosal and the alisphenoid, and a sphenofrontal foramen are all present. In the medial wall of the orbit, the ethmoid foramen is placed dorsal to M2; the ethmoturbinals are moderate in size; the sphenopalatine foramen is bordered by the maxillary, ethmoid, and palatine bones; and the optic foramen is moderate in size and slightly posterior to M3. The paraoccipital process is small. The incisive foramina are long and extend posteriorly to the anterior margins of the first molars, not between, and are widest behind the premaxillary-maxillary suture; the posterior margins are rounded (fig. 17B). The mesopterygoid fossa is broad and expanded anteriorly, the roof is closed, and the sides are subparallel; the palatal median process is present (in 78% of examined specimens). The parapterygoid fossa is triangular, shallow, and without vacuities. The foramen ovale is moderate in size, the alisphenoid strut is present, and the middle lacerate foramen is narrow but conspicuous. The auditory bullae are small, flask shaped, and moderately inflated with short and broad Eustachian tubes; the stapedia process of bulla is reduced. The internal carotid canal is bounded by the basioccipital and the ectotympanic (auditory bulla), but not by the periotic. The basioccipital is moderately broad, the mastoid (the occipital exposure of the periotic) is either imperforate or has only a small fenestra. The lamina of the malleus is squarish and not deep, and the orbicular apophysis is elongated without a basal constriction (fig. 18B). The processus brevis of the incus is long, narrow, and delicate.

Teeth: The upper incisors are orthodont with orange enamel on their anterior surfaces. The upper molar rows are moderately long (4.8–5.5 mm). The upper molars are brachyodont and pentalophodont (sensu Hershkovitz, 1962) without interpenetration of the labial and lin-

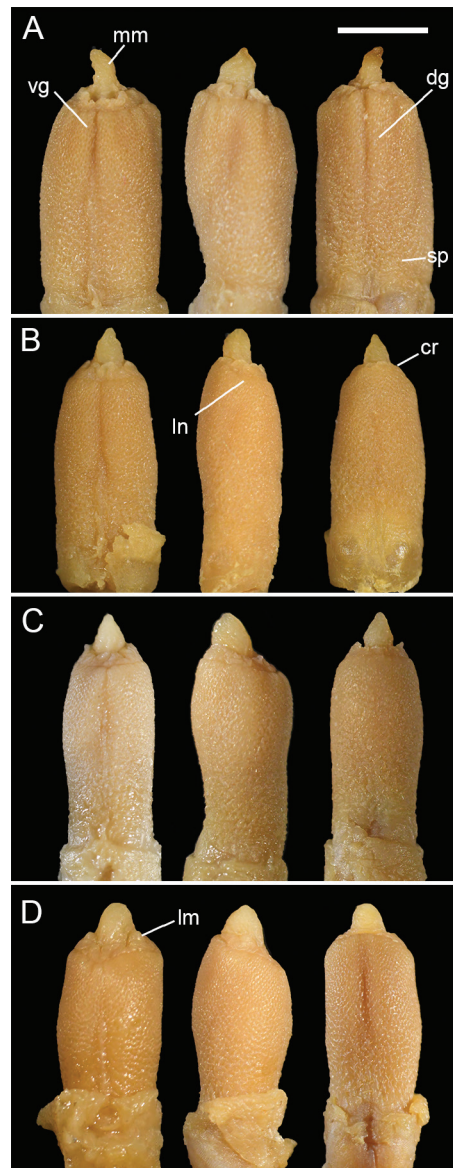


FIGURE 20. Ventral, lateral, and dorsal views of glans penis of four species of *Thomasomys*: **A**, *T. cinereus* (MUSM 38493); **B**, *T. lojapiuranus* (MUSM 23761); **C**, *T. shallqukucha* (MUSM 46887); **D**, *T. pagaibambensis* (MUSM 40965). Abbreviations: **cr**, crater; **dg**, dorsal groove; **lm**, lateral bacular mound; **ln**, lateral notch; **mm**, medial bacular mound; **sp**, spines; **vg**, ventral groove. Scale bar = 2 mm.

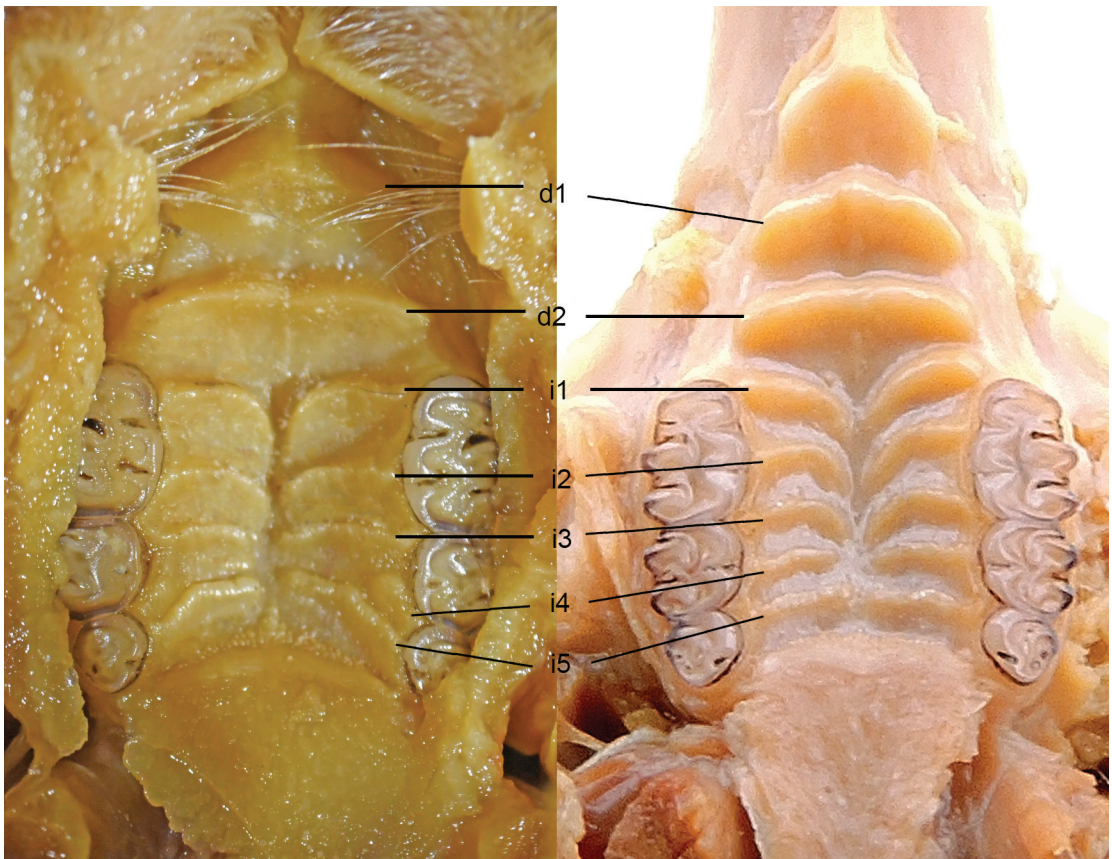


FIGURE 21. Soft palate of *Thomasomys cinereus* (MUSM 17299) and *T. lojapiuranus* (MUSM 23761) showing differences in the palatal rugae. Abbreviations: **d1–d2**, diastemal palatal rugae; **i1–i5**, interdigital rugae.

gual flexi; labial and lingual cingula are not developed; and accessory labial roots are absent. The procingulum of M1 is slightly narrower than the protocone-paracone cusp pair, and the anteromedian flexus is weak or coalesced. The anteroloph is conspicuous and the paraflexus is recurved. The paraloph is oriented transversally to the median mure, to the base of the mesoloph, or the mesoloph. The mesoloph is narrow and well developed and reaches the labial margin of the tooth. The metaflexus is slightly curved. The posteroloph is coalesced with the metacone. M2 exhibits a strong anteroloph with a recurved paraflexus; the mesoloph is narrow and complete, the metaflexus is comma shaped, and the posteroloph is coalesced with the metacone. M3 is smaller compared to M2; its paraf-

lexus is conspicuous but the hypoflexus is reduced (fig. 19B).

On the lower molars, the main cuspids are conspicuous and slightly alternating. The first lower molar (m1) has a weak anteromedian flexid; the protolophid and anterolophid are short and quickly coalesced; the anterolabial and anterolingual cingula are poorly developed; the mesoflexid is narrow and recurved; the entoflexid is small or coalesced; the posteroflexid is narrow and almost straight; the hypoflexid is narrow and oriented perpendicularly; and the mesolophid is narrow but complete. On m2, the mesolophid is short and the anterolabial cingulum is small. The m3 has a subtriangular occlusal shape produced by the less developed entoconid; the mesoflexid and

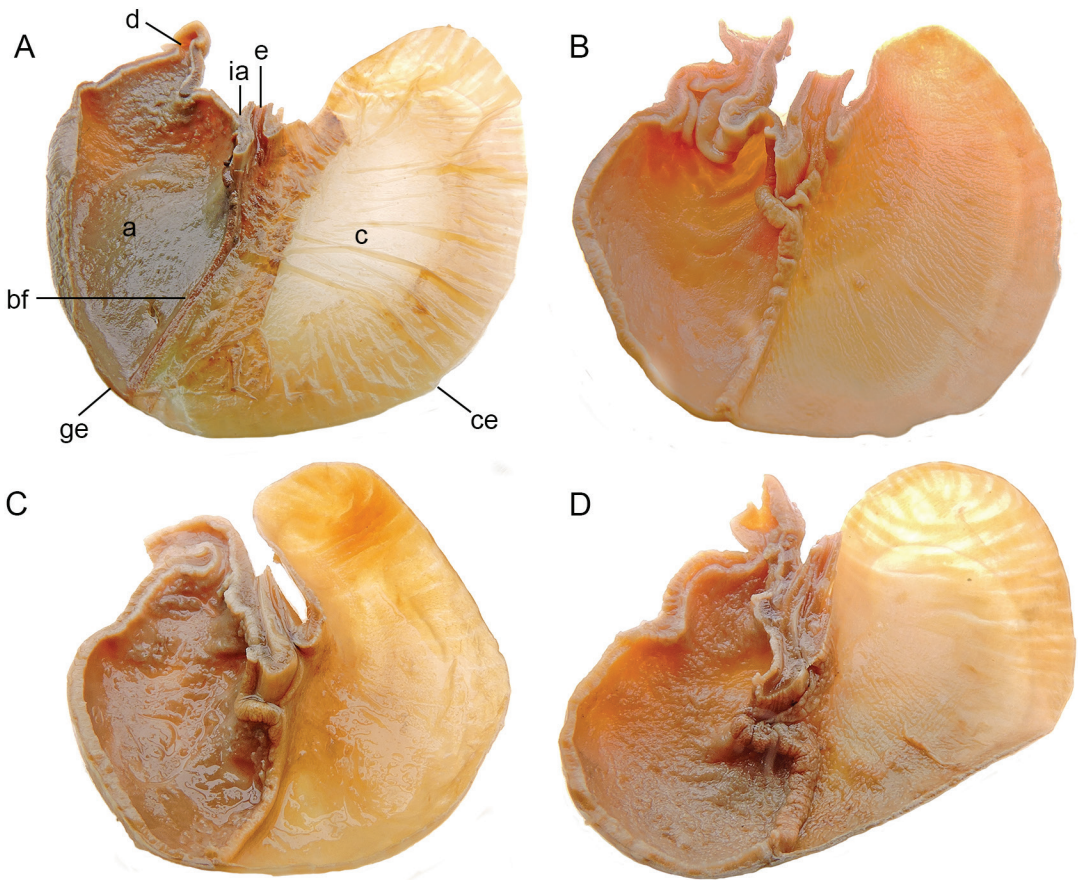


FIGURE 22. Stomach morphology in four species of *Thomasomys*: **A**, *T. cinereus* (MUSM 38497); **B**, *T. lojapiuranus* (MUSM 23761); **C**, *T. shallqkucha* (MUSM 46871); **D**, *T. pagaibambensis* (MUSM 40965). Abbreviations: **a**, antrum; **bf**, bordering fold; **c**, corpus; **ce**, cornified epithelium; **d**, duodenum; **e**, esophagus; **ge**, glandular epithelium; **ia**, incisura angularis.

hypoflexid are conspicuous; and the postero-flexid is coalesced (fig. 19F).

Mandible: The coronoid process is long, narrow, falciform, and taller than the condylar process, producing a deep sigmoid notch. The angular process is well developed and on the same plane as or slightly anterior to the condylar process. The ventral border of the mandible is deeply concave. The capsular process of the lower incisor alveolus is absent (fig. 24).

Hyoid apparatus: Hyoid morphology like that described for *Thomasomys cinereus* (observation made only in one specimen).

Penis: Two fluid-preserved male specimens (MUSM 23760, 23761) were examined. The glans is medium size, subcylindrical, relatively long (4.48 mm), and narrow (2.28 mm) (fig. 20B). A dorsal groove is absent, and a ventral groove is exhibited as a shallow sulcus. The external surface of the glans is covered by small epidermal spines overall except along the crater rim. The spineless crater lip circumscribes the entire crater opening and is separated from the spinous epithelium by a thick fold. Distally, the glans is not divided on the lateral sides, but a shallow notch is present (fig. 20B). The medial bacular mound projects prominently from the crater lip

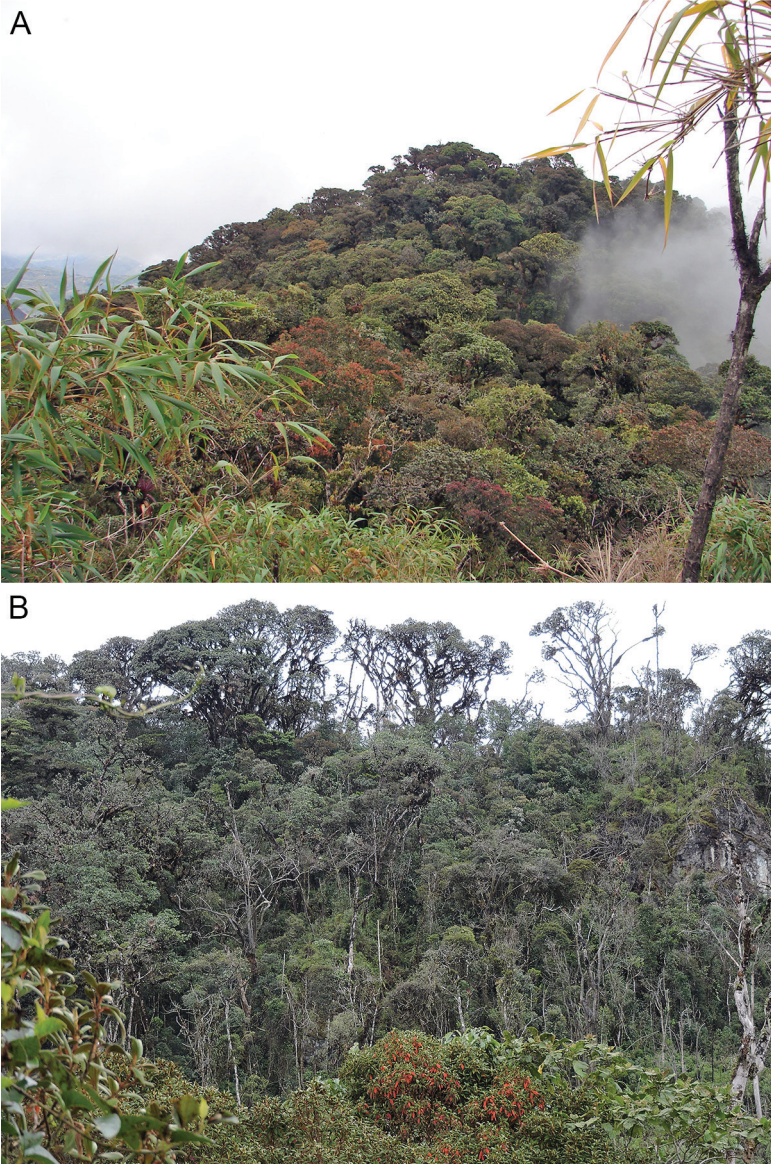


FIGURE 23. Habitat views of *Thomasomys cinereus* (A, P.N. Cutervo, Cajamarca) and *T. shallqkucha* (B, Kañaris, Lambayeque, Peru). Both photos by Víctor Pacheco.

and is thus visible externally; the lateral bacular mounds are much smaller than in *Thomasomys cinereus*, lack ornamentation, and are not visible externally. The tip of the medial bacular mound is broad and oriented vertically or slightly ventrally oriented. The urethral flaps are small, conical, deeply buried within the crater, and lack

ornamentation. The dorsal papilla is small, conical, and lack spines or other ornamentation.

Palatal rugae: Two complete (diastemal) and five incomplete (interdental) transverse palatal ridges like in *Thomasomys cinereus*, except that the interdental ruga i4 extends to the palate midline and the interdental ruga i5 is nearly straight (fig. 21).

Stomach: The stomach corresponds to the unilocular-hemiglandular morphotype (Carleton, 1973; Pacheco, 2003). The incisura angularis is shallow, and the bordering fold is thicker and crosses the lesser curvature of the stomach slightly anterior to the incisura angularis; the bordering fold also gently recurves to the left but not beyond the esophageal orifice (fig. 22B).

Gall bladder: Present.

Reproductive glands: Macroscopic preputial glands are absent.

Skeleton: The vertebral count is 7 cervical, 13 thoracic, 6 lumbar, 4 sacral, and 37 to 40 caudal vertebrae; and the same skeletons each have 13 pairs of ribs. The supratrochlear fenestra of humerus is usually absent (6 of 7 samples). The first caudal vertebra has chevron bones fused forming a closed arch, mostly without a spinous process (in 5 of 7 examined specimens). As described by Pacheco (2003), on the calcaneus, the trochlear process levels its posterior articular facet; and the peroneal process of the fifth metatarsal is moderately long but not extending to the proximal edge of the cuboid.

Karyotype: Unknown.

MEASUREMENTS OF HOLOTYPE: GSL, 33.1; CIL, 30.15; CML, 19.52; LOF, 10.5; LN, 12.03; RL, 11.28; LD, 8.94; LIF, 6.31; LM, 5.15; BIF, 2.67; BR, 5.39; BPB, 3.36; BM1, 1.7; BN, 4.27; LIB, 5.2; ZB, 17.56; BB, 14.15; BZP, 2.73; DI, 1.7; HBC, 9.35; MFB, 2.45. Measurements of additional specimens are provided in table 3.

DISTRIBUTION: *Thomasomys lojapiuranus* is distributed in the montane forests of the western slope of the department of Piura, in northern Peru, and the province of Loja in southern Ecuador. All examined specimens are from north of the Huancabamba depression, most of them in the headwaters of the Río Huancabamba, a main tributary of the Río Chamaya (fig. 1). The altitudinal range is from 1198 m (but see Remarks) to 3481 m.

TAXONOMIC COMPARISONS: *Thomasomys lojapiuranus* differs from *T. cinereus* by its brownish dorsal pelage (vs. grizzled ashy gray to dark gray in *T. cinereus*); whitish gray or pale brown ven-

tral pelage (vs. pale yellowish or pale gray); mystacial vibrissae long, extending behind the posterior margin of pinnae by about half the pinnae length when laid back alongside the head (vs. shorter in *T. cinereus*, table 4); tail longer than head-and-body length (Tail% = 117±11% vs. 103±8%) and mostly unicolored (vs. moderately bicolored); thenar and hypothenar pads separated by a distinct gap (vs. thenar and hypothenar pads closely approximated); zygomatic notches shallow (vs. deep [55%] or shallow in *T. cinereus*); incisive foramina long, but never extending posteriorly between the first upper molars (vs. usually extending between the first upper molars in *T. cinereus*); stapedial process of bulla reduced (vs. conspicuous); orbicular apophysis elongated without basal constriction (vs. knob shaped in *T. cinereus*); M1 anteromedian flexus, M3 hypoflexus, and m1 anteromedian flexid weak (vs. all these traits distinct; table 4). *T. lojapiuranus* also differs from *T. cinereus* in the morphology of glans penis by exhibiting a lateral notch, lack of dorsal groove, and spineless urethral flaps and dorsal papilla. Additionally, interdental ruga i4 extends to the palatal midline (vs. interdental ruga i4 shorter in *T. cinereus*).

Thomasomys lojapiuranus differs from *T. shallqukucha* by its long mystacial vibrissae that extend conspicuously behind the posterior margin of pinnae when laid back alongside the head (vs. mystacial vibrissae shorter, barely extending behind the posterior margin of the pinnae in *T. shallqukucha*); plantar surface of hind foot pale (vs. dark); zygomatic notch shallow (vs. very shallow); interparietal bone moderately long anteroposteriorly (vs. conspicuously long anteroposteriorly); incisive foramina long, extending posteriorly to the anterior margins of the first molars (vs. short, not approaching the anterior margins of the first molars); palatal median process usually present (vs. absent); Eustachian tube short and broad (vs. short and narrow); orbicular apophysis elongated without basal constriction (vs. elongated with basal constriction on anterior margin); M1 anteromedian flexus, M3 hypoflexus, and m1 anteromedian flexid weak (vs. all



FIGURE 24. Dorsal, ventral, and lateral views of the cranium and mandible of *Thomasomys lojapiuranus* (MUSM 23758, holotype), an adult female from Parimarca Alto, Huancabamba province, Piura department, Peru. Scale bar = 10 mm.

flexi distinct; table 4). *Thomasomys lojapiuranus* also differs from *T. shallkukucha* in the morphology of glans penis by presenting a lateral notch.

Thomasomys lojapiuranus differs from *T. pagaibambensis* by having a tail without a white tip (vs. tip usually white in *T. pagaibambensis*); plantar surface of hind foot pale (vs. slightly

darker); zygomatic plates moderately sloped backward (vs. vertically oriented); zygomatic process of maxilla and zygomatic process of squamosal closely approximated (vs. processes distinctly separated by a narrow jugal); incisive foramina long, extending posteriorly to the anterior margins of the first molars (vs. short, not approaching the

anterior margins of the first molars); palatal median process usually present (vs. usually absent); Eustachian tube short and broad (vs. short and narrow); orbicular apophysis elongated without basal constriction (vs. elongated with basal constriction and recurved); capsular process of lower incisor alveolus absent (vs. distinctly swollen; table 4). *Thomasomys lojapiuranus* also differs from *T. pagaibambensis* in penis morphology by exhibiting a lateral notch and lack of dorsal groove, and in stomach morphology by exhibiting a shallower incisura angularis and a bordering fold little recurved to the left.

Thomasomys lojapiuranus could also be confused with some species of similar size of the Cinereus Group from Ecuador, such as *T. silvestris*, *T. caudivarius*, and the recently described *T. salazari*. However, *T. lojapiuranus* has the tail proportionally shorter (Tail% = 117%), whereas *T. silvestris*, *T. caudivarius*, and *T. salazari* have the tail longer (Tail% >130%; Brito et al., 2019: table 2). *Thomasomys lojapiuranus* has a broad rostrum with anterior half of nasals expanded that clearly differs from the narrower rostrum and nasals of *T. caudivarius*, *T. salazari*, and *T. silvestris* (fig. 24; Brito et al., 2019: fig. 6, S2). Also, the cranium of *T. lojapiuranus* has a more rectangular dorsal profile versus a more triangular profile in *T. caudivarius*, *T. salazari*, and *T. silvestris* (fig. 12B; Brito et al., 2019: fig. 6, S2). Additional comparisons are presented in table 4 (this work) and Brito et al. (2019: table 2).

NATURAL HISTORY: This species inhabits the humid montane forests of northern Peru and southern Ecuador, which has also been called the Peruvian Yungas ecoregion of the Tropical and Subtropical Moist Broadleaf Forest biome (Dinerstein et al., 2017). At several collecting localities, the vegetation consisted of high shrubs and small trees, 10 to 15 m high.

Among specimens with reproductive data, 13 males were collected from July to August (usually considered the dry season); eight of them had scrotal testes (length >10 mm) and five had abdominal testes (length ≤9 mm). No data is available for the wet season. Among 24 female

specimens collected in July and August, 18 specimens had closed vagina (75%); three females had embryos (one with a fetus on the left ovary; the second with two embryos, one on each side; and the third with three embryos, two on the left, one on the right side); and three females were lactating; suggesting that during the dry season most specimens of *T. lojapiuranus* are in nonreproductive condition. Six specimens collected in November and December had no embryos.

Stomach contents of four specimens contained insect remains and seeds. Some nematodes were also found in the antrum.

In Yacurí National Park, Ecuador, *Thomasomys lojapiuranus* is sympatric with *T. taczanowskii* and *T. caudivarius* (Lee et al., 2018).

ETYMOLOGY: It is a pleasure to dedicate this species to the people of Loja and Piura departments, from Ecuador and Peru, respectively, who share similar costumes and traditions. We recognize in the distributional range of this mouse the fact that nature does not observe political boundaries.

REMARKS: Brito et al.'s (2019: fig. 3) phylogenetic analysis of the Cinereus Group contains several problematic identifications. Among others, they identified several specimens that appear as terminals in a phylogenetic tree (QCAZ 15612–15630) as *Thomasomys cinereus*. The authors did not report the collection localities of those specimens, but according to Lee et al. (2015: fig. 1), these were collected in 2015 near Laguna Negra (4.71308°S, 79.43025°W; 3407 m) in Loja province, Ecuador. We found that the sequences of four of these specimens are not *T. cinereus* sensu stricto nor any of the new species reported here (table 1, fig. 4). Additionally, Brito et al. (2019: apéndice 1) identified several specimens (QCAZ 16230, 16231, 16328–16330) from Jimbura (4.71167°S, 79.4403°W; 3226 m) as *T. cinereus* or “*Thomasomys* sp. 2” (Brito et al., 2019: fig 3); based on our sequence analyses (fig. 4), we would identify these specimens as *T. lojapiuranus*. Lastly, we sequenced one specimen (MEPN 12549) from Espinola, Parque Nacional Yacurí, Loja (4.719803°S, 79.439031°W; 3274 m)

that Brito et al. (2019) identified morphologically as *T. cinereus* and determined that it too is *T. lojapiuranus* (fig. 4).

Several specimens from Piura, Huancabamba, Canchaque, Tambo, at 1198 m (FMNH 83444–83454) were collected at an unusually low elevation for *Thomasomys* (Pacheco 2015). Unusually too, most of the habitat around Canchaque corresponds to dry forest (VP, personal obs.), which suggests that the elevation provided for those specimens is inaccurate. On the other hand, two specimens were collected nearby (15 road km E Canchaque; LSMZ 19315, 19316) but at 1737 m, which suggests that the locality of the FMNH specimens is likely correct, but perhaps not the elevation. The latter locality (at 1737 m) would be the lowest elevation record for *T. lojapiuranus* if the elevation data of the FMNH specimens were not considered.

***Thomasomys shallqukucha*, new species**

Shallqa *Thomasomys*

Figures 6C, 8, 9, 10C, 11C, 11G, 12C, 13C, 14, 15C, 16C, 17C, 18C, 19C, 19G, 20C, 22C, 25

Thomasomys cinereus, Pacheco 2015; part, not Thomas, 1882

HOLOTYPE: An adult male specimen in the Museo de Historia Natural de la Universidad Nacional Mayor de San Marcos (MUSM 46875). The holotype is a fluid-preserved specimen with skull removed, collected by Víctor Pacheco (field number VPT 4685) on 14 October 2016.

PARATYPES: Nineteen paratypes from the same locality (MUSM 46870–46874, 46876–46889).

TYPE LOCALITY: Peru, Department of Lambayeque, Province of Ferreñafe, District of Kañaris, Geomarca; 6.098573°S, 79.239928°W. 3266 m above sea level.

DIAGNOSIS: A medium-sized *Thomasomys* (table 3) that can be distinguished from its congeners by the following combination of characters: pelage dark brownish; metatarsal patch pale

brownish; tail long, unicolored, without a white tip; thenar and hypothenar pads separated; plantar surface of hind foot dark; nasals long, expanded anteriorly, and tapering posteriorly to lacrimal; zygomatic notches very shallow; interparietal bone conspicuously long anteroposteriorly; zygomatic plate moderately sloped backward; incisive foramina short, extending posteriorly close to the anterior margin of the first molar; palatal median process absent; Eustachian tube short and narrow; stapedia process of bulla reduced; bullae flask shaped and moderately inflated; capsular process of lower incisors alveolus absent; M1 anteromedian flexus distinct; M3 hypoflexus distinct; and m1 anteromedian flexid distinct.

MORPHOLOGICAL DESCRIPTION: *Thomasomys shallqukucha* is a medium-size species (HBL = 116–142 mm) with long, soft, and dense dorsal fur (about 14 mm). Dorsal pelage is dark brown (Vandyke Brown, color 221; Sepia, color 219) with slate colored basally (Blackish Neutral Gray, color 82). Ventral pelage is Pearl Gray (color 81) or Pale Neutral Gray (color 86) with individual hairs slate colored basally, and moderately countershaded with dorsal pelage (figs. 8, 9). The ears are moderately long (EL = 19–26 mm) and dark brown. Postauricular patches are not conspicuous. The mystacial vibrissae are short, extending slightly behind the posterior margin of pinnae when laid back alongside the head. The supraorbital vibrissae are short, not extending to the posterior margins of pinnae when laid back alongside the head. The genal 1 vibrissae are absent. The tail is on average longer than the combined length of head and body (Tail% = 119), comparatively thick, unicolored without a white tip. The manus is pale brown with digit II larger than digit V. The hindfeet are moderately long (HFL = 30–33 mm) with metatarsals pale brownish. The plantar surface of the hind foot is dark. The thenar and hypothenar pads are separated by a conspicuous gap (fig. 10C). Digit I of the hind foot (hallux) is moderately long, its claw extending close to or to the first interphalangeal joint of dII. Digit V of hind foot is long, with



FIGURE 25. Dorsal, ventral, and lateral views of the cranium and mandible of *Thomasomys shallqukucha* (MUSM 46874, paratype); an adult male from Geomarca, Kañaris district, Ferreñafe province, Lambayeque department, Peru. Scale bar = 10 mm.

claw extending about half the length of phalanx 2 of dIV.

Cranium: The skull is moderately large (CIL = 30.4–32.5 mm) with flat or barely convex profile without a bump on the frontal region. The rostrum is relatively long and moderately broad. A rostral tube is absent, and the gnathic process

is small (figs. 12C, 15C). The nasals are long and tapering; the anterior half are expanded; the posterior margins are narrow, extending posteriorly to the lacrimals and beyond the premaxillae. The zygomatic notches are extremely shallow (fig. 13C). The interorbital region is moderately broad and hourglass shaped with rounded margins,

and the frontal sinuses are relatively inflated. The braincase is wide and squarish. The lateral parietal processes are moderately large and subtriangular. The interparietal is wide and long anteroposteriorly, straplike in some specimens, but rhomboidal in others (fig. 14). The zygomatic arches converge anteriorly to a moderate degree or subparallel. The zygomatic plates are moderately broad, subequal in breadth to the length of M1, with the anterior margins slightly sloped backward (fig. 15C). The premaxillae are conspicuously produced anteriorly beyond the incisors (fig. 15C). The zygomatic processes of the maxilla and of the squamosal are closely approximated (fig. 16). The postglenoid foramen is small and placed anterior to a relatively larger subsquamosal fenestra. The tegmen tympani is robust and overlaps a distinct suspensory process of squamosal. The carotid circulatory pattern is pattern 1 (sensu Voss, 1988): a stapedial foramen, a groove on the inner surface of the squamosal and the alisphenoid, and a sphenofrontal foramen are all present. In the medial wall of the orbit, the ethmoid foramen is placed dorsal to M2; the ethmoturbinals are moderate in size; the sphenopalatine foramen is bordered by the maxillary, ethmoid, and palatine bones; and the optic foramen is moderate in size and slightly posterior to M3. The paraoccipital process is small. The incisive foramina are short and extend posteriorly to just in front of the anterior margins of the first molars, and are widest at the premaxillary-maxillary suture (fig. 17C). The palate is short and wide (sensu Hershkovitz, 1962). The mesopterygoid fossa is broad (in 68% of examined specimens), expanded anteriorly, with subparallel sides; a median posterior process of the palate is absent. The sphenopalatine vacuities are absent or produced as small slits along the basi-sphenoid and the presphenoid. The parapterygoid fossa is triangular, shallow, and perforated by a vacuity. The foramen ovale is small, the alisphenoid strut is present, and the middle lacerate foramen is relatively wide. The auditory bullae are flask shaped, moderately inflated, with short and narrow Eustachian tubes; the stapedial pro-

cess of bulla is reduced. The internal carotid canal is bounded by the basioccipital and the ectotympanic (auditory bulla), but not the periotic. The basioccipital is moderately broad, and the mastoid (the occipital exposure of the periotic) is either imperforate or has only a small fenestra. The lamina of the malleus is squarish and not deep, and the orbicular apophysis is elongated, with a basal constriction on the anterior margin (fig. 18C). The processus brevis of the incus is narrow and delicate.

Teeth: The upper incisors are orthodont with orange enamel on their anterior surfaces. The upper molar rows are moderately long (5.1–5.4 mm). The upper molars are brachyodont and pentalophodont (sensu Hershkovitz, 1962) without interpenetration of the labial and lingual flexi; labial and lingual cingula are not developed; the accessory labial roots are absent. The procingulum of M1 is slightly narrower than the protocone-paracone cusp pair, and the antero-medial flexus conspicuously divides a slightly smaller anterolingual conule from a larger anterolabial conule. The anteroloph is conspicuous and the paraflexus is recurved. The paraloph is oriented transversally to the median mure or the base of the mesoloph. The mesoloph is well developed and reaches perpendicularly the labial margin of the tooth; the metaflexus is nearly straight. The posteroloph is absent. M2 exhibits a strong anteroloph with a recurved paraflexus; the mesoloph is mostly absent or very reduced, the metaflexus is comma shaped, and the posteroloph is coalesced with the metacone. M3 is smaller than M2; its paraflexus, mesoflexus, and hypoflexus are conspicuous; and its metacone is obsolete (fig. 19C).

On the lower molars, the main cuspids are conspicuous and slightly alternating. The first lower molar (m1) has a narrow anteroconid and a distinct anteromedian flexid; the protolophid and anterolophid are short or coalesced; the anterolabial and anterolingual cingula are poorly developed. The mesoflexid is narrow and curved; the entoflexid is small or coalesced; the posteroflexid is narrow and almost straight; the hypo-

flexid is broad and oriented perpendicularly; and the mesolophid is very short or coalesced with the entoconid. On m2, the mesolophid is usually absent or short; and the anterolabial cingulum is conspicuous. The m3 has a subtriangular occlusal shape produced by the less developed entoconid; the mesoflexid and hypoflexid are conspicuous; and the posteroflexid is enclosed in an island (fig. 19G).

Mandible: The coronoid process is long, slender, and falciform. The angular process is short and anterior than the condylar process. The capsular process of the lower incisor alveolus is absent (fig. 25).

Hyoid apparatus: Hyoid morphology like that described for *Thomasomys cinereus* (observation made in six specimens).

Penis: Three fluid-preserved male specimens (MUSM 46875, 46883, 46887) were examined. The glans is medium sized, subcylindrical, relatively long (4.4 mm), and narrow (2.2 mm) (fig. 20C). The external surface is covered by epidermal spines overall except along the crater rim, which is spineless; dorsal and ventral grooves are absent, and the ventral notch is shallow. The crater lip circumscribes the entire crater opening and is separated from the spinous epithelium by a thick fold. The medial bacular mound is large, conical, and projects prominently from the crater lip; the lateral bacular mounds are small, deep, and barely visible externally. The tip of the medial bacular mound is oriented vertically. The urethral flaps are small, conical, and deeply buried within the crater; their tips are well separated and lack spines or other ornamentation. The dorsal papilla is very small, deep, rounded, and lack spines or other ornamentation.

Palatal rugae: Unknown.

Stomach: The stomach corresponds to the unilocular-hemiglandular morphotype (Carleton, 1973; Pacheco, 2003). The incisura angularis is shallow, and the bordering fold is thick and crosses the lesser curvature of the stomach slightly anterior to the incisura angularis; the bordering fold also recurves moderately to the left but not beyond the esophageal orifice (fig. 22C).

Gall bladder: Present.

Reproductive glands: Unknown.

Skeleton: Unknown.

Karyotype: Unknown.

MEASUREMENTS OF HOLOTYPE: GSL, 34.07; CIL, 31.46; CML, 20.3; LOF, 11.09; LN, 13.04; LD, 9.62; RL, 12.65; LIF, 6.64; LM, 5.25; BIF, 2.43; BR, 5.15; BPB, 3.35; BM1, 1.77; BN, 4.69; LIB, 5.05; ZB, 17.26; BB, 13.82; BZP, 2.63; DI, 1.78; HBC, 8.96; MFB, 2.40. Measurements of additional specimens are provided in table 3.

DISTRIBUTION: *Thomasomys shallqukucha* has a restricted distribution near the northeastern border of the department of Lambayeque, Peru. The Río Kañaryaku flows through this region to the Río Huancabamba, which ultimately joins the Río Marañón on the eastern versant of the Andes. All records are also west of the Río Chotano and south of the Huancabamba Depression (fig. 1). The altitudinal range is from 2550 m to 3330 m.

TAXONOMIC COMPARISONS: *Thomasomys shallqukucha* differs from *T. cinereus* by its dark brownish dorsal pelage (vs. grizzled ashy gray to dark gray in *T. cinereus*); metatarsals pale brownish (vs. whitish); tail longer than head and body length (Tail% = $[119 \pm 6]$, vs. $[103 \pm 8]$ %) and unicolored (vs. moderately bicolor); plantar surface of hind foot dark (vs. pale); the thenar and hypothenar pads separated by a distinct gap (vs. thenar and hypothenar pads closely approximated); zygomatic notches very shallow (vs. deep [55%] or shallow); interparietal conspicuously long anteroposteriorly (vs. moderately long); zygomatic plates slightly sloped backward (vs. vertically oriented); incisive foramina short, not approaching the anterior margins of the first molars (vs. long, and usually extended posteriorly between the first molars); median palatal process absent (vs. usually present); bullae moderately inflated (vs. not inflated); stapedial process of bulla reduced (vs. conspicuous); orbicular apophysis elongated with basal constriction on anterior margin (vs. knob shaped; table 4). Also, the glans penis of *T. shallqukucha* lacks dorsal and ventral grooves,

and the urethral flaps and dorsal papilla lack spines, whereas the glans penis of *T. cinereus* exhibits a conspicuous dorsal groove and a ventral shallow groove, and the urethral flaps and dorsal papilla exhibit some spines.

Thomasomys shallqukucha differs from *T. pagaibambensis* by its short mystacial vibrissae that barely extend behind the posterior margin of pinnae when laid back alongside the head (vs. longer vibrissae that extend conspicuously behind the posterior margin of pinnae); tail without a white tip (vs. tail usually white tipped); zygomatic notches very shallow (vs. shallow; fig. 13); zygomatic plates gently sloping backward (vs. vertically oriented); zygomatic process of maxilla and zygomatic process of squamosal closely approximated (vs. processes separated by a narrow jugal); orbicular apophysis elongated with basal constriction on anterior margin (vs. elongated with basal constriction and recurved); capsular process of lower incisor alveolus indistinct (vs. distinctly swollen); M3 hypoflexus distinct (vs. weak; table 4). Also, the stomach of *T. shallqukucha* has a shallower incisura angularis and the bordering fold is not markedly recurved to the left, whereas the stomach of *T. pagaibambensis* has a deeper incisura angularis and the bordering fold is distinctly recurved to the left (fig. 22); and the glans penis of *T. shallqukucha* lacks a dorsal groove and a distinct notch on the ventral wall, whereas the glans penis in *T. pagaibambensis* has a shallow dorsal groove and a conspicuous ventral notch.

Thomasomys shallqukucha is unlikely to be sympatric with *T. silvestris*, *T. caudivarius*, or *T. salazari*; nonetheless, *T. shallqukucha* could be readily differentiated from them by its broader rostrum and nasals, its extremely reduced zygomatic notch, and its short incisive foramina.

NATURAL HISTORY: This species inhabits the montane forests of northern Peru, which has also been called the Peruvian Yungas ecoregion of the Tropical and Subtropical Moist Broadleaf Forests biome (Dinerstein et al., 2017) (fig. 23B). The main tree components of the montane forests of Kañaris are members of Lauraceae (*Persea*,

Ocotea, *Nectandra*), Cunoniaceae (*Weinmannia*), Podocarpaceae (*Podocarpus*), Cecropiaceae (*Cecropia*), Myrtaceae (*Myrcianthes*), Moraceae (*Ficus*), Rubiaceae (*Cinchona*), Bignoniaceae (*Tabebuia*), Arecaceae (*Ceroxylon*), and tree ferns of the genus *Nephelea* (Llata-Quiroz and López-Mesones, 2005). In these forests, *Thomasomys shallqukucha* is sympatric with *T. taczanowskii* and *T. cf. aureus*.

Among specimens of *Thomasomys shallqukucha* with reproductive data, 10 males were collected in October (usually considered dry season); four had abdominal testes and six had scrotal testes; and one male specimen collected in November had scrotal testes. Of 10 females collected in October (dry season), three had closed vaginas, two had open vaginas, and five were lactating. Four female specimens collected in November had closed vaginas.

The stomach contents of two specimens contained insect remains and seeds. Some nematodes were also found in the antrum.

ETYMOLOGY: The name *shallqukucha* is a compound of two words in the Lambayeque dialect of Quichua: *shallqua* means “Jalca”: a Paramo-like ecoregion, typical of northwestern Peru (Weigend 2002, 2004)—and *ukucha* means “rodent.” The community of Kañaris speaks the Lambayeque dialect of Quichua, and it is probably one of the few Quichuan-speaking communities in northern Peru. This species is dedicated to the region of Kañaris, its people, and their interest in maintaining their montane forests.

***Thomasomys pagaibambensis*, new species**

Pagaibamba *Thomasomys*

Figures 6D, 8, 9, 10D, 11D, 11H, 12D, 13D, 15D, 16D, 17D, 18D, 19D, 19H, 20D, 22D, 26

Thomasomys cinereus, Pacheco 2015; part, not Thomas, 1882

HOLOTYPE: An adult female specimen in the Museo de Historia Natural de la Universidad Nacional Mayor de San Marcos (MUSM 40986).

The holotype is a skin, skull, and carcass, all in good condition, collected by Edith Salas Perez (field number ESP 384) on 29 September 2007.

PARATYPES: Twenty-three specimens from the same locality MUSM 40968–40985; 40987–40990.

TYPE LOCALITY: Peru, Department of Cajamarca, Province of Chota, District of Quericoto, Pagaibamba. 6.429585°S, 79.05792°W; 2902 m above sea level.

DIAGNOSIS: A medium-sized *Thomasomys* (table 3) that differs from its congeners by the following combination of characters: dorsal pelage brownish; metatarsal patch pale brownish; tail long, unicolored, usually with a white tip; thenar and hypothenar pads separated; plantar surface of hind foot slightly dark; nasals long with anterior half expanded; zygomatic notches shallow; interparietal bone wide and long anteroposteriorly; zygomatic plate with anterior margin vertical; incisor foramina short, approaching posteriorly in front of the anterior margins of the first molars; palate median process absent or indistinct; zygomatic process of the maxilla distinctly separated from the zygomatic process of the squamosal by a narrow jugal; capsular process of lower incisors alveolus distinctly swollen; M1 anteromedian flexus distinct; M3 hypoflexus reduced, and m1 anteromedian flexid distinct.

MORPHOLOGICAL DESCRIPTION: *Thomasomys pagaibambensis* is a medium-sized species (HBL = 121–158 mm) with long, soft, and dense dorsal fur (about 14 mm). Dorsal pelage is brownish (Clay Color, color 26 or Dark Drab, color 119B) with individual hairs slate colored basally. Ventral pelage is Pale Horn Color (color 92) or Pale Neutral Gray (color 86) with individual hairs slate-colored basally, and moderately counter-shaded with dorsal pelage (figs. 8, 9). The ears are moderately long (EL = 20–24 mm) and dark brown. Postauricular patches are not conspicuous. The mystacial vibrissae are long, extending behind the posterior margin of the pinnae when laid back alongside the head. The supraorbital vibrissae are short, extending barely to the posterior margin of the pinnae when laid back

alongside the head. The genal 1 vibrissae are absent. The tail is longer than combined length of head and body (Tail% = 122), comparatively thick, unicolored, and usually with a white tip. The hindfeet are moderately long (HFL = 28–34 mm) with metatarsals pale brownish. The manus are also pale brown. The plantar surface of hind foot is slightly dark. The thenar and hypothenar pads are widely separated (fig. 10D). Digit I of the hind foot (hallux) is moderately long, its claw extending close or to the first interphalangeal joint of dII. Digit V of hind foot is long, with claw extending about half the length of phalanx 2 of dIV.

Cranium: The skull is moderately long (CIL = 29.8–33.3 mm) with a flat or barely convex profile and a bump on the frontal region. The rostrum is relatively long and moderately broad (fig. 11D). A rostral tube is absent, and the gnathic process is small (figs. 12D, 15D). The nasals are long and tapering; the anterior half are expanded; the posterior margins are narrow, extending to the lacrimals and beyond the premaxillae. The zygomatic notches are shallow (fig. 13D). The interorbital region is moderately broad and hourglass shaped with rounded margins, and the frontal sinus are relatively inflated. The braincase is wide and oval shape. The lateral parietal processes are moderately large and subtriangular. The interparietal is wide and long anteroposteriorly, straplike, or rhomboidal. The zygomatic arches converge anteriorly to a moderate degree. The zygomatic plates are moderately broad, in breadth longer than the length of M1, and vertically oriented (fig. 15D). The premaxillae are conspicuously produced anteriorly beyond the incisors (fig. 15D). The zygomatic process of the maxilla is distinctly separated from the zygomatic process of the squamosal by a long and narrow jugal (fig. 16). The postglenoid foramen is small and placed anterior to a relatively larger subsquamosal fenestra. The tegmen tympani is robust and overlaps a distinct suspensory process of squamosal. The carotid circulatory pattern is pattern 1 (sensu Voss, 1988): a stapedia foramen, a groove on the inner surface of the squa-

mosal and the alisphenoid, and a sphenofrontal foramen all present. In the medial wall of the orbit, the ethmoid foramen is placed dorsal to M2; the ethmoturbinals are relatively small; the sphenopalatine foramen is bordered by the maxillary, ethmoid, and palatine bones; the optic foramen is moderate in size and is slightly posterior to M3. The paraoccipital process is larger and curved. The incisive foramina are usually short (in 84% of examined specimens) and extend posteriorly in front of the anterior margins of the first molars, and slightly broad with the anterior and posterior margins narrow (fig. 17D). The palate is short and wide (sensu Hershkovitz, 1962). The mesopterygoid fossa is broad, lyre shaped; a median posterior process of the palate is absent (in 77% of examined specimens) or poorly developed (23%). The sphenopalatine vacuities are absent or are represented by narrow slits along the basisphenoid and presphenoid bones. The parapterygoid fossa is triangular and shallow. The foramen ovale is of moderate size, the alisphenoid strut is present, and the middle lacerate foramen is narrow but conspicuous. The auditory bullae are flask shaped, moderately inflated, with short and narrow Eustachian tubes; the stapedia process of bulla is reduced. The internal carotid canal is bounded by the basioccipital and the ectotympanic (auditory bulla), but not by the petiotic. The basioccipital is moderately broad, and the mastoid (the occipital exposure of the petiotic) is either imperforate or has only a small fenestra. The lamina of the malleus is squarish and not deep; the orbicular apophysis is elongated and recurved, with a basal constriction (fig. 18D). The processus brevis of incus is narrow and delicate.

Teeth: The upper incisors are orthodont with orange enamel on their anterior surfaces. The upper molar rows are moderately long (5–5.8 mm). The upper molars are brachyodont and pentalophodont (sensu Hershkovitz, 1962) without interpenetration of the labial and lingual flexi; labial and lingual cingula are not developed; and the accessory labial roots are absent. The procingulum of M1 is slightly narrower than

the protocone-paracone cusp pair, and the anteromedian flexus is distinct. The anteroloph is conspicuous but usually coalesced with the anterocone and the paraflexus is recurved. The paraloph is oriented transversally to the median mure, and sometimes to the base of the mesoloph. The mesoloph is well developed and reaches perpendicularly the labial margin of the tooth; the metaflexus is slightly curved; and the posteroloph is absent. M2 exhibits a strong anteroloph with a recurved paraflexus; the mesoloph is narrow, complete, and reaches the labial margin of the tooth; the metaflexus is comma-shaped, and the posteroloph is coalesced with the metacone. M3 is much smaller than M2, only its paraflexus is distinct, and its hypoflexus is mostly absent or reduced (fig. 19D).

On the lower molars, the main cuspids are conspicuous and slightly alternating. The first lower molar (m1) has a distinct anteromedian flexid; the protolophid and the anterolophid are short or coalesced; the anterolabial and anterolingual cingula are poorly developed; the mesoflexid is narrow and curved; the entoflexid is coalesced; the posteroflexid is narrow and slightly curved; the hypoflexid is broad, deep, and oriented slightly transversally; and the mesolophid is narrow and complete or coalesced with the entoconid in adult or older specimens. On m2, the mesolophid is short and the anterolabial cingulum is small. On m3, the mesoflexid and hypoflexid are conspicuous; but its posteroflexid is reduced or absent (fig. 19H).

Mandible: The coronoid process is long, slender, and falciform. The angular process is short and anterior than the condylar process. The capsular process of the lower incisor alveolus is distinctly swollen (fig. 26).

Hyoid apparatus: Hyoid morphology like that described for *Thomasomys cinereus* (observation made in six specimens).

Penis: Three fluid-preserved male specimens (MUSM 40965, 40998, 41004) were examined. The glans is subcylindrical, comparatively short (4 mm), and wide (2.34 mm) (fig. 20D). The external surface is covered by epidermal spines



FIGURE 26. Dorsal, ventral, and lateral views of the cranium and mandible of *Thomasomys pagaibambensis* (MUSM 39527), an adult female from Alto Pagaibamba, Querocoto district, Chota province, Cajamarca department, Peru. Scale bar = 10 mm.

overall except along the crater rim, which is spineless. A dorsal shallow groove and a distinct ventral notch are present. Laterally, the glans is undivided. The crater lip circumscribes the entire crater opening and is separated from the spinous epithelium by a thick fold. The medial bacular

mound is large and conical, projecting beyond the crater lip; the lateral bacular mounds are small and barely project beyond the crater lip. The tip of the medial bacular mound is oriented vertically. The urethral flaps are small, conical, and deeply buried within the crater; their tips are

well separated and lack ornamentation. The dorsal papilla is large, conical, and lack spines or other ornamentation.

Palatal rugae: Unknown.

Stomach: The stomach corresponds to the unilocular-hemiglandular morphotype (Carleton, 1973; Pacheco, 2003). The incisura angularis is comparatively deeper, and the bordering fold is also comparatively thicker and crosses the lesser curvature of the stomach slightly anterior to the incisura angularis; the bordering fold recurves to the left slightly beyond the esophageal orifice (fig. 22D).

Gall bladder: Present.

Reproductive glands: Macroscopic preputial glands are absent.

Skeleton: The vertebral count is 7 cervical, 13 thoracic, 6 lumbar, 4 sacral, and 41 caudal vertebrae; and the same skeletons each have 13 pairs of ribs. The supratrochlear fenestra of humerus is usually absent (5 of 6 examined specimens). The first caudal vertebrae have chevron bones unfused (in 5 of 6 examined specimens). On the calcaneus, the trochlear process levels its posterior articular facet. The peroneal process of the fifth metatarsal is moderately long but does not extend to the proximal edge of the cuboid.

Karyotype: Unknown.

MEASUREMENTS OF HOLOTYPE: GSL, 34.52; CIL, 31.78; CML, 20.88; LOF, 10.89; LN, 13.56; RL, 12.44; LD, 9.2; LIF, 6.31; LM, 5.7; BIF, 2.56; BR, 5.71; BPB, 3.57; BM1, 1.71; BN, 4.08; LIB, 5.45; ZB, 18.23; BB, 14.1; BZP, 2.63; DI, 1.76; HBC, 9.44; MFB, 2.77. Measurements of additional specimens are provided in table 3.

DISTRIBUTION: *Thomasomys pagaibambensis* is distributed in the mountains of the Pagaibamba Protection Forests, province of Chota, department of Cajamarca, Peru. All records are also south of the Huancabamba Depression, west of Río Chotano, and north of Río Chancay (fig. 1). The elevation range is from 2530 m to 3370 m.

TAXONOMIC COMPARISONS: *Thomasomys pagaibambensis* differs from *T. cinereus* by its brownish dorsal pelage (vs. grizzled ashy gray to dark gray in *T. cinereus*); mystacial vibrissae long,

extending posteriorly behind margin of pinnae when laid back alongside the head (vs. shorter in *T. cinereus*, table 4); metatarsal pale brown (vs. whitish); tail longer than head-and-body length (Tail% = $[122 \pm 8]$, vs. $[103 \pm 8]$ %), unicolored (vs. moderately bicolor), and tip usually white (vs. a tail without a white tip); plantar surface of hind foot slightly dark (vs. pale); thenar and hypothenar pads separated by a distinct gap (vs. thenar and hypothenar pads closely approximated); zygomatic notch shallow (vs. deep [55%] or shallow in *T. cinereus*); interorbital region moderately broad (vs. narrow); frontal sinus relatively inflated (vs. not inflated); interparietal conspicuously long anteroposteriorly (vs. moderately long, fig. 14); the zygomatic process of the maxilla and the zygomatic process of the squamosal are separated by a narrow jugal bone (vs. both processes closely approximated); incisive foramina short, not approaching the anterior margins of the first molars (vs. usually extending between the first upper molars in *T. cinereus*); palatal median process usually absent (vs. present); bullae moderately inflated (vs. small, not inflated); stapedial process of bulla reduced (vs. distinct); orbicular apophysis elongated with basal constriction and recurved (vs. knob shaped); capsular process distinctly swollen (vs. absent); M3 hypoflexus reduced (vs. distinct in *T. cinereus*). Also, the stomach of *T. pagaibambensis* has a deeper incisura angularis and a thicker bordering fold more recurved to the left, whereas the stomach of *T. cinereus* has a shallower incisura angularis and a thinner bordering fold not recurved to the left (fig. 22); and the glans penis in *T. pagaibambensis* is comparatively smaller with a conspicuous ventral notch and a shallow dorsal groove, whereas the glans penis in *T. cinereus* exhibits a shallow ventral notch and a conspicuous dorsal groove.

Thomasomys pagaibambensis is unlikely to be sympatric with *T. silvestris*, *T. caudivarius*, or *T. salazari*; nonetheless, *T. pagaibambensis* could be readily differentiated from them by its broader rostrum and nasals, its larger interparietal, and its short incisive foramina.

NATURAL HISTORY: This species inhabits the montane forests of the Pagaibamba Cordillera, which is part of the Peruvian Yungas ecoregion of the Tropical and Subtropical Moist Broadleaf Forests biome (Dinerstein et al., 2017) and the Jalca ecoregion, above 3200 m, which has also been called the Cordillera Central Páramo (Dinerstein et al., 2017). In the Jalca, there is a predominance of grasses of the family Poaceae (*Stipa*, *Festuca*, and *Calamagrostis*), and trees of the families Asteraceae (*Werneria*) and Rosaceae (*Polylepis*) occur on rocky slopes (Roncal-Rabanal, 2018). Extensive data on the flora and fauna of Bosque de Protección Pagaibamba was recently summarized by Roncal-Rabanal (2018).

In the montane forests of Pagaibamba Protected forests, *Thomasomys pagaibambensis* is sympatric with *T. taczanowskii*, *T. pyrrhonotus*, and *T. cf. aureus*; and the thomasomyine *Chilomys instans* (Medina et al., 2016). Medium and large mammals (i.e., *Cuniculus taczanowskii*, *Dinomys branickii*, *Sylvilagus andinus*, *Leopardus pardalis*, *Puma concolor*, *Lycalopex culpaeus*, *Tremarctos ornatus*, *Conepatus chinga*, *Eira barbara*, *Mustela frenata*, *Tapirus pinchaque*, *Mazama* sp., *Odocoileus virginianus*) have also been reported (Jiménez et al., 2010; Diaz and Pacheco, 2022).

Among specimens with reproductive data, seven males were collected in September and October (usually considered dry season); all had abdominal testes (length ≤ 10 mm). Among specimens collected in May and November (wet season), nine had scrotal testes and two had abdominal testes. Of 17 females collected in September and October (dry season), 13 had closed vaginas, and four had open vaginas. Of 17 specimens collected in April, May, and November (wet season), 10 had closed vaginas, six had open vaginas, and one was pregnant.

The stomach contents of four specimens contained some insect remains and seeds. One of them was full of seeds of *Greigia* sp. (Bromeliaceae) and large unidentified nematodes in the antrum.

ETYMOLOGY: The species epithet refers to the type locality, which is located in the Pagaib-

amba Protected Forest in the Cordillera Pagaibamba, one of the few relict forests in the department of Cajamarca.

DISCUSSION

This study is based on the largest series of morphological specimens closely related to *Thomasomys cinereus* and the largest mitochondrial DNA dataset ever assembled for the species in its previously understood sense. Our phylogenetic analyses of cytochrome *b* sequence data together with our morphological comparisons of voucher material suggest that *T. cinereus* sensu lato (Pacheco, 2015) is a species complex composed of at least four distinct lineages, herein referred to *T. cinereus* sensu stricto and three new species: *T. lojapiuranus* from the montane forests of the Peruvian department of Piura and the Ecuadorean province of Loja; *T. shallqukucha* from the mountains of the department of Lambayeque (Peru); and *T. pagaibambensis* from the Cordillera Pagaibamba, department of Cajamarca (Peru). Of these taxa, *T. lojapiuranus* is distributed north of the Huancabamba Depression—long recognized as a biogeographically important feature of the tropical Andes (e.g., by Parker et al., 1985)—whereas *T. cinereus*, *T. shallqukucha*, and *T. pagaibambensis* are distributed south of this landscape feature.

In addition, our phylogenetic analyses confirm the monophyly of the Cinereus Group as defined by Pacheco (2015) and as emended in the Introduction to this report. Although weakly supported, the Cinereus Group now consists of at least 18 currently recognized species (*T. australis*, *T. bombycinus*, *T. caudivarius*, *T. cinereus*, *T. cinnamomeus*, *T. daphne*, *T. erro*, *T. fumeus*, *T. hudsoni*, *T. lojapiuranus*, *T. onkiro*, *T. pagaibambensis*, *T. paramorum*, *T. salazari*, *T. shallqukucha*, *T. silvestris*, *T. ucucha*, *T. vulcani*) and two candidate species from Ecuador (*Thomasomys* sp. 1 and *Thomasomys* sp. 2). Future revisionary research will doubtless increase this tally. In particular, our species delimitation results suggest that *T. daphne* includes two candidate taxa as

previously suggested by Pacheco (2015: 642). As discussed above (in Remarks in the account for *T. lojapiuranus*), our results corrected identifications for several terminal taxa previously sequenced by Lee et al. (2018) and Brito et al. (2019) and support the hypothesis that their “*Thomasomys* sp. 1” (herein also *Thomasomys* sp. 1) is another candidate species. However, their “*T. cinereus*” (here *Thomasomys* sp. 2) appears to be more closely related to *T. salazari* and *T. caudivarius* than to *T. cinereus* sensu stricto and likely also represents an undescribed taxon. Therefore, the Cinereus Group potentially comprises at least 21 species based on these molecular results.

Bruto et al. (2019) recognized four clades (labelled A–D) within the Cinereus Group, of which clade B consisted only of *T. erro*. Of their three multispecies lineages, clades A and C were strongly supported in our analyses, whereas clade D was only weakly supported, probably due to denser taxon sampling in this report. To be more conservative, we opt to recognize only two strongly supported multispecies clades within the Cinereus Group (fig. 4). Our clade A (which corresponds to the clade A of Brito et al. [2019]) includes *Thomasomys fumeus*, *T. bombycinus*, *T. vulcani*, *T. australis*, *T. daphne*, and *Thomasomys* sp. 3 (sensu Pacheco, 2003), whereas our clade B includes *T. caudivarius*, *T. cinereus*, *T. cinnameus*, *T. hudsoni*, *T. lojapiuranus*, *T. pagaibambensis*, *T. paramorum*, *T. salazari*, *T. shallqukucha*, *T. silvestris*, *T. ucucha*, and two candidate species from Ecuador (*Thomasomys* sp. 1 and *Thomasomys* sp. 2). Only two species are orphaned by this scheme—*T. erro* and *T. onkiro*—because their relationships remain inadequately supported in our analyses.

In spite of our improved understanding of the phylogenetic relationships within the Cinereus Group, these results remain preliminary and incomplete. Sequence data from additional genes are clearly needed, and several species of the Cinereus Group from Colombia and Venezuela are still unrepresented by genetic data (i.e., *T. cinereiventer*, *T. contradic-*

tus, *T. dispar*, *T. emeritus*, *T. hylophilus*, *T. laniger*, *T. monochromos*, *T. niveipes*, and *T. vestitus*). Pacheco (2015) included 23 species in his Cinereus group, which now additionally includes *T. salazari*, *T. lojapiuranus*, *T. pagaibambensis*, *T. shallqukucha*, and the three candidate unnamed species listed in table 1. With a potential total of 30 taxa, the Cinereus Group is by far the largest of the seven species groups proposed by Pacheco (2015) within *Thomasomys*.

Among other remaining phylogenetic issues, evidence for the monophyly of *Thomasomys* and for the interrelationships among currently recognized species groups remains unconvincing. Several phylogenies that have recovered a monophyletic *Thomasomys* with different genetic markers (*cytb*, IRBP, BRCA1, GRH, RAG1, Acp5; Schenk et al., 2013; Steppan and Schenk, 2017; Parada et al., 2013, 2015; Lee et al., 2011, 2015, 2018; Brito et al., 2019, 2021; Ruelas and Pacheco, 2021a) have sampled only a limited number of species, and none has included representatives of all species groups. About half the currently recognized species have yet to be included in any phylogenetic analysis, so Pacheco (2003)’s hypothesis of *Thomasomys* as a polyphyletic genus diagnosed by morphological characters still awaits a formal molecular-phylogenetic evaluation. Similarly, the monophyly of Pacheco’s (2003, 2015) seven species groups remains untested with molecular data. Although the results of several molecular analyses partially support Pacheco’s species-group classification (see Salazar-Bravo and Yates, 2007; Lee et al., 2018; Brito et al., 2019), other results are incongruent.¹ Because this is not the place to enumerate such inconsistent analytic results nor to explain the real or assumed misidentifications on which some of them are based, we reserve such topics for future reports.

¹ For example, Brito et al. (2019) recovered *Thomasomys kalinowskii* (sequence AF108678) is a sister taxon to the Baeps and Notatus groups rather than as member of the Incanus Group as proposed by Pacheco (2003, 2015).

BIOGEOGRAPHIC IMPLICATIONS

The Huancabamba Depression (also called the Huancabamba Deflection) transects the departments of Piura, Lambayeque, and Cajamarca in northern Peru. In this region, the Andes reach their lowest elevation point at the Abra de Porculla (2145 m), and they make a rather abrupt change in direction from NW/SE to SW/NE (Gansser, 1973; Duellman, 1979; Jaillard et al., 1990). The Huancabamba Depression has been proposed as a barrier between northern and central Andean faunas because it is thought to limit the dispersion of species living at high elevation (Parker et al., 1985; Patterson et al., 1992; Pacheco and Patterson, 1992; Albuja and Patterson, 1996; Vivar et al., 1997; Duellman and Pramuk, 1999; Pacheco, 2002; Lunde and Pacheco, 2003). The habitat in the Huancabamba Depression is mostly open shrubby vegetation or dry forests (Linares-Palomino, 2004) that have a mammalian fauna resembling those of adjacent lowland forests (Ruelas and Pacheco, 2021b). Such habitats are not inhabited by species of *Thomasomys* (Pacheco, 2015) and—consistent with its hypothesized role as a dispersal barrier—the Huancabamba Depression appears to separate the distribution of *T. lojapiuranus* in the north from the distributions of the other three species in this complex (*T. cinereus*, *T. shallqukucha*, and *T. pagaibambensis*), which are all found to the south. Of the latter, *T. shallqukucha* and *T. pagaibambensis* are both distributed in the Cordillera Occidental, and no major river has previously been suggested as a potential barrier between the small ranges that they occupy. However, the Río La Leche (which originates in the Cordillera Occidental and flows westward to the Pacific Ocean; fig. 1) might be such a barrier. Although the montane forests of the Kañaris and Pagaibamba ranges are apparently continuous, the data compiled and analyzed in this report suggest that *T. shallqukucha* and *T. pagaibambensis* are independently evolving lineages evolving despite their geographic proximity (about 35 km separates their known distributional ranges).

Similarly, the distributions of *T. pagaibambensis* and *T. cinereus* are separated by a map distance of only about 45 km, with no known intervening barrier. However, the Río Maichil in Cajamarca department (a tributary of the Río Chancay that runs westward to the Pacific Ocean) might be acting as a barrier, as might the dry-forested valley of the Río Chotano, the floor of which is mostly below 2000 m. To our knowledge, these minor rivers (La Leche, Maichil, Chotano) and the valleys they occupy have never previously been suggested as zoogeographic barriers, and additional collecting is needed to test their local importance as drivers of biodiversity south of the Huancabamba Depression.

Although we have not explicitly tested the hypothesis of isolation by distance among taxa in the *Thomasomys cinereus* complex, the F_{ST} values we computed among them are similar and appear uncorrelated with geographic proximity. For example, the F_{ST} value between *T. lojapiuranus* and *T. pagaibambensis* on the one hand and between *T. pagaibambensis* and *T. cinereus* on the other are the same (0.87) in spite of the fact that the geographic distributions of *T. lojapiuranus* and *T. pagaibambensis* are separated by about 390 km, whereas the distributions of *T. pagaibambensis* and *T. cinereus* are separated by about 50 km. Also, the highest fixation index we computed ($F_{ST} = 0.96$) was that between *T. shallqukucha* and *T. pagaibambensis*, which are geographically closer to one another than to either of the other species.

Although its geographic range is smaller now than was previously thought, *Thomasomys cinereus* is still widely distributed: from the Río Marañón westward to the Pacific versant of the Cordillera Occidental, a large extent of montane forest, jalca, and puna. The northern and southern limits of this distribution are still not precisely known, although they might correspond to the Río Chancay on the north, and Río Tablachaca and Río Crisnejas on the south. Morphological and genetic variability within *T. cinereus* sensu stricto appears to be geographically structured, and the average intraspecific

genetic distance we computed for this species (1.39%) is substantially higher than the corresponding values for *T. lojapiuranus*, *T. shal-lukucha*, and *T. pagaibambensis* (0.22%–0.39%). At present, montane forests within the geographic range of *T. cinereus* are highly fragmented, probably due to human interventions that date to pre-Hispanic times (Sylvester et al., 2017), but also by naturally occurring nonforest (puna or jalca) vegetation. Because our collection data suggest that *T. cinereus* is closely associated with montane forest, its current distribution suggests that either most of this region was once covered by montane forests that have since disappeared by natural or anthropogenic causes or that the species actually survives at low densities in open habitats.

Thomasomys cinereus is not known to occur east of the Río Marañón despite frequent and extensive collecting in the eastern cordillera dating back to the late 19th century (Thomas, 1894, 1926a, 1926b, 1926c, 1927a, 1927b; Osgood, 1914; Thomas and Leger, 1926; Gardner and Romo R., 1993; Leo L. and Gardner, 1993; Ruelas et al., 2021), so its absence in the eastern cordillera is unlikely to be a sampling artifact. Pacheco (2015) suggested that the Río Marañón is a formidable dispersal barrier for species of *Thomasomys*, as it apparently is also for species of *Akodon* (Jiménez et al., 2013), *Neacomys* (Hurtado and Pacheco 2017), *Phyllotis* (Pacheco et al., 2014; Rengifo and Pacheco, 2015), and *Nephelomys* (Ruelas et al., 2021).

Taking a larger biogeographic perspective, our results suggest that species richness of the Cinereus Group is higher in the Northern Andes (north of the Huancabamba Depression; i.e., from Venezuela to northern Peru) than it is in the Central Andes (south of the Huancabamba Depression), where only a few species are known to occur (i.e., *T. daphne*, *T. australis*, and *T. onkiro*), all to the east of the Río Marañón (Pacheco, 2015). This biogeographic pattern is consistent with Voss's (2003) suggestion that Ecuador is a center of endemism for *Thomasomys*. Previous studies (Brito et al., 2019, 2021;

Ruelas and Pacheco, 2021a) also support this pattern—at least for the Cinereus and Baeops groups—but we should emphasize that other congeneric clades (including the Notatus, Incanus, Macrotis, and Oreas groups) are endemic to the montane forests of the Central Andes east of the Río Marañón (Pacheco, 2015).

Ongoing taxonomic research will doubtless refine our biogeographic knowledge of *Thomasomys*. Among other currently deficient data, several additional species remain to be described (Pacheco (2003, 2015; Lee et al., 2018; Brito et al., 2019; Brito et al., 2021; Ruelas and Pacheco, 2021a), mostly in the Aureus and Cinereus groups. The discovery of new species is not unexpected because analyses of molecular sequence data have revealed the existence of cryptic species in several other sigmodontine genera, including *Neacomys* (Sánchez-Vendizú et al., 2018; Semedo et al., 2020), *Nephelomys* (Ruelas et al., 2021), and *Rhipidomys* (Brito et al., 2017). This taxonomic research and accumulating new records of *Thomasomys* (e.g., Moreno-Cárdenas and Novillo-Gonzalez, 2020; Pacheco, 2021) are improving our knowledge of the diversity and distribution of the genus, but we are still far from a comprehensive analysis of diversification and biogeography of these quintessentially montane-forest rodents.

ACKNOWLEDGMENTS

We thank R. Cadenillas, K. Cervantes, L. Huamani, C. Jiménez, E. Rengifo, M. Peralta, E. Salas, A. Solis, C. Tello, L. Luna-Wong, S. Velazco, and E. Vivar, who have collected with us or independently several specimens of *Thomasomys cinereus* sensu lato for the MUSM collection employed in this work. J.L. Patton, M.D. Carleton, D. Lunde, R.S. Voss, B.D. Patterson, P. Myers, M.S. Hafner, L. Albuja, S. Burneo, and P. Jenkins graciously allowed access to specimens under their care and/or facilitated the visit to their institution (to V.P.). Special thanks to Lucía Luna-Wong, who kindly provided the photographs of the holotype of *Thomasomys cinereus*,

and to Mario López Mesones for sharing his deep knowledge of the Lambayeque region. Klaus Cervantes identified seeds found in stomach contents and shared his expertise on habitat description. Gerardo Lamas helped resolve issues of taxonomic nomenclature. Financial support was provided by INNOVATE (formerly FINCyT) with Contract No. 402-PNIPC-PIBA-2014 (to VP), which funded several expeditions to northern Peru and implemented our Laboratory of Evolutionary Biology in the Mammalogy Department of the MUSM. Additional support came from the Vicerrectorado de Investigación y Posgrado de la Universidad Nacional Mayor de San Marcos (UNMSM) with the projects B1710043e, B18104092e, B19100991, and B20100321 (to the Study Group Diversidad de Mamíferos y sus Parásitos [DIMAPA] lead by VP). We thank Guillermo D'Elia for his help with molecular analyses at the beginning of the project, and Pablo Moreno for kindly sharing some samples from Ecuador. Silvia Diaz efficiently helped to handle specimens and the database, and skillfully improved and composed the figures.

REFERENCES

- Albuja, L., and B.D. Patterson. 1996. A new species of northern shrew-opossum (Paucituberculata: Caenolestidae) from the Cordillera del Cóndor, Ecuador. *Journal of Mammalogy* 77: 41–53.
- Anderson, S., and T.L. Yates. 2000. A new genus and species of phyllotine rodent from Bolivia. *Journal of Mammalogy* 81: 18–36.
- Anthony, H.E. 1923. Preliminary report on Ecuadorean mammals. No. 3. *American Museum Novitates* 55: 1–14.
- Anthony, H.E. 1924. Preliminary report on Ecuadorean mammals. No. 4. *American Museum Novitates* 114: 1–6.
- Anthony, H.E. 1925. New species and subspecies of *Thomasomys*. *American Museum Novitates* 178: 1–4.
- Anthony, H.E. 1926. Preliminary report on Ecuadorean mammals. No. 7. *American Museum Novitates* 240: 1–6.
- Baker, R.J., and R.D. Bradley. 2006. Speciation in mammals and the genetic species concept. *Journal of Mammalogy* 87: 643–662.
- Bandelt, H.J., P. Forster, and A. Röhl. 1999. Median-joining networks for inferring intraspecific phylogenies. *Molecular Biology and Evolution* 16: 37–48.
- Bangs, O. 1900. List of the mammals collected in the Santa Marta region of Colombia by W.W. Brown, Jr. *Proceedings of the New England Zoological Club* 1: 87–102.
- Bouckaert, R. et al. 2019. BEAST 2.5: an advanced software platform for Bayesian evolutionary analysis. *PLOS Computational Biology* 15: e1006650.
- Bradley, R.D., and R.J. Baker. 2001. A test of the genetic species concept: cytochrome *b* sequences and mammals. *Journal of Mammalogy* 82: 960–973.
- Brito, J.M., et al. 2017. New species of arboreal rat of the genus *Rhipidomys* (Cricetidae, Sigmodontinae) from Sangay National Park, Ecuador. *Neotropical Biodiversity* 3: 65–79.
- Brito, J., et al. 2019. Diversidad insospechada en los Andes de Ecuador: filogenia del grupo “cinereus” de *Thomasomys* y descripción de una nueva especie (Rodentia, Cricetidae). *Mastozoología Neotropical* 26: 308–330.
- Brito, J., S. Vaca-Puente, C. Koch, and N. Tinoco. 2021. Discovery of the first Amazonian *Thomasomys* (Rodentia, Cricetidae, Sigmodontinae): a new species from the remote Cordilleras del Cóndor and Kutukú in Ecuador. *Journal of Mammalogy* 102 (2): 615–635.
- Brown, J.C. 1971. The description of mammals. 1. The external characters of the head. *Mammals Review* 1: 151–168.
- Brown, J.C., and D.W. Yalden. 1973. The description of mammals. 2. Limbs and locomotion of terrestrial mammals. *Mammals Review* 3: 107–134.
- Carleton, M.D. 1973. A survey of gross stomach morphology in New World Cricetinae (Rodentia, Muroidea), with comments on functional interpretations. *Miscellaneous Publications of the Museum of Zoology University of Michigan* 146: 1–43.
- Carleton, M.D. 1980. Phylogenetic relationships in Neotomine-Peromyscine rodents (Muroidea) and a reappraisal of the dichotomy within New World Cricetinae. *Miscellaneous Publications of the Museum of Zoology University of Michigan*, 157: 1–146.
- Carleton, M.D., and G.G. Musser. 1984. Muroid rodents. In S. Anderson and J.K. Jones, Jr. (editors), *Orders and families of Recent mammals of the world*: 289–379. New York: John Wiley and Sons.
- Carleton, M.D., and G.G. Musser. 1989. Systematic studies of oryzomyine rodents (Muridae, Sigmo-

- dontinae): a synopsis of *Microryzomys*. Bulletin of the American Museum of Natural History 191: 1–83.
- Coues, E. 1884. *Thomasomys*, a new subgeneric type of *Hesperomys*. American Naturalist 18: 1275–1275.
- Darriba, D., G.L. Taboada, R. Doallo, and D. Posada. 2012. jModelTest 2: more models, new heuristics and parallel computing. Nature Methods 9: 772.
- D'Elía, G. 2003. Phylogenetics of Sigmodontinae (Rodentia, Muroidea, Cricetidae), with special reference to the akodont group, and with additional comments on historical biogeography. Cladistics 19: 307–323.
- de Queiroz, K., 2007. Species concepts and species delimitation. Systematic Biology 56: 879–886.
- Díaz, S., and V. Pacheco. 2022. Confirmation of the occurrence of Andean cottontail, *Sylvilagus andinus* (Thomas, 1897) (Leporidae, Lagomorpha), in Peru. Check List 18 (4): 867–873.
- Dinerstein, E., et al. 2017. An ecoregion-based approach to protecting half the terrestrial realm. Bioscience 67: 534–545.
- Duellman, W.E. 1979. The herpetofauna of the Andes: patterns of distribution, origin, differentiation and present communities. In W.E. Duellman (editor), The South American herpetofauna: its origin, evolution and dispersal: 371–459. Lawrence, KS: University of Kansas Natural History Museum.
- Duellman, W.E., and J.B. Pramuk. 1999. Frogs of the genus *Eleutherodactylus* (Anura: Leptodactylidae) in the Andes of northern Peru. Scientific Papers, Natural History Museum, University of Kansas 13: 1–78.
- Durden, L.A., and G.G. Musser. 1994. The sucking lice (Insecta, Anoplura) of the world: a taxonomic checklist with records of mammalian hosts and geographical distributions. Bulletin of the American Museum of Natural History 218: 1–90.
- Esselstyn, J. 2017. LSMZ Mammals Collection. Louisiana State University Museum of Natural Science. Occurrence dataset [doi: 10.15468/wxiqf6] via GBIF (<http://www.gbif.org/occurrence/45912597>), accessed March 15, 2019.
- Excoffier, L., and H.E.L. Lischer. 2010. Arlequin suite ver 3.5: a new series of programs to perform population genetics analyses under Linux and Windows. Molecular Ecology Resources 10: 564–567.
- Excoffier, L., P.E. Smouse, and J.M. Quattro. 1992. Analysis of molecular variance inferred from metric distances among DNA haplotypes: application to human mitochondrial DNA restriction data. Genetics 131: 479–491.
- Fujisawa, T., and T.G. Barraclough. 2013. Delimiting species using single-locus data and the generalized mixed Yule coalescent approach: A revised method and evaluation on simulated data sets. Systematic Biology 62: 707–724.
- Gansser, A. 1973. Facts and theories on the Andes (26th William Smith lecture). Journal of the Geological Society of London 129 (2): 93–131.
- Gardner, A.L., and M. Romo R. 1993. A new *Thomasomys* (Mammalia: Rodentia) from the Peruvian Andes. Proceedings of the Biological Society of Washington 106: 762–774.
- Gyldenstolpe, N. 1932. A manual of Neotropical sigmodont rodents. Kungliga Svenska Vetenskapsakademien Handlingar 11 (3): 1–164.
- Hanson, J.D. 2008. Molecular phylogenetics of Oryzomyini: does a multigene approach help resolve a systematic conundrum? Ph.D. dissertation, [[DEPARTMENT?]], Texas Tech University, Texas.
- Hershkovitz, P. 1962. Evolution of Neotropical cricetine rodents (Muridae) with special reference to the phyllotine group. Fieldiana: Zoology 46:1–524.
- Hooper, E.T., and B.S. Hart. 1962. A synopsis of recent North American microtine rodents. Miscellaneous Publications, Museum of Zoology, University of Michigan 120: 1–68.
- Hooper, E.T., and G.G. Musser. 1964. The glans penis in neotropical cricetines (family Muridae) with comments on classification of muroid rodents. Miscellaneous Publications, Museum of Zoology, University of Michigan 123: 1–57.
- Howell, A.B. 1926. Anatomy of the woodrat (Monograph of the American Society of Mammalogy 1). Baltimore: Williams and Wilkins.
- Hurtado, N., and V. Pacheco. 2017. Revision of *Neacomys spinosus* (Thomas, 1882) (Rodentia: Cricetidae) with emphasis on Peruvian populations and the description of a new species. Zootaxa 4242 (3): 401–440.
- Jaillard, E., P. Soler, G. Carlier, and T. Mourier. 1990. Geodynamic evolution of the northern and central Andes during early to middle Mesozoic times: a Tethyan model. Journal of the Geological Society, London 141: 1009–1022.
- Jiménez, C., et al. 2010. Camera trap survey of medium and large mammals in a montane rainforest of northern Peru. Revista Peruana de Biología 17 (2): 191–196.
- Jiménez, C.F., V. Pacheco, and D. Vivas. 2013. An introduction to the systematics of *Akodon orophilus* Osgood, 1913 (Rodentia: Cricetidae) with the

- description of a new species. *Zootaxa* 3669: 223–242.
- Johnson, P.T. 1972. Sucking lice of Venezuelan rodents, with remarks on related species (Anoplura). *Brigham Young University Science Bulletin, Biological Series* 17: 1–62.
- Korkmaz, S., D. Goksuluk, and G. Zararsiz. 2014. MVN: An R Package for Assessing Multivariate Normality. *R Journal* 6: 151–162.
- Kuch, M., et al. 2002. Molecular analysis of an 11,700-year-old rodent midden from the Atacama Desert, Chile. *Molecular Ecology* 11: 913–924.
- Kumar, S., G. Stecher, and K. Tamura. 2016. MEGA7: Molecular evolutionary genetics analysis version 7.0 for bigger datasets. *Molecular Biology and Evolution* 33: 1870–1874.
- Lance, R.F., M.L. Kennedy, and P.L. Leberg. 2000. Classification bias in discriminant function analyses used to evaluate putatively different taxa. *Journal of Mammalogy* 81 (1): 245–249.
- Lee, T.E., C. Boada-Terán, A.M. Scott, S.F. Burneo, and J.D. Hanson. 2011. Small mammals of Sangay National Park, Chimborazo Province and Morona Santiago Province, Ecuador. *Occasional Papers, Museum of Texas Tech University* 305: 1–16.
- Lee, T.E., Jr., et al. 2015. Small mammals of Guandera Biological Reserve, Carchi Province, Ecuador and comparative Andean small mammal ecology. *Occasional Papers of the Museum of Texas Tech University* 334: 1–17.
- Lee, T.E., Jr., et al. 2018. Mammals of Yacuri National Park, Loja, Province, Ecuador. *Occasional Papers of the Museum of Texas Tech University* 357: 1–17.
- Lee, T.E., Jr., N. Tinoco, and J. Brito. 2022. A new species of Andean mouse of the genus *Thomasomys* (Cricetidae, Sigmodontinae) from the eastern Andes of Ecuador. *Vertebrate Zoology* 72: 219–233.
- Leo, L.M., and A.L. Gardner. 1993. A new species of a giant *Thomasomys* (Mammalia: Muridae: Sigmodontinae) from the Andes of northcentral Peru. *Proceedings of the Biological Society of Washington* 106: 417–428.
- Letunic, I., and P. Bork. 2016. Interactive Tree of Life (iTOL) v3: an online tool for the display and annotation of phylogenetic and other trees. *Nucleic Acids Research* 44: W242–W245.
- Linares-Palomino, R. 2004. Los bosques tropicales estacionalmente secos: II. Fitogeografía y composición florística. *Arnaldoa* 11: 103–138.
- Llatas-Quiroz, S., and M. López-Mesones. 2005. Bosques montanos-relictos en Kañaris (Lambayeque, Perú). *Revista Peruana de Biología* 12 (2): 299–308.
- Luna, L., and V. Pacheco. 2002. A new species of *Thomasomys* (Muridae: Sigmodontinae) from the Andes of southeastern Peru. *Journal of Mammalogy* 83: 834–842.
- Lunde, D.P., and V. Pacheco. 2003. Shrew opossums (Paucituberculata: *Caenolestes*) from the Huanca-bamba region of east Andean Peru. *Mammal Study* 28 (2): 145–148.
- Medina, C.E., et al. 2016. Primer registro del ratón colombiano del bosque *Chilomys instans* (Cricetidae: Rodentia) en Cajamarca: actualizando el listado de mamíferos del Perú. *Revista Peruana de Biología* 23: 315–320.
- Milazzo, M.L., M.N.B. Cajimat, M.H. Richter, R.D. Bradley, and C.F. Fulhorst. 2017. Muleshoe virus and other hantaviruses associated with neotomine or sigmodontine rodents in Texas. *Vector-Borne and Zoonotic Diseases* 17: 720–729.
- Moreno-Cárdenas, P.A., and M. Novillo-Gonzalez. 2020. First record of *Thomasomys cinereus* Thomas, 1882 (Rodentia, Cricetidae, Sigmodontinae) in Ecuador. *Therya* 11 (1): 41–45.
- Myers, P., J.L. Patton, and M.F. Smith. 1990. A review of the boliviensis group of *Akodon* (Rodentia: Sigmodontinae), with emphasis on Peru and Bolivia. *Miscellaneous Publications, Museum of Zoology, University of Michigan* 177: iv + 1–104.
- Nguyen, L.T., H.A. Schmidt, A. von Haeseler, and B.Q. Minh. 2015. IQ-TREE: A fast and effective stochastic algorithm for estimating maximum likelihood phylogenies. *Molecular Biology and Evolution* 32: 268–274.
- Osgood, W.H. 1912. Mammals from western Venezuela and eastern Colombia. *Field Museum of Natural History, Zoological Series* 10: 32–67.
- Osgood, W.H. 1914. Mammals of an expedition across northern Peru. *Field Museum of Natural History, Zoological Series* 10 (12): 143–185.
- Pacheco, V. 2002. Mamíferos del Perú. In G. Ceballos and J. Simonetti (editors), *Diversidad y conservación de los mamíferos neotropicales*, CONABIO-UNAM: 503–550. Mexico: Universidad Nacional Autónoma de México.
- Pacheco, V. 2003. Phylogenetic analyses of the *Thomasomyini* (Muroidea: Sigmodontinae) based on morphological data. Ph.D. dissertation, City University of New York, New York.
- Pacheco, V. 2015. Genus *Thomasomys* Coues, 1884. In J.L. Patton, U.F.J. Pardiñas, and G. D'Elia (editors),

- Mammals of South America, vol. 2, rodents: 617–682. Chicago: University of Chicago Press.
- Pacheco, V. 2021. Range extension of *Thomasomys princeps* (Thomas, 1895) (Rodentia, Sigmodontinae) and first record in Venezuela. *Check List* 17 (2): 385–393.
- Pacheco, V., and B.D. Patterson. 1992. Systematics and biogeographic analyses of four species of *Sturnira* (Chiroptera: Phyllostomidae), with emphasis on Peruvian forms. *Memorias del Museo de Historia Natural, Universidad Nacional Mayor de San Marcos* 21: 57–81.
- Pacheco, V., E.M. Rengifo, and D. Vivas. 2014. A new species of leaf-eared mouse, genus *Phyllotis* Waterhouse, 1837 (Rodentia: Cricetidae) from northern Peru. *Therya* 5 (2): 481–508.
- Pacheco, V., J.L. Patton, and G. D'Elía. 2015. Tribe Thomasomyini Steadman and Ray, 1982. In J.L. Patton, U.F.J. Pardiñas, and G. D'Elía (editors), *Mammals of South America*, vol. 2, rodents: 571–574. Chicago: University of Chicago Press.
- Parada, A., U.F.J. Pardiñas, J. Salazar-Bravo, G. D'Elía, and R.E. Palma. 2013. Dating an impressive Neotropical radiation: molecular time estimates for the Sigmodontinae (Rodentia) provide insights into its historical biogeography. *Molecular Phylogenetics and Evolution* 66 (3): 960–968.
- Parada, A., G. D'Elía, and R.E. Palma. 2015. The influence of ecological and geographical context in the radiation of neotropical sigmodontine rodents. *BMC Evolutionary Biology* 15: 172.
- Parada, A., J. Hanson, and G. D'Elía. 2021. Ultraconserved Elements improve the resolution of difficult nodes within the rapid radiation of Neotropical sigmodontine rodents (Cricetidae: Sigmodontinae). *Systematic Biology* 70: 1090–1100.
- Parker, T.A. III, T.S. Schulenberg, G.R. Graves, and M.J. Braun. 1985. The avifauna of the Huancabamba Region, northern Peru. *Ornithological Monographs* 36: 169–197.
- Patterson B.D., V. Pacheco, and M.V. Ashley. 1992. On the origins of the western slope region of endemism: systematics of fig-eating bats, genus *Artibeus*. *Memorias del Museo de Historia Natural, Universidad Nacional Mayor de San Marcos* 21: 189–205.
- Patton, J.L. 1987. Patrones de distribución y especiación de fauna de mamíferos de los bosques nublados andinos del Perú. *Anales del Museo de Historia Natural de Valparaíso* 17: 87–94.
- Patton, J.L., and M.N.F. da Silva. 1995. A review of the spiny mouse genus *Scolomys* (Rodentia: Muridae: Sigmodontinae) with the description of a new species from the western Amazon of Brazil. *Proceedings of the Biological Society of Washington* 108: 319–337.
- Percequillo, A.R., P.R. Gonçalves, and J.A. de Oliveira. 2004. The rediscovery of *Rhagomys rufescens* (Thomas, 1886), with a morphological redescription and comments on its systematic relationships based on morphological and molecular (Cytochrome *b*) characters. *Mammalian Biology* 69: 238–257.
- Polo-Gonzales, M.A. 2020. Nematofauna del género *Thomasomys* Coues, 1884 (Rodentia: Cricetidae) en el bosque relicto de Cachil (provincia Contumazá, departamento Cajamarca, Perú). Tesis de Biólogo con Mención en Zoología, Facultad de Ciencias Biológicas, Universidad Nacional Mayor de San Marcos, Lima, Perú.
- Pons, J., et al. 2006. Sequence-based species delimitation for the DNA taxonomy of undescribed insects. *Systematic Biology* 55: 595–609.
- Puillandre, N., A. Lambert, S. Brouillet, and G. Achaz. 2011. ABGD, Automated barcode gap discovery for primary species delineation. *Molecular Ecology* 21: 1864–1877.
- Puillandre, N., S. Brouillet, and G. Achaz. 2021. ASAP: assemble species by automatic partitioning. *Molecular Ecology Resources* 21: 609–620.
- Quay, W.B. 1954. The anatomy of the diastemal palate in microtine rodents. *Miscellaneous Publications of the Museum of Zoology, University of Michigan* 86: 1–41.
- R Core Team 2022. R: a language and environment for statistical computing. Vienna, Austria. Online resource (<https://www.R-project.org/>).
- Rambaut, A., A.J. Drummond, D. Xie, G. Baele, and M.A. Suchard. 2018. Posterior summarization in Bayesian phylogenetics using Tracer 1.7. *Systematic Biology* 67: 901–904.
- Reig, O.A. 1977. A proposed unified nomenclature for the enameled components of the molar teeth of the Cricetidae (Rodentia). *Journal of Zoology* 181: 227–241.
- Reig, O.A. 1980. A new fossil genus of South American cricetid rodents allied to *Wiedomys*, with an assessment of the Sigmodontinae. *Journal of Zoology* 192: 257–281.
- Rengifo, E., and V. Pacheco. 2015. Taxonomic revision of the Andean leaf-eared mouse, *Phyllotis andium* Thomas 1912 (Rodentia: Cricetidae), with the description of a new species. *Zootaxa* 4018: 349–380.

- Roncal-Rabanal, M.R. 2018. Línea base de flora y fauna del bosque de protección Pagaibamba, en el marco del proyecto 'Recuperación del servicio ambiental hídrico de área de amortiguamiento del bosque de protección Pagaibamba, distrito de Querocoto, Provincia de Chota, región Cajamarca.' Cajamarca: Talleres Gráficos de CIMAGRAF S.A.C.
- Ronquist, F., et al. 2012. MrBayes 3.2: efficient Bayesian phylogenetic inference and model choice across a large model space. *Systematic Biology* 61: 539–542.
- Ruelas, D., and V. Pacheco. 2021a. A new species of *Thomasomys* Coues, 1884 (Rodentia: Sigmodontinae) from the montane forests of northern Peru with comments on the "aureus" group. *Revista Peruana de Biología* 28 (3): e19912.
- Ruelas, D., and V. Pacheco. 2021b. Small mammals from the Seasonally Dry Tropical Forests of the Huallaga River basin and new records for San Martín department, Peru. *Check List* 17 (3): 877–894.
- Ruelas, D., V. Pacheco, B. Inche, and N. Tinoco. 2021. A preliminary review of *Nephelemys albigularis* (Tomes, 1860) (Rodentia: Cricetidae), with the description of a new species from the Peruvian montane forests. *Zootaxa* 5027 (2): 175–210.
- Salazar-Bravo, J., and T.L. Yates. 2007. A new species of *Thomasomys* (Cricetidae: Sigmodontinae) from central Bolivia. In D.A. Kelt, E.P. Lessa, J. Salazar-Bravo, and J.L. Patton (editors). *The quintessential naturalist, honoring the life and legacy of Oliver P. Pearson: 747–774*. University of California Publications in Zoology 134: xii + 1–981.
- Sánchez-Vendizú, P., V. Pacheco, and D. Vivas-Ruiz. 2018. An introduction to the systematics of small-bodied *Neacomys* (Rodentia: Cricetidae) from Peru with descriptions of two new species. *American Museum Novitates* 3913: 1–38.
- Schenk, J.J., K.C. Rowe, and S.J. Steppan. 2013. Ecological opportunity and incumbency in the diversification of repeated continental colonizations by muroid rodents. *Systematic Biology* 62 (6): 837–864.
- Semedo, T.B.F. et al. 2020. Systematics of Neotropical spiny mice, genus *Neacomys* Thomas, 1900 (Rodentia: Cricetidae), from Southeastern Amazonia, with descriptions of three new species. *American Museum Novitates* 3958: 1–43.
- Smith, M.F., and J.L. Patton. 1993. The diversification of South America murid rodents: evidence from mitochondrial DNA sequence data for Akodontini tribe. *Biological Journal of the Linnean Society* 50: 149–177.
- Smith, M.F., and J.L. Patton. 1999. Phylogenetic relationships and the radiation of sigmodontine rodents in South America: evidence from cytochrome b. *Journal of Mammalian Evolution* 6: 89–128.
- Smith, M.F., D.A. Kelt, and J.L. Patton. 2001. Testing models of diversification in mice in the *Abrothrix olivaceus/xanthorhinus* complex in Chile and Argentina. *Molecular Ecology* 10: 397–405.
- Smith, F.B. 1975. *Naturalist's color guide*. New York: American Museum of Natural History.
- Sprague, J.M. 1941. A study of the hyoid apparatus of the Cricetinae. *Journal of Mammalogy* 22: 296–310.
- Steppan, S.J., and J.J. Schenk. 2017. Muroid rodent phylogenetics: 900-Species tree reveals increasing diversification rates. *PLoS ONE* 12 (8): e0183070.
- Sylvester, S.P., et al. 2017. Relict high-Andean ecosystems challenge our concepts of naturalness and human impact. *Scientific Reports* 7: 3334.
- Thomas, O. 1882. On a collection of rodents from North Peru. *Proceedings of the Zoological Society of London*: 98–111.
- Thomas, O. 1884. On a collection of Muridae from central Peru. *Proceedings of the Zoological Society of London* (part III): 393–403.
- Thomas, O. 1894. Descriptions of some new Neotropical Muridae. *Annals and Magazine of Natural History* 6 (14): 346–366.
- Thomas, O. 1895. On small mammals from Nicaragua and Bogota. *Annals and Magazine of Natural History* 6 (16): 55–60.
- Thomas, O. 1896. On new small mammals from the Neotropical region. *Annals and Magazine of Natural History* 6 (18): 301–314.
- Thomas, O. 1898. On seven new small mammals from Ecuador and Venezuela. *Annals and Magazine of Natural History* 7 (1): 451–457.
- Thomas, O. 1906. Notes on South-American rodents. *Annals and Magazine of Natural History* 18: 442–448.
- Thomas, O. 1917. Preliminary diagnoses of new mammals obtained by the Yale–National Geographic Society Peruvian Expedition. *Smithsonian Miscellaneous Collections* 68 (4): 1–3.
- Thomas, O. 1926a. The Godman-Thomas expedition to Peru.— II. On mammals collected by Mr. Hendee in north Peru between Pacasmayo and Chachapoyas. *Annals and Magazine of Natural History* 9 (17): 610–616.
- Thomas, O. 1926b. The Godman-Thomas expedition to Peru.— III. On mammals collected by Mr. R.W. Hendee in the Chachapoyas region of north Peru.

- Annals and Magazine of Natural History 9 (18): 156–167.
- Thomas, O. 1926c. The Godman-Thomas expedition to Peru.— IV. On mammals collected by Mr. R.W. Hendee north of Chachapoyas, province of Amazonas, north Peru. Annals and Magazine of Natural History 9 (18): 345–349.
- Thomas, O. 1927a. The Godman- Thomas expedition to Peru.— V. On mammals collected by Mr. R.W. Hendee in the province of San Martin, N. Peru, mostly at Yurac Yacu. Annals and Magazine of Natural History 9 (19): 361–373.
- Thomas, O. 1927b. The Godman- Thomas expedition to Peru.— VI. On mammals from the upper Hualлага and neighbouring highlands. Annals and Magazine of Natural History 9 (20): 594–608.
- Thomas, O., and J.S. Leger. 1926. The Godman-Thomas expedition to Peru.— IV. On mammals collected by Mr. R.W. Hendee north of Chachapoyas, Province of Amazonas, north Peru. Annals and Magazine of Natural History 9 (18): 345– 49.
- Tribe, C.J. 1996. The neotropical rodent genus *Rhipidomys* (Cricetidae: Sigmodontinae): a taxonomic revision. Ph.D. dissertation, University College, London.
- Trouessart, E.L. 1898. Catalogus mammalium tam viventium quam fossilium, nova editio. Tomus 1. Berlin: R. Friedliinder and Sohn.
- Vivar, E., V. Pacheco, and M. Valqui. 1997. A new species of *Cryptotis* (Insectivora: Soricidae) from northern Peru. American Museum Novitates 3202: 1–15.
- Voss, R.S. 1988. Systematics and ecology of ichthyomyine rodents (Muroidea): patterns of morphological evolution in a small adaptive radiation. Bulletin of the American Museum of Natural History 188: 259–493.
- Voss, R.S. 1991. An introduction to the Neotropical muroid rodent genus *Zygodontomys*. Bulletin of the American Museum of Natural History 244: 1–113.
- Voss, R.S. 1993. A revision of the Brazilian muroid rodent genus *Delomys* with remarks on “thomasomyine” characters. American Museum Novitates 3073: 1–44.
- Voss, R.S. 2003. A new species of *Thomasomys* (Rodentia: Muridae) from eastern Ecuador, with remarks on mammalian diversity and biogeography in the Cordillera Oriental. American Museum Novitates 3421: 1–47.
- Wahlert, J.H. 1985. Cranial foramina of rodents. In W.P. Luckett and J.L. Hartenberger (editors), Evolutionary relationships among rodents, a multidisciplinary analysis: 311–332. New York: Plenum Press.
- Weigend, M. 2002. Observations on the biogeography of the Amotape-Huancabamba zone in northern Peru. Botanical Review 68: 38–54.
- Weigend, M. 2004. Additional observations on the biogeography of the Amotape-Huancabamba zone in northern Peru: defining the south-eastern limits. Revista Peruana de Biología 11: 127–134.
- Zavodszky, A.M., and G.A. Russo. 2020. Comparative and functional morphology of chevron bones among mammals. Journal of Mammalogy 101 (2): 403–416.
- Zhang, J., P. Kapli, P. Pavlidis, and A. Stamatakis. 2013. A general species delimitation method with applications to phylogenetic placements. Bioinformatics 29: 2869–2876.

APPENDIX 1

SELECTED COLLECTING LOCALITIES

List of examined specimens of *Thomasomys cinereus*, *T. lojapiuranus*, *T. pagaibambensis*, and *T. shallqkucha* with their respective localities.

Names of the largest administrative unit (department, state, etc.) within each country are italicized and geographic coordinates are provided.

Thomasomys cinereus

PERU

- Cajamarca*, Cajamarca, Encañada (**locality 40**: 6.944976°S, 78.362122°W; MUSM 42453, 42454).
- Cajamarca*, Cajamarca, Páramo de Cajamarca (not located; BNMH 0.3.15.4, 0.3.15.5).
- Cajamarca*, Cajamarca, Quengorrio (**locality 37**: 6.8446100°S, 78.4318300°W; MUSM 38350).
- Cajamarca*, Cajamarca, San Juan de Yerbabuena (**locality 38**: 6.9766300°S, 78.3799800°W; MUSM 38351, 38352).
- Cajamarca*, Celendín, CCPP La Florida (**locality 47**: 7.041686°S, 78.137400°W; MUSM 38005).
- Cajamarca*, Celendín, CCPP Lalucma (**locality 46**: 6.923999°S, 78.244523°W; MUSM 38006).
- Cajamarca*, Celendín, CCPP Sorochuco (**locality 45**: 6.893929°S, 78.244760°W; MUSM 38007).
- Cajamarca*, Celendín, Coñicorgue (**locality 41**: 6.8330600°S, 78.3149600°W; MUSM 38349, 38493–38495).
- Cajamarca*, Celendín, El Punre (**locality 44**: 6.994457°S, 78.279074°W; MUSM 39369–39373).
- Cajamarca*, Celendín, Hacienda El Punre (**locality 43**: 7.007557°S, 78.288909°W; MUSM 38008).
- Cajamarca*, Celendín, Laguna Milpo (**locality 42**: 6.975250°S, 78.307950°W; MUSM 34949).
- Cajamarca*, Celendín, Porvenir (**locality 39**: 6.977116°S, 78.379967°W; MUSM 38496, 38497).
- Cajamarca*, Contumaza, Bosque Cachil (**locality 48**: 7.395183°S, 78.780277°W; MUSM 51108–51113, 51115–51117, 52399–52406).
- Cajamarca*, Cutervo, Cutervo (**locality 24**: 6.378980°S, 78.817920°W; BMNH 81.9.7.29).
- Cajamarca*, Cutervo, Parque Nacional Cutervo, 100 m over Tragadero (**locality 25**: 6.249972°S, 78.766528°W; MUSM 46716).
- Cajamarca*, San Miguel, Seques (**locality 26**: 6.900000°S, 79.300000°W; AMNH 73127, 73129).
- Cajamarca*, San Miguel, Taulis (**locality 27**: 6.833300°S, 79.166670°W; AMNH 73136, 73147).
- Cajamarca*, Santa Cruz, 2 Km E Montesecco (**locality 28**: 6.857110°S, 79.098200°W; MUSM uncatalogued [VPT 1629, VPT 1640, VPT 1650]).
- Cajamarca*, Santa Cruz, 3.81 km NE from Montesecco (**locality 29**: 6.8437300°S, 79.0812540°W; MUSM 46756–46759; UMMZ 178461, 178463, 178467, 178482, 178488).
- Cajamarca*, Santa Cruz, 35 mi NW Cajamarca (**locality 30**: 6.971760°S, 78.987800°W; MVZ 137937–137939).
- Cajamarca*, Santa Cruz, Alcaparrosa, T 28 (**locality 34**: 6.786230°S, 78.890020°W; MUSM 25704).
- Cajamarca*, Santa Cruz, Bancuyoc, T 07 (**locality 32**: 6.823410°S, 78.903620°W; MUSM 25705).
- Cajamarca*, Santa Cruz, Bosque San Pedro (**locality 33**: 6.806293°S, 78.896919°W; MUSM 46909).
- Cajamarca*, Santa Cruz, La Zanja y La Redonda (**locality 35**: -6.821666°S, -78.88166°W; MUSM 23346).
- Cajamarca*, Santa Cruz, Pampa Verde (**locality 31**: 6.814830°S, 78.912050°W; MUSM 25706–25708).

- Cajamarca*, Santa Cruz, Pisit T 25 (**locality 36**: 6.811390°S, 78.870520°W; MUSM 25709).
- La Libertad*, Daniel A. Carrión, La Arena (**locality 51**: 7.88955°S, 78.13786°W; MUSM 24136–24142, 24166–24172).
- La Libertad*, Daniel A. Carrión, South of Huamachuco (**locality 50**: 7.814830°S, 78.050030°W; BMNH 0.6.6.12).
- La Libertad*, Gran Chimú, La Clambay (**locality 49**: 7.622123°S, 78.435071°W; MUSM 52972, 52973).
- La Libertad*, Santiago de Chuco, Cachicadán (**locality 55**: 8.0646300°S, 78.1732100°W; MUSM 17285–17299, 17302).
- La Libertad*, Santiago de Chuco, El Fundo Río Chuyuhual (**locality 54**: 7.933627°S, 78.220142°W; MUSM 41102, 41103, 42008–42012).
- La Libertad*, Santiago de Chuco, Lagunas del Norte, río Chuyuhual (**locality 53**: 7.9304800°S, 78.2180200°W; MUSM 24928).
- La Libertad*, Santiago de Chuco, Lagunas Norte, río Perejil, San Pedro (**locality 52**: 7.9262000°S, 78.2790800°W; MUSM 24774).
- Thomasomys lojapiuranus*
ECUADOR
- Loja*, Espindola, Guardianía, Parque Nacional Yacuri National (**locality 2**: 4.7124700°S, 79.44067°W; MEPN 12549).
- Loja*, Espindola, Parque Nacional Yacuri 10.1 (**locality 4**: 4.725244°S, 79.434502°W; QCAZ 15641).
- PERU
- Piura*, Ayabaca, Aypate (4.70756179°S, 79.57981948°W; (**locality 1**: MUSM uncatalogued: ASA06, ASA11, ASA12, ASA16, ASA23, ASA27; MUSM 38501).
- Piura*, Ayabaca, Bosque de Huamba, 44 km E Ayabaca (**locality 3**: 4.718720°S, 79.530850°W; MUSM 511).
- Piura*, Huancabamba, Pariamarca Alto (**locality 6**: 5.158670°S, 79.549010°W; MUSM 23758–23762).
- Piura*, Huancabamba, 15 road Km E Canchaque (**locality 12**: 5.400000°S, 79.464660°W; LSUMZ 19315, 19316).
- Piura*, Huancabamba, 33 road Km SW Huancabamba (**locality 13**: 5.455450°S, 79.662160°W; LSUMZ 19301–19314, 19707, 20313).
- Piura*, Huancabamba, Cerro Chinguela, ca. 5 km NE Zapalache (**locality 5**: 5.116666°S, 79.383333°W; LSUMZ 27147).
- Piura*, Huancabamba, Cruz Blanca, ca. 33 rd. Km SW Huancabamba (**locality 7**: 5.333333°S, 79.533333°W; LSUMZ 27045–27081, 27130–27146).
- Piura*, Huancabamba, Tambo (**locality 9**: 5.350000°S, 79.550000°W; FMNH 81297–81299, 81301–81306, 81308–81312, 81325–81330, 81334, 81336).
- Piura*, Huancabamba, Canchaque (**locality 11**: 5.400000°S, 79.600000°W; FMNH 83444–83454).
- Piura*, Huancabamba, El Tambo (**locality 10**: 5.3594000°S, 79.5511000°W; USNM 304535–304537).
- Piura*, Huancabamba, Sondorillo, Ulpamache (**locality 8**: 5.338900°S, 79.491400°W; USNM 551643).
- Thomasomys pagaibambensis*
PERU
- Cajamarca*, Chota, El Mirador, Agua de Montaña (**locality 18**: 6.380954°S, 79.126427°W; MUSM 40961–40967).
- Cajamarca*, Chota, La Granja, Qda. Agua de la Montaña (**locality 17**: 6.359960°S, 79.142670°W; MUSM 40357, 40358, 41591).
- Cajamarca*, Chota, Pagaibamba (**locality 22**: 6.432256°S, 79.070808°W; MUSM 40968–40990).
- Cajamarca*, Chota, Pagaibamba Alto (**locality 23**: 6.433360°S, 79.072210°W; MUSM 39524–39527).
- Cajamarca*, Chota, Pagaibamba Bajo (**locality 20**: 6.419030°S, 79.058920°W; MUSM 39528–39532).

Cajamarca, Chota, Pagaibamba Medio (**locality 21**: 6.427160°S, 79.065380°W; MUSM 39533–39536, 40991–40995).

Cajamarca, Chota, Paja Blanca (**locality 19**: 6.389970°S, 79.126910°W; MUSM 39537–39556, 40996–41011).

Thomasomys shallqukucha

PERU

Lambayeque, Lambayeque, Bosque de Chiñama (**locality 16**: 6.100000°S, 79.433330°W; MUSM 5095).

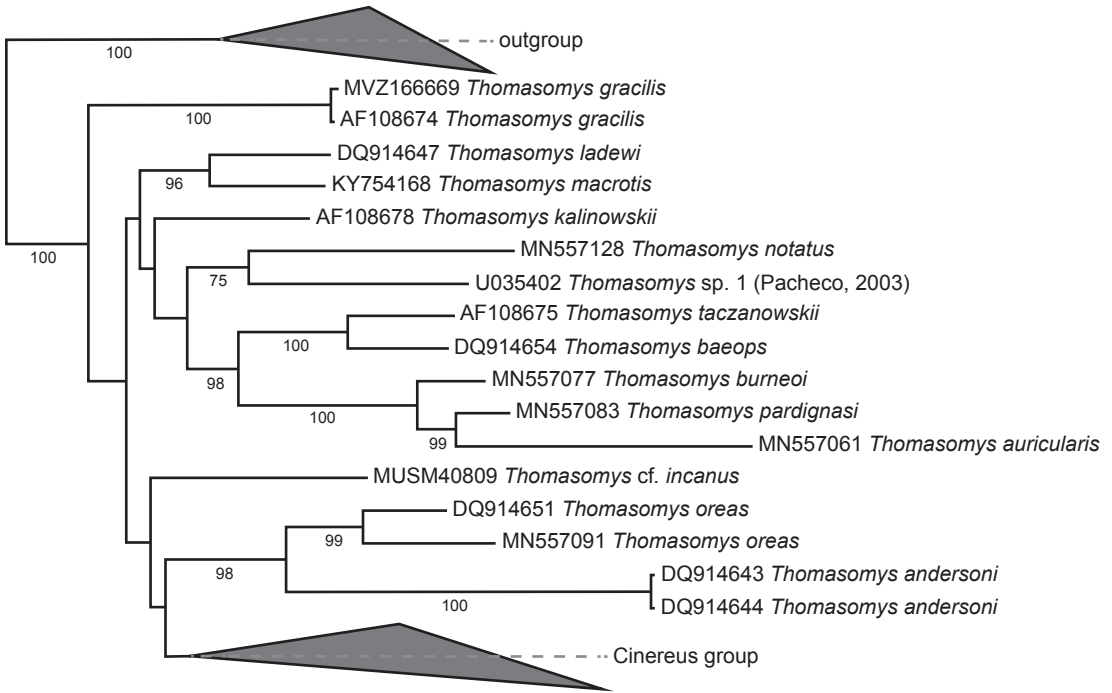
Lambayeque, Ferreñafe, Geomarca (**locality 15**: 6.095835°S, 79.240488°W; MUSM 46870–46889).

Lambayeque, Ferreñafe, Palomapampa (**locality 14**: 6.0746110°S, 79.2495280°W; MUSM 47227–47231).

APPENDIX 2

PHYLOGENETIC RELATIONSHIPS OF *THOMASOMYS* BASED ON MAXIMUM-LIKELIHOOD ANALYSIS

Phylogenetic tree resulting from Maximum-Likelihood Analysis for species of *Thomasomys*. The content of the Cinereus Group is expanded in figure 4. Values below the branches are the bootstrap support.



APPENDIX 3

ANOVA TEST RESULTS

ANOVA test results with post-hoc Tukey-Kramer test comparing *Thomasomys cinereus* sensu stricto, *T. lojapiuranus*, sp. nov., *T. shallqkucha*, sp. nov., and *T. pagaibambensis*, sp. nov., using 13 variables with normal distribution. The meaning of the abbreviations of the variables are explained in Material and Methods. Abbreviations: **F**, F value; **p**, p-value; **diff**, mean differences; **lwr**, lower confidence interval; **upr**, upper confidence interval. Statistically significant values are shown in bold ($P < 0.05$).

Variables	ANOVA		Tukey-Kramer test				
	F	P	Species	diff	lwr	upr	p
CML	14.054	6.41E-08	<i>cinereus</i> - <i>lojapiuranus</i>	0.006	-0.359	0.372	1.000
			<i>cinereus</i> - <i>pagaibambensis</i>	0.611	0.248	0.974	0.000
			<i>cinereus</i> - <i>shallqkucha</i>	0.449	-0.074	0.971	0.036
			<i>lojapiuranus</i> - <i>pagaibambensis</i>	0.604	0.254	0.955	0.000
			<i>lojapiuranus</i> - <i>shallqkucha</i>	-0.442	-0.956	0.072	0.036
			<i>pagaibambensis</i> - <i>shallqkucha</i>	0.162	-0.350	0.674	0.746
LN	6.6112	3.57E-04	<i>cinereus</i> - <i>lojapiuranus</i>	-0.261	-0.712	0.189	0.258
			<i>cinereus</i> - <i>pagaibambensis</i>	0.336	-0.111	0.784	0.085
			<i>cinereus</i> - <i>shallqkucha</i>	0.139	-0.505	0.784	0.902
			<i>lojapiuranus</i> - <i>pagaibambensis</i>	0.598	0.166	1.029	0.000
			<i>lojapiuranus</i> - <i>shallqkucha</i>	-0.401	-1.034	0.233	0.190
			<i>pagaibambensis</i> - <i>shallqkucha</i>	0.197	-0.435	0.829	0.754
LD	12.777	2.61E-07	<i>cinereus</i> - <i>lojapiuranus</i>	0.265	-0.011	0.542	0.015
			<i>cinereus</i> - <i>pagaibambensis</i>	0.481	0.206	0.756	0.000
			<i>cinereus</i> - <i>shallqkucha</i>	0.567	0.171	0.962	0.000
			<i>lojapiuranus</i> - <i>pagaibambensis</i>	0.216	-0.049	0.481	0.052
			<i>lojapiuranus</i> - <i>shallqkucha</i>	-0.302	-0.691	0.087	0.071
			<i>pagaibambensis</i> - <i>shallqkucha</i>	-0.086	-0.473	0.302	0.897
LIF	14.56	3.71E-08	<i>cinereus</i> - <i>lojapiuranus</i>	-0.413	-0.614	-0.213	0.000
			<i>cinereus</i> - <i>pagaibambensis</i>	-0.190	-0.389	0.010	0.016
			<i>cinereus</i> - <i>shallqkucha</i>	-0.268	-0.555	0.020	0.019
			<i>lojapiuranus</i> - <i>pagaibambensis</i>	0.224	0.031	0.417	0.002
			<i>lojapiuranus</i> - <i>shallqkucha</i>	-0.146	-0.428	0.137	0.362
			<i>pagaibambensis</i> - <i>shallqkucha</i>	0.078	-0.203	0.360	0.813
LM	14.377	4.52E-08	<i>cinereus</i> - <i>lojapiuranus</i>	-0.199	-0.318	-0.080	0.000
			<i>cinereus</i> - <i>pagaibambensis</i>	0.010	-0.108	0.128	0.993
			<i>cinereus</i> - <i>shallqkucha</i>	-0.117	-0.288	0.053	0.132
			<i>lojapiuranus</i> - <i>pagaibambensis</i>	0.209	0.095	0.323	0.000
			<i>lojapiuranus</i> - <i>shallqkucha</i>	-0.082	-0.249	0.086	0.410
			<i>pagaibambensis</i> - <i>shallqkucha</i>	0.127	-0.040	0.294	0.078

APPENDIX 3 *continued*

Variables	ANOVA		Tukey-Kramer test				
	F	P	Species	diff	lwr	upr	p
BPB	10.995	1.95E-06	<i>cinereus - lojapiuranus</i>	-0.103	-0.244	0.037	0.095
			<i>cinereus - pagaibambensis</i>	0.130	-0.010	0.269	0.019
			<i>cinereus - shallqkucha</i>	-0.081	-0.282	0.120	0.579
			<i>lojapiuranus - pagaibambensis</i>	0.233	0.098	0.368	0.000
			<i>lojapiuranus - shallqkucha</i>	-0.023	-0.220	0.175	0.983
			<i>pagaibambensis - shallqkucha</i>	0.211	0.014	0.407	0.005
BN	3.9477	1.00E-02	<i>cinereus - lojapiuranus</i>	0.111	-0.075	0.296	0.235
			<i>cinereus - pagaibambensis</i>	-0.043	-0.227	0.141	0.880
			<i>cinereus - shallqkucha</i>	0.172	-0.094	0.437	0.173
			<i>lojapiuranus - pagaibambensis</i>	-0.154	-0.331	0.024	0.035
			<i>lojapiuranus - shallqkucha</i>	-0.061	-0.322	0.200	0.879
			<i>pagaibambensis - shallqkucha</i>	-0.215	-0.475	0.045	0.048
LIB	35.233	< 2.2e-16	<i>cinereus - lojapiuranus</i>	0.097	-0.028	0.222	0.070
			<i>cinereus - pagaibambensis</i>	0.370	0.246	0.494	0.000
			<i>cinereus - shallqkucha</i>	0.288	0.110	0.467	0.000
			<i>lojapiuranus - pagaibambensis</i>	0.273	0.154	0.393	0.000
			<i>lojapiuranus - shallqkucha</i>	-0.192	-0.367	-0.016	0.004
			<i>pagaibambensis - shallqkucha</i>	0.082	-0.093	0.257	0.451
BZP	1.2581	2.92E-01	<i>cinereus - lojapiuranus</i>	-0.042	-0.162	0.077	0.676
			<i>cinereus - pagaibambensis</i>	-0.017	-0.136	0.101	0.966
			<i>cinereus - shallqkucha</i>	0.056	-0.115	0.227	0.726
			<i>lojapiuranus - pagaibambensis</i>	0.025	-0.090	0.139	0.902
			<i>lojapiuranus - shallqkucha</i>	-0.098	-0.266	0.070	0.253
			<i>pagaibambensis - shallqkucha</i>	-0.073	-0.241	0.094	0.506
DI	11.966	6.47E-07	<i>cinereus - lojapiuranus</i>	0.057	0.002	0.112	0.007
			<i>cinereus - pagaibambensis</i>	0.103	0.048	0.157	0.000
			<i>cinereus - shallqkucha</i>	0.061	-0.018	0.139	0.073
			<i>lojapiuranus - pagaibambensis</i>	0.046	-0.007	0.099	0.031
			<i>lojapiuranus - shallqkucha</i>	-0.004	-0.081	0.073	0.999
			<i>pagaibambensis - shallqkucha</i>	0.042	-0.035	0.119	0.306
HBC	13.444	1.25E-07	<i>cinereus - lojapiuranus</i>	-0.071	-0.246	0.105	0.578
			<i>cinereus - pagaibambensis</i>	0.248	0.073	0.422	0.000
			<i>cinereus - shallqkucha</i>	0.003	-0.249	0.254	1.000
			<i>lojapiuranus - pagaibambensis</i>	0.318	0.150	0.487	0.000
			<i>lojapiuranus - shallqkucha</i>	-0.073	-0.320	0.174	0.782
			<i>pagaibambensis - shallqkucha</i>	0.245	-0.001	0.492	0.011

APPENDIX 4

FACTOR LOADINGS FOR PRINCIPAL COMPONENTS AND DISCRIMINANT FUNCTION ANALYSES

Factor loadings of principal components analyses (PC1, PC2, PC3), discriminant function analysis (DF1, DF2, DF3), and percentage of variance from 17 morphometric variables of *Thomasomys cinereus*, *T. lojapiuranus*, *T. shallqukucha*, and *T. pagaibambensis*.

Variables	PC1	PC2	PC3	DF1	DF2	DF3
CML	0.205	0.117	0.016	26.221	5.335	-0.413
LOF	0.151	0.039	0.081	-27.455	4.473	7.380
LN	0.327	0.183	0.023	-1.073	-6.365	-7.452
LD	0.275	0.272	-0.121	15.397	12.726	1.168
LIF	0.234	-0.123	0.338	-9.635	-13.832	-17.069
LM	0.175	-0.052	0.123	-1.539	-25.612	8.441
BIF	0.279	-0.547	0.378	1.204	1.653	2.408
BR	0.246	-0.313	0.007	-11.275	-4.504	-1.757
BPB	0.391	0.205	0.198	0.062	-10.366	0.267
BM1	0.155	-0.104	-0.140	2.515	11.192	-19.594
BN	0.237	-0.312	-0.770	-1.870	1.773	-3.235
LIB	0.141	0.385	0.009	14.429	-3.932	-18.379
ZB	0.230	0.147	0.053	7.411	-14.716	29.402
BB	0.070	-0.094	-0.071	-12.915	25.428	13.249
BZP	0.391	-0.128	-0.091	-3.681	7.310	-7.763
DI	0.244	0.279	-0.191	11.016	5.307	9.673
HBC	0.071	0.197	0.046	5.628	-11.499	1.092
% variance	31.75	12.79	11.77	52.48	41.53	5.98

APPENDIX 5

RESULTS OF PRINCIPAL COMPONENTS ANALYSES

Plots of the first two principal components (PC) for pairwise analyses of craniodental measurement data for **A.** *Thomasomys cinereus* versus *T. lojapiuranus*, **B.** *T. cinereus* versus *T. pagaibambensis*, **C.** *T. cinereus* versus *T. shallqukucha*, **D.** *T. lojapiuranus* versus *T. pagaibambensis*, **E.** *T. lojapiuranus* versus *T. shallqukucha*, and **F.** *T. pagaibambensis* versus *T. shallqukucha*. Symbols used: *T. cinereus* sensu stricto (circles), *T. lojapiuranus* (diamonds), *T. pagaibambensis* (triangles), and *T. shallqukucha* (squares). Percentages of variance are shown into parenthesis.

